C H A P T E R - IV

R E S U L T S

4.1 GENERAL INTRODUCTION

In this chapter the results obtained by (1) chronopotentiometry, (2) cyclic voltammetry, (3) chronoamperometry and (4) sampled current voltammetry for the redox reactions of Pb^{++}, Co^{++}, Ni^{++}, Fe^{+++} and Cu^{++} ions are given. A full description of the results, of the calculations of transfer coefficients, transition times, quarter-wave potentials, diffusion coefficients etc. are given for lead only for each technique, as the processes are only repetitions for other elements.

4.2 CHRONOPOTENTIOMETRY

Chronopotentiometric experiments were performed in the manner described in the earlier chapter. The concentrations of the electroactive substance and current densities were the parameters which were changed for the investigation. The apparatus and the three electrode cell have been described in the earlier chapter. A repetition of the procedure is not warranted. The details for the data obtained and the mode of obtaining the data are described for lead only, as the processes are repetitive for other elements.

4.2.1 Lead

The solute used was $Pb(NO_3)_2$ which was dehydrated under vacuum at 383 K for 24 hrs. The residue was tested for any decomposition of nitrate. The mechanism of dehydration and so the complete absence of moisture was explained in the earlier chapter. The weight of solvent was kept constant through the series of experiments as the solvent was not disturbed and the solute was added to the same solvent to increase the concentration. The volume of the solvent was calculated using equation 3.1.

Chronopotentiograms were recorded as a function of concentration and current strength. The former was varied from 0.5 to 1.5 mole cm^{-3} and the latter from 200 to 400 uA. The area of the foil platinum electrode was 2.23 cm^2 and hence the current densities varied from 89.7 to 179.4 $\mu A\ cm^{-2}$. Both forward and reverse chronopotentiograms were recorded.

Fig. 4.2.1 gives a typical chronopotentiogram of lead in the nitrate melt at 423 K. Table 4.2.1 lists the current strengths used, the concentration of the solute and the transition time measured for the forward reaction. The method of measuring the transition times has already been described. The reverse curve was ill defined and ill shaped and hence no reliable data could be obtained from the curve. Exhaustive compilation of data has not been given but only typical values have been reported in Table 4.2.1.

In any chronopotentiogram the first criterion which has to be looked into is to test whether the reaction is

Table 4.2.1

Chronopotentiometric Data on Pb^{++} Ion in (Li, Na, K) NO_3 Eutectic at 423 $\pm$ 2 K (Forward)

Concentration $C \times 10^6$ mole cm^{-3}	Current $i \times 10^6$ A	Transition Time τ_f s	$\frac{i \times \tau_f^{1/2}}{C}$ A $s^{1/2}$ mole cm^3	Diffusion coefficient $(D_o) \times 10^6$ cm^2 s^{-1}
0.51	300	3.94	1168	9.40
	250	6.00	1200	9.96
	200	8.40	1137	8.92
0.76	400	5.04	1151	9.21
	300	6.96	1015	7.15
	250	9.60	993	6.85
	200	13.80	953	6.31
1.02	400	6.30	1287	6.56
	350	7.20	1204	5.26
	300	9.20	1167	5.10
			mean	7.47

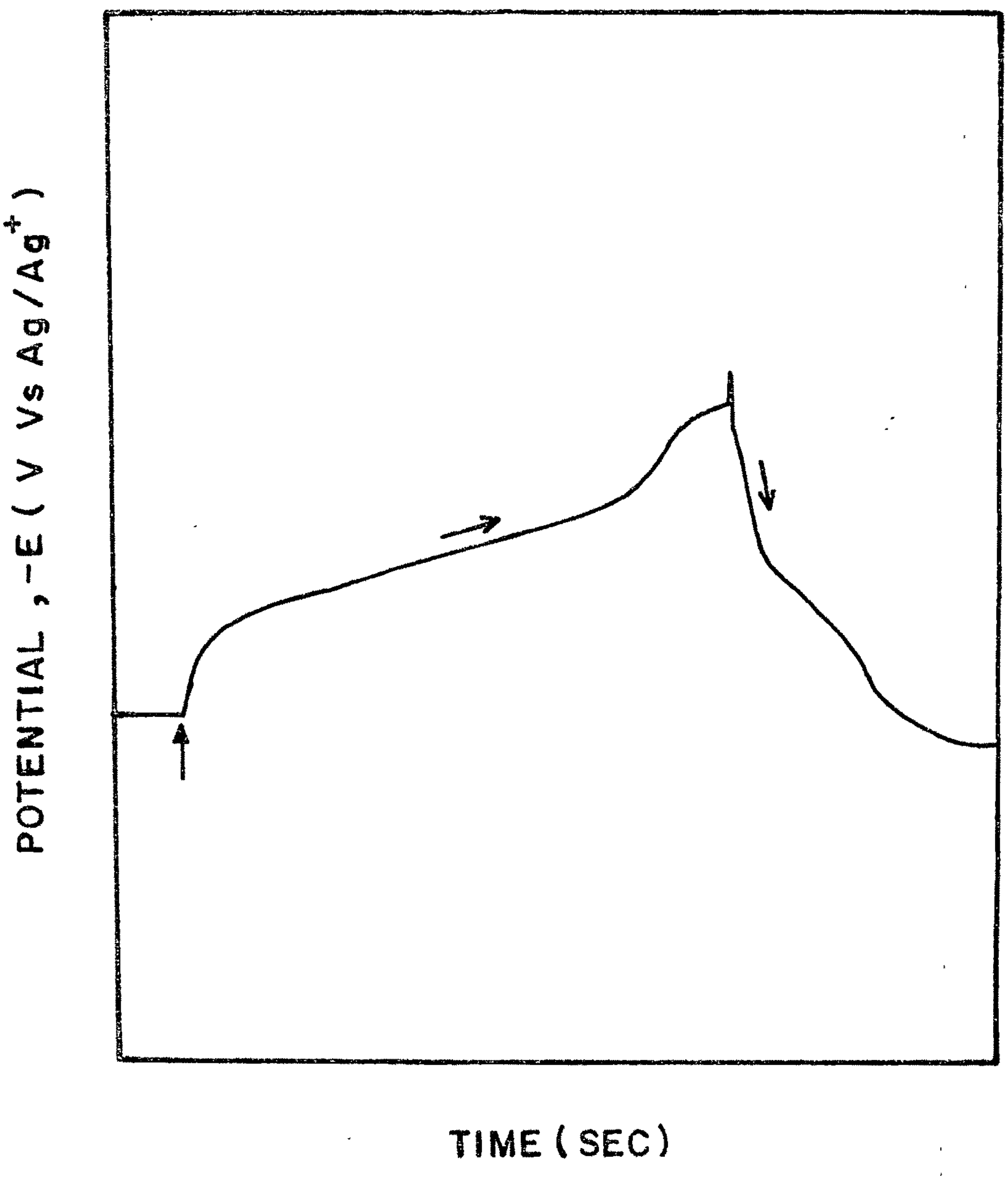

FIG. 4.2.1. A TYPICAL CHRONOPOTENTIOGRAM OF Pb^{++} ION IN (Li, Na, K) NO_3 EUTECTIC AT 423 ± 2K

diffusion controlled or not. This is verified from the constancy of the factor $\frac{i\tau^{\frac{1}{2}}}{C}$ where i is the current in amperes, τ the transition time in seconds and C is the concentration of the electroactive solute in moles cm^{-3}. As can be seen from Table 4.2.1 the factor $\frac{i\tau^{\frac{1}{2}}}{C}$ remained constant within experimental errors and uncertainties. After having ascertained that the reaction is diffusion controlled the Sand's equation

$$\tau^{\frac{1}{2}} = \frac{\pi^{\frac{1}{2}} n F D_o^{\frac{1}{2}} C}{2 i^o} \qquad 2.3$$

was employed to calculate diffusion coefficients. In this equation τ is the transition time in s, n is the number of electrons involved, F is the Faraday i.e., 96,500 coulombs, D_o is the diffusion constant of the Pb^{++} ion in $cm^2 s^{-1}$, C the concentration of the active electrolyte in mole cm^{-3} and i^o the current densities in A. cm^{-2}. The values of $(D_o)_f$ so calculated are listed in Table 4.2.1 together with the values of $i\,\tau^{\frac{1}{2}}/_C$. Sand's equation can be used in any chronopotentiometric process, irrespective of whether it is reversible or irreversible.

The values of $E\,\tau/_4$ were then obtained from the several chronopotentiograms. It was found that $E\,\tau/_4$ varied with current densities and concentration and not necessarily in a regular or predictable fashion. This has been observed

Table 4.2.2

Chronopotentiometric Data of Pb^{++} Ion in (Li, Na, K)NO_3 Eutectic at 423 ± K

Current density = 89.7 $\mu A/cm^2$

τ = 13.8 s

E V vs Ag/ Ag^+	t s	$\log\left[\frac{\tau^{\frac{1}{2}} - t^{\frac{1}{2}}}{t^{\frac{1}{2}}}\right]$	$\log\left[\frac{\tau^{\frac{1}{2}} - t^{\frac{1}{2}}}{\tau^{\frac{1}{2}}}\right]$
-0.24	1.2	+2.388	-0.152
-0.28	2.4	+1.395	-0.234
-0.31	3.6	+0.956	-0.311
-0.34	4.8	+0.694	-0.387
-0.38	6.0	+0.515	-0.468
-0.44	7.2	+0.383	-0.556
-0.50	8.4	+0.280	-0.658
-0.55	9.6	+0.197	-0.780
-0.65	10.8	+0.129	-0.938

by Reinmuth[60] in several other cases. Reinmuth has compiled diagnostic features for the kinetic scheme for chronopotentiometry (Section 2.2.7).

The potential of the time - potential graph should vary very abruptly at time $t = 0$ (nglecting the charging of the double layer) for a totally irreversible electrode process involving only one rate determining step. This is virtually the case as can be seen from Fig. 4.2.2. Again if the linear plot of E vs $\ln\left[\frac{\tau^{\frac{1}{2}} - t^{\frac{1}{2}}}{t^{\frac{1}{2}}}\right]$ yields a slope of $\frac{RT}{nF}$, then the reaction can be deemed to be reversible. In this case t is the time elapsed from the start of the electrolysis to the time at which any value of E is reached. Thus E is the potential at time t. The value of t are listed against values of E in Table 4.2.2. Having found that this plot did not show any linear relationship, (Fig. 4.2.3), a plot of E vs $\log\left[1 - (t/\tau)^{\frac{1}{2}}\right]$ was drawn. A linear relationship was obtained with a slope of 0.513, which was equal to $\frac{2.303\,RT}{\alpha_c n_\alpha F}$. Thus the value of $\alpha_c n_\alpha$ was deduced to be 0.164. The relationship is shown in Fig. 4.2.3. This value of 0.164 was found to be reasonably constant at different current densities and had a variation of only $\pm$ 0.009 which would not very much affect the magnitude of the rate constants to be calculated from this value.

In the above computation the basic equation[61]

$$E = \frac{RT}{\alpha_c n_\alpha F} \ln \frac{nFAC\,k^o_{f,h}}{i} + \frac{RT}{\alpha_c n_\alpha F} \ln \left[\left(\frac{\tau^{\frac{1}{2}} - t^{\frac{1}{2}}}{\tau^{\frac{1}{2}}}\right)\right] \qquad \text{......... 2.8}$$

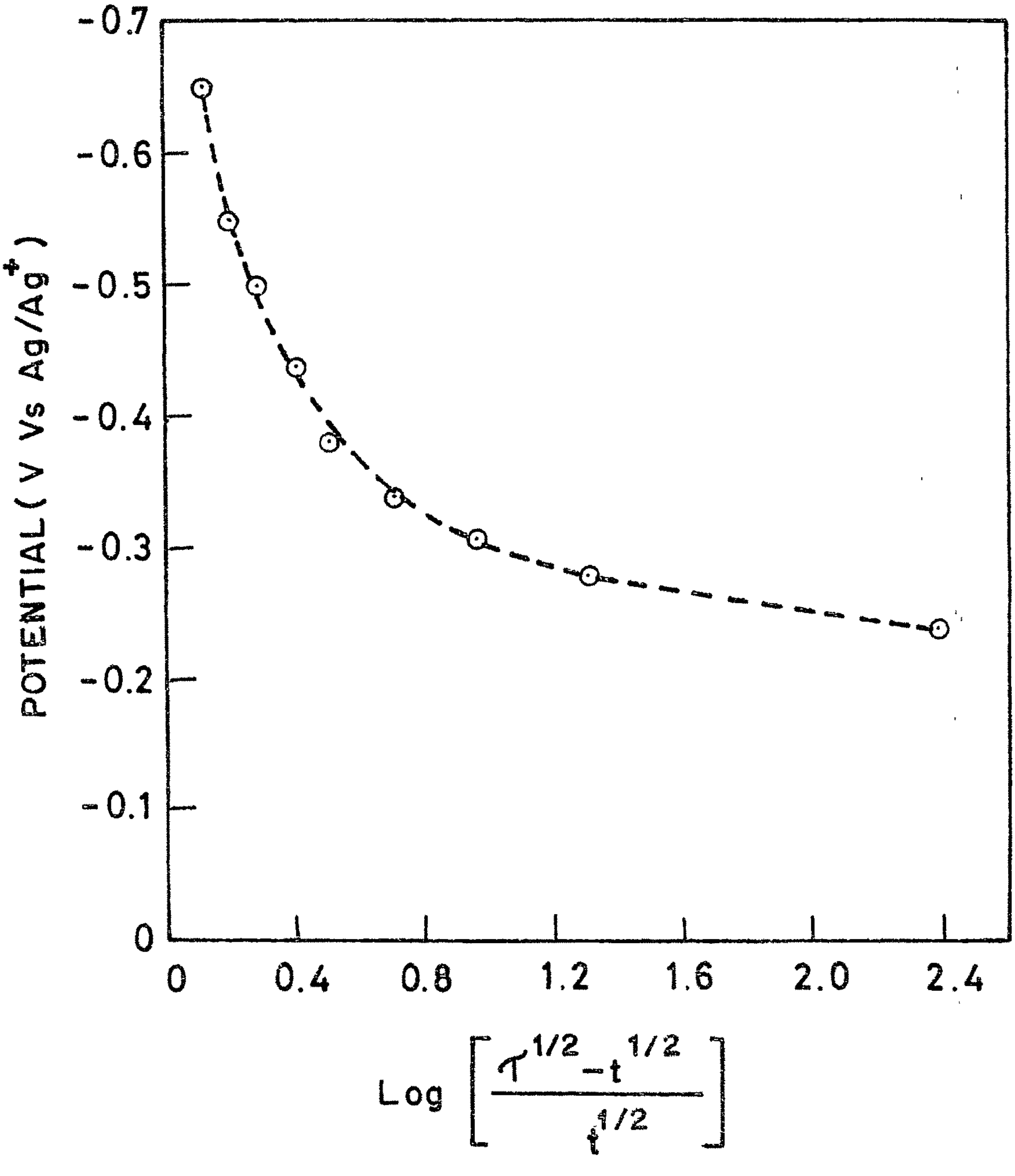

FIG.4.2.2. LOG PLOT FOR FINDING OUT REVERSIBILITY.

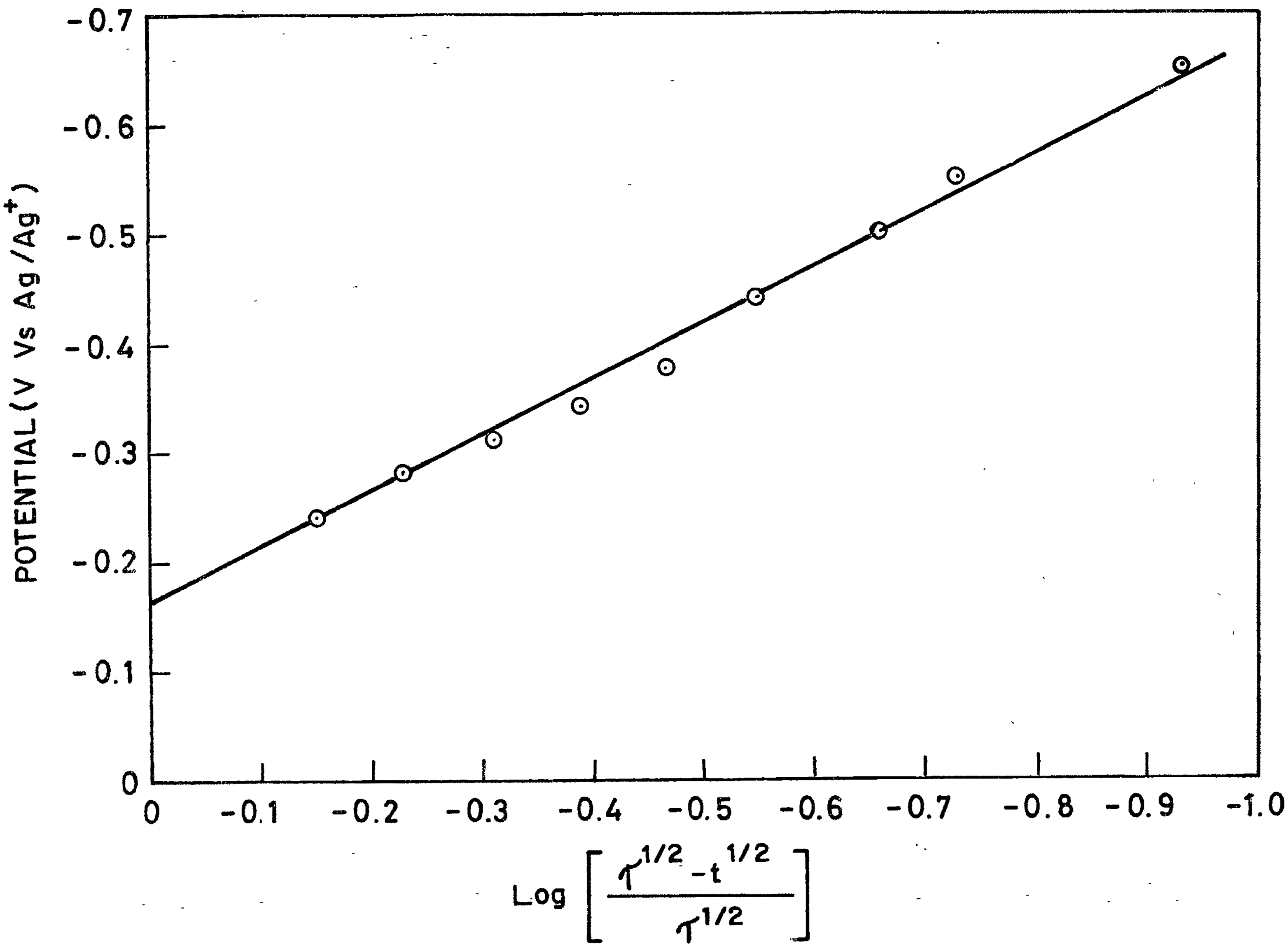

FIG.4:2.3. LOG PLOT FOR FINDING OUT $\alpha_c n_\alpha$ AND $E_t = O$.

was used. In the above equation the intercept will be equal to the first term on the R.H.S. At this juncture the log terms disappear and E can be termed at $E_{t=0}$

$$\text{Thus} \quad E_{t=0} = \frac{R\,T}{\alpha_c\,n_\alpha} \ln \frac{n F C\, k^o_{f,h}}{i^o} \qquad 4.1$$

With the knowledge of $\alpha_c\, n_\alpha$ and the intercept $E_{t=0}$, one can find out $k^o_{f,h}$. The value of $k^o_{f,h}$ has been then calculated.

Table 4.2.3 lists all the pertinent information that can be obtained from the forward and backward chronopotentiograms. All the terms have been explained in the text. In the case of Pb^{++}, attempts to get reliable results from the reverse curve were not successful and so were abandoned.

4.2.2 Cobalt

Chronopotentiograms of Co^{++} ions in nitrate melt were taken as a function of current densities and concentrations. $Co(NO_3)_2$ was taken as the electroactive solute and the area of the working electrode was 0.181 cm^2. The current densities were varied from 4 to 3 mA cm^{-2} or 4000 to 3000 $\mu A\ cm^{-2}$. Both forward and backward chronopotentiograms were obtained as well-difined curves, even though at the start of the electrolysis the change in current was abrupt. The factors $\frac{i\,\tau_f^{1/2}}{C}$ and $\frac{i\,\tau_r^{1/2}}{C}$ were found to be constant within experimental errors indicating that the reaction is diffusion controlled. These

Table 4.2.3

Electrochemical Chronopotentiometric Constants of Pb^{++} Ion in (Li, Na, K) NO_3 Eutectic at 423 ± 2 K

1. $E_{\tau/4,f}$ = -0.340 V vs Ag/Ag^{+}

2. $(D_o)_f$ = 7.47×10^{-6} $cm^2\ s^{-1}$

3. Slope of plot of

   E vs $\log\left[\dfrac{\tau^{1/2} - t^{1/2}}{t^{1/2}}\right]$ plot not linear

4. Slope of plot of

   E vs $\log\left[\dfrac{\tau^{1/2} - t^{1/2}}{\tau^{1/2}}\right]$ = 0.513

5. $\alpha_c n_\alpha$ = 0.64 $E_{t=0}$ = -0.062 V vs NHE

6. $\log k^o_{f,h}$ = -3.344 $k^o_{f,h}$ = 4.53×10^{-4} $cm\ s^{-1}$

quantities varied in magnitude due to the difference in the values of τ_f and τ_r. Actually the average ratio of the factor from experiments of different current densities and concentration was found to be 2.88, a factor very near to 3 indicating a possible reversible reaction. The diffusion coefficients of Co^{++} ion calculated from both the forward and reverse reactions, therefore, would change only nominally, i.e., not in the power function. The reverse diffusion coefficients were found to be smaller than the forward values.

Tables 4.2.4 and 4.2.5 list the above mentioned parameters and Tables 4.2.6 and 4.2.7 the above parameters for forward and backward reactions, respectively. The diffusion coefficients obtained using Sand's equation are also listed in these tables. A typical chronopotentiogram of Co^{++} ions is also drawn in Fig. 4.2.4.

In order to ascertain whether the reaction is reversible or irreversible and the extent of reversibility, a graph of E vs log $\left[1-(\tau/_t)^{\frac{1}{2}}\right]$ was then plotted and this graph is shown in Fig. 4.2.5. The data used for plotting was taken from one curve, the details of which are given in Table 4.2.8. The slope of this line was calculated be 0.017 which would yield an value of n as 5. This would point out to an irreversible reaction and therefore a plot of E vs log $\left[1-(t/\tau)^{\frac{1}{2}}\right]$ was drawn. This plot is shown in Fig. 4.2.6 The plot was found to be linear with the slope equal to 0.188.

Table 4.2.4

Chronopotentiometric Data on Co^{++} Ion in $(Li, Na, K)NO_3$ Eutectic at 423 $\pm$ 2 K (Forward)

Concentration $C \times 10^5$ mole cm^{-3}	Current $i \times 10^6$ A	Transition time τ_f s	$\frac{i \times \tau_f^{1/2}}{C}$ A $s^{1/2}$ mole $^{-1}$ cm^3	Diffusion coefficient $(D_o)_f \times 10^6$ cm^2 s^{-1}
2.94	850	7.44	78.87	6.30
	800	8.40	78.35	3.54
	750	9.36	78.03	3.47
	700	10.56	77.38	3.41
	650	11.52	75.09	3.21
	600	12.00	70.69	2.85
	550	13.44	68.58	2.68
	500	16.32	68.71	2.69
			mean	3.09

Table 4.2.5

Chronopotentiometric Data on Co^{++} Ion in (Li, Na, K) NO_3 Eutectic at 423 $\pm$ K (Forward)

Concentration $C \times 10^5$ mole cm^{-3}	Current $i \times 10^6$ A	Transition time τ_f S	$\frac{i \times \tau_f^{1/2}}{C}$ $A\,s^{1/2}$ $mole^{-1}$ cm^3	Diffusion coefficient $(D_o)_f \times 10^6$ cm^2 s^{-1}
3.91	900	7.68	63.78	4.10
	800	11.52	69.30	4.86
	750	13.52	70.53	5.01
	700	17.76	75.44	5.73
	650	22.56	78.96	6.28
	600	24.96	76.66	5.92
	550	26.88	73.00	5.36
	500	40.88	81.67	6.72
				mean 5.50

Table 4.2.6

Chronopotentiometric Data on Co^{++} Ion in (Li, Na, K)NO_3 Eutectic at 423 $\pm$ 2 K (Reverse)

Concentration $C \times 10^5$ mole cm^3	Current $i \times 10^6$ A	Transition time τ_r s	$\frac{i \times \tau_r^{1/2}}{C}$ A $s^{1/2}$ mole	Diffusion coefficient cm^3 $(D_o)_r \times 10^6$ cm^2 s^{-1}
2.94	850	2.16	42.50	1.03
	800	2.64	44.22	1.11
	750	2.84	41.45	1.05
	650	4.80	48.44	1.34
	600	5.76	49.00	1.37
	550	6.24	46.77	1.25
	500	7.68	47.13	1.27
			mean	1.20

Table 4.2.7

Chronopotentiometric Data on Co^{++} Ion in (Li, Na, K)NO_3 Eutectic at 423 ± 2 K (Reverse)

Concentration $C \times 10^5$ mole cm^3	Current $i \times 10^6$ A	Transition time τ_f s	$\frac{i \times \tau_f^{1/2}}{C}$ $A\, s^{1/2}\, mole^{-1} cm^3$	Diffusion coefficient $(D_{o_r}) \times 10^6$
3.91	900	5.04	51.67	2.69
	800	5.28	47.01	2.23
	750	6.72	49.71	2.49
	650	7.20	44.60	2.00
	600	8.64	45.10	2.05
	550	10.88	46.39	2.17
	500	13.44	46.87	2.21
			mean	2.27

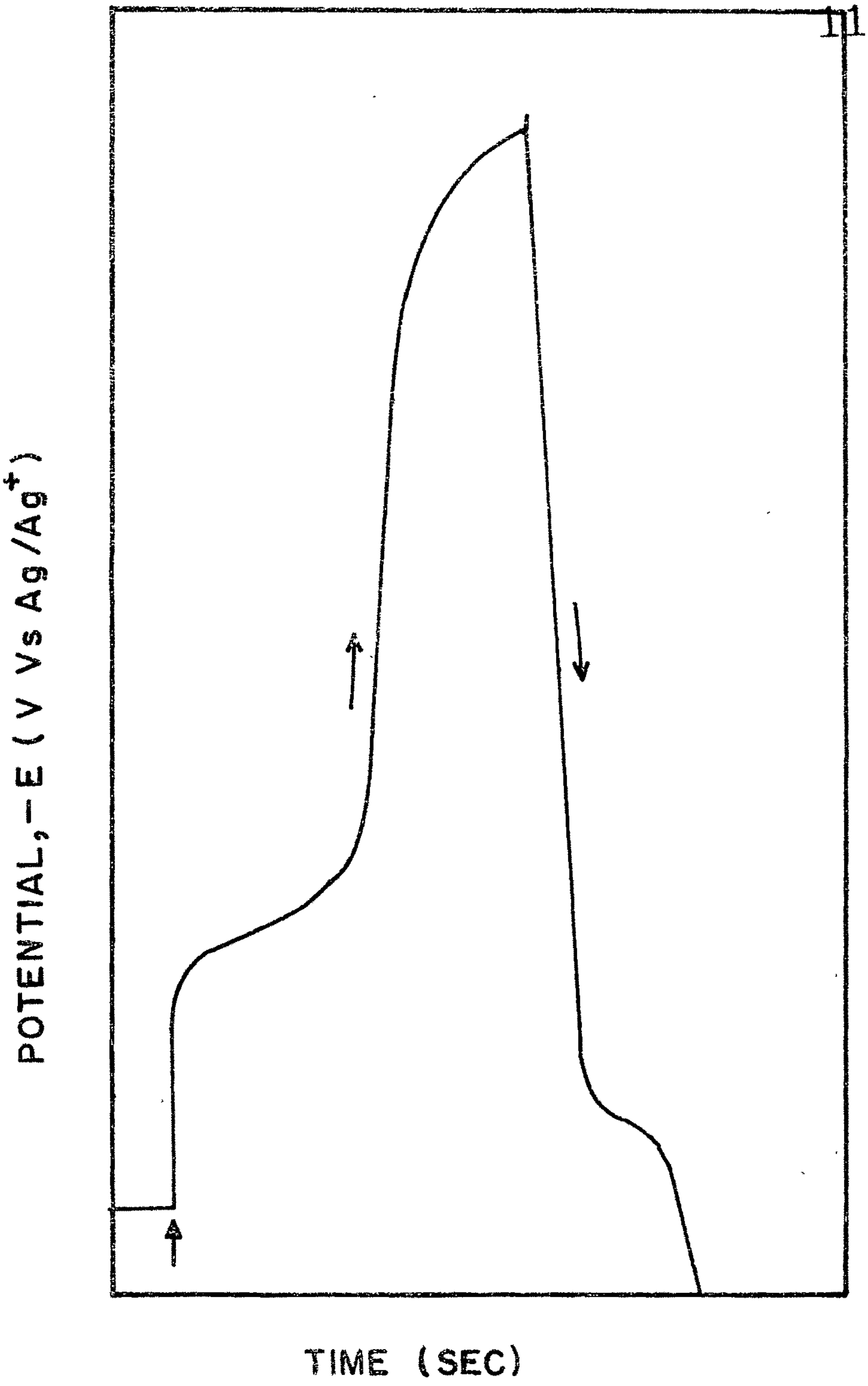

FIG. 4.2.4. A TYPICAL CHRONOPOTENTIOGRAM OF Co^{++} ION IN (Li, Na, K) NO_3 EUTECTIC AT 423 ± 2K.

Table 4.2.8

Chronopotentiometry of Co^{++} Ion in (Li, Na, K) NO_3
Eutectic at 423 ± 2 K

Current density = 2762 $\mu A\ cm^{-2}$

τ = 15.84 s

E V vs Ag/Ag^+	t s	$\log\left[\frac{\tau^{1/2} - t^{1/2}}{t^{1/2}}\right]$	$\log\left[\frac{\tau^{1/2} - t^{1/2}}{\tau^{1/2}}\right]$
-0.450	1.92	+1.872	+0.272
-0.500	3.84	+1.031	+0.013
-0.515	5.76	+0.658	-0.182
-0.540	7.68	+0.436	-0.360
-0.560	9.60	+0.285	-0.546
-0.600	11.52	+0.173	-0.763
-0.650	13.44	+0.087	-1.067
-0.700	15.36	+0.015	-1.810

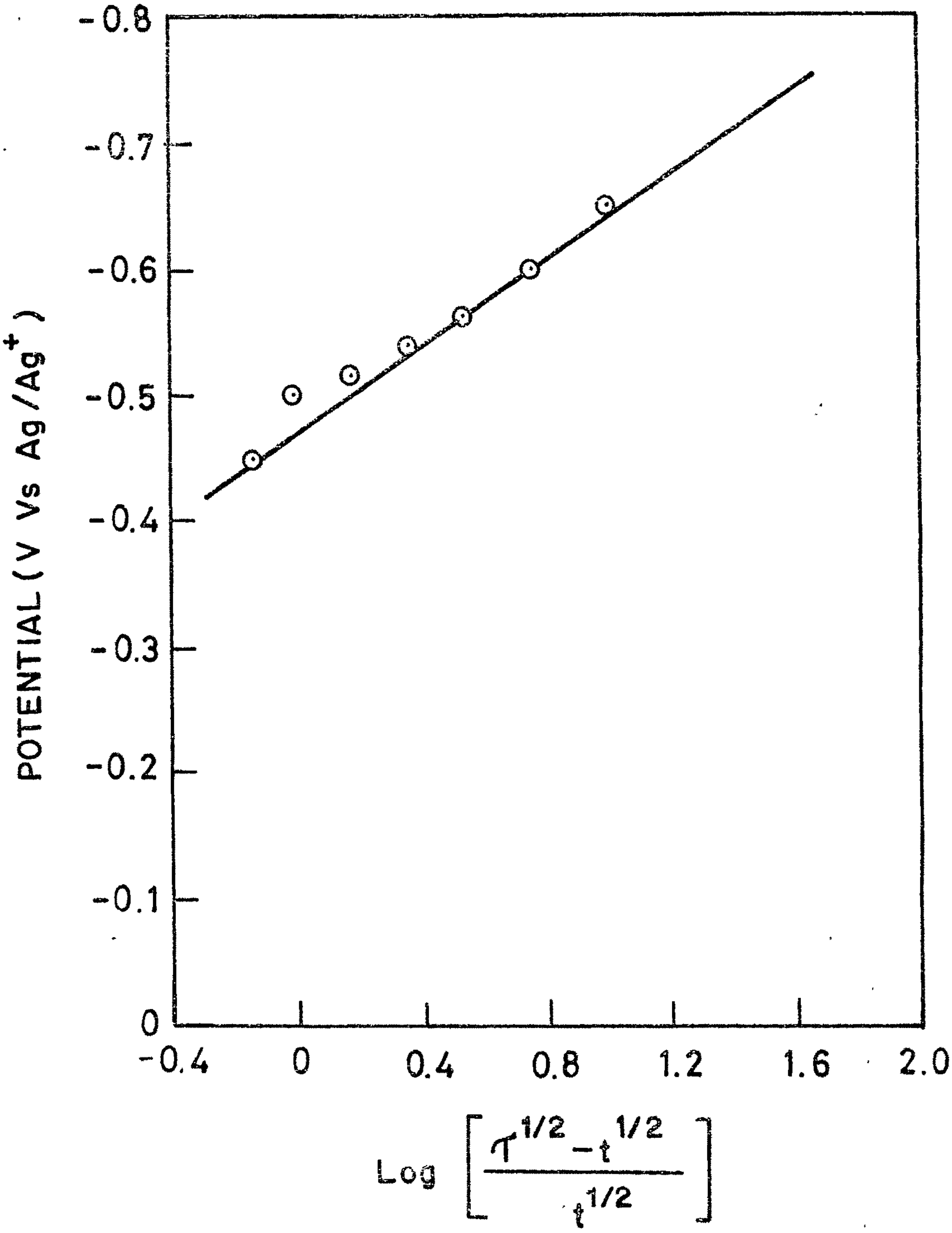

FIG. 4.2.5. LOG PLOT FOR FINDING OUT REVERSIBILITY.

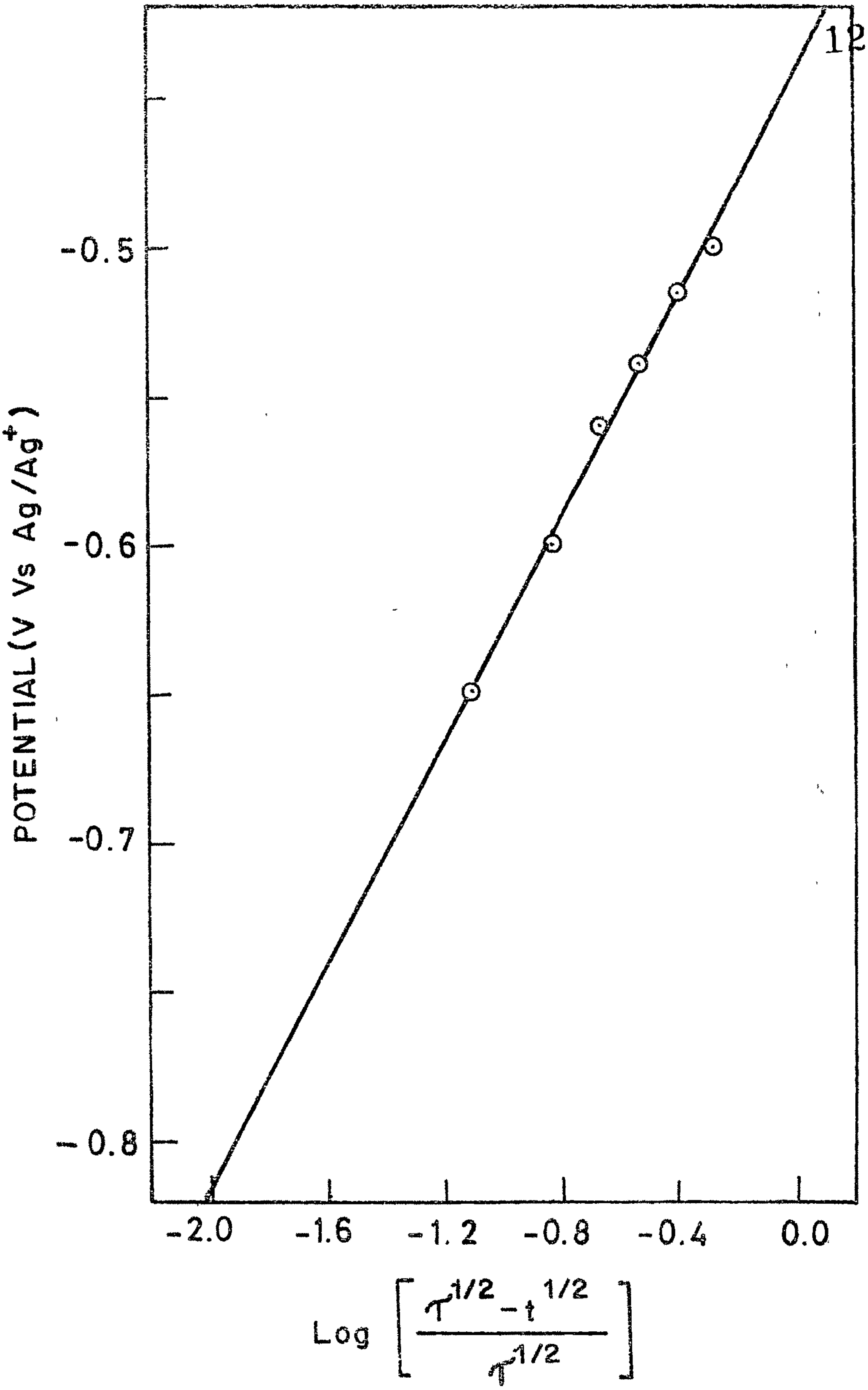

FIG. 4.2.6. LOG PLOT FOR FINDING OUT $\alpha_c n_\alpha$ AND $E_{t=0}$.

As this slope is equal to $\frac{2.303\,R\,T}{\alpha_c\, n_\alpha}$, the transfer coefficient or the kinetic shape parameters $\alpha_c\, n_\alpha$ was calculated to 0.446. This value was reasonably constant at different current densities and had a variation of nearly $\pm$ 0.015. The magnitude of the rate constants will be not reflected in the rate constants due to this small variation.

The values of $E\,\tau/4$ were then obtained for both the forward and reverse reactions. The variation of $E\,\tau/4$ for different current densities was not regular.

The rate constants for electron transfer were then calculated from the intercept of the plot in Fig. 4.2.6.

The available relevant information from this study of the chronopotentiometry of Co^{++} has been summarised in Table 4.2.9.

4.2.3 Nickel

In the case of nickel also, chronopotentiograms in nitrate melt were taken as a function of current densities and concentrations. Nickelous nitrate was taken as the electroactive solute. The current densities were varied from 0.2 to 0.05 mA cm^{-2} or 200 to 67 $\mu A\ cm^{-2}$. The reduction in current densities compared to those used in cobalt is due to the larger area of the working electrode. Both forward and backward chronopotentiograms were obtained as well defined curves. However, it was found that it was not possible to get reverse chronopotentiograms at the same current densities as for which the forward curves were taken. Fig. 4.2.7 gives a

Table 4.2.9

Electrochemical Chronopotentiometric Constants of Co^{++} Ions in (Li, Na, K) NO_3 Eutectic at 423 ± 2 K

1. $E_{\tau/4_f}$ = −0.490 V vs Ag/Ag^+

2. $E_{\tau/4_r}$ = −0.05 V vs Ag/Ag^+

3. Ratio of τ_f/τ_r = 2.88 (mean)

4. $(D_o)_f$ = 4.32×10^{-6} $cm^2\ s^{-1}$

   $(D_o)_r$ = 1.74×10^{-6} $cm^2\ s^{-1}$

5. Slope of

   Plot of $\log\left[\frac{\tau^{\frac{1}{2}} - t^{\frac{1}{2}}}{t^{\frac{1}{2}}}\right]$ vs E = 0.017

6. Slope of

   Plot of $\log\left[\frac{\tau^{\frac{1}{2}} - t^{\frac{1}{2}}}{\tau^{\frac{1}{2}}}\right]$ vs E = 0.188

7. $\alpha_c n_\alpha$ = 0.446 . $E_{t=0}$ = −0.337 V vs NHE

8. Log $k^o_{f,h}$ = −12.00 $k^o_{f,h}$ = 1×10^{-12} $cm\ s^{-1}$

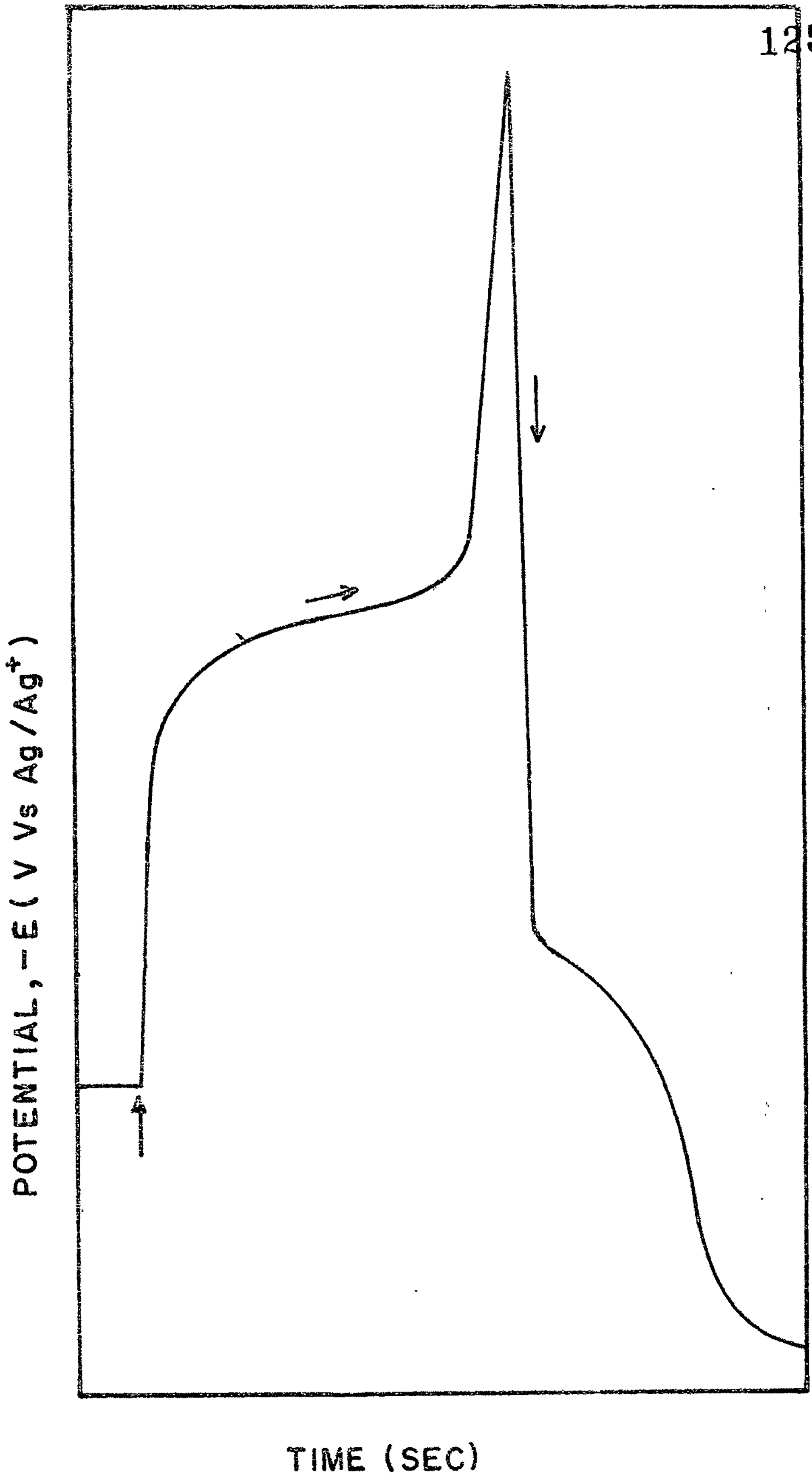

FIG. 4.2.7. A TYPICAL CHRONOPOTENTIOGRAM OF Ni^{++} ION (Li, Na, K)NO_3 EUTECTIC AT 423±2K.

typical chronopotentiogram obtained in the series of experiments. Table 4.2.10 lists the values of the concentration, current strength, the transition time obtained and the factor $\frac{i \times \tau_f^{1/2}}{C}$. Similarly the same factors for the reverse curves are given for in Table 4.2.11. As can be seen from Tables 4.2.10 and 4.2.11 the factor $\frac{i \times \tau^{1/2}}{C}$ remains constant showing that the reactions were diffusion controlled. The factor $\frac{i \times \tau_f^{1/2}}{C}$ was higher in magnitude than $\frac{i \times \tau_r^{1/2}}{C}$ due to the ratio τ_f / τ_r being of the order of 2.48. This factor points out to an irreversible process. The diffusion coefficients were, as usual, calculated using Sand's equation and are listed in Tables 4.2.10 and 4.2.11 for the forward and reverse processes respectively.

In order to accertain the reversibility of the process a graph of E vs log$\left[\frac{\tau^{1/2} - t^{1/2}}{t^{1/2}}\right]$ (Fig. 4.2.8) was then plotted and the relevant data given in Table 4.2.12. The slope of the straight line obtained was 0.075 and the value of n, calculated from this slope works out to be 0.089, a value which does not confirm with the normal value of 2 for Ni^{++} ion. Therefore log $\left[1 - (t/\tau)^{1/2}\right]$ was plotted against E, the potential values, the relevant data for which are given in Table 4.2.12. This graph is depicted in Fig. 4.2.9 and the linear curve yielded a slope of 0.117, from which the value of the transfer coefficient $\alpha_c n_\alpha$ works out to be 0.718. It was confirmed that the variation in this value with different current strengths

Table 4.2.10

Chronopotentiometric Data on Ni^{++} Ion in (Li, Na, K)NO_3 Eutectic at 423 ± 2 K (Forward)

Concentration $C \times 10^6$ mole cm^{-3}	Current $i \times 10^6$ A	Transition time τ_f s	$\frac{i \times \tau_f^{1/2}}{C}$ A $s^{1/2}$ $mole^{-1}$ cm^3	Diffusion coefficient $(D_o)_f \times 10^6$ $cm^2\ s^{-1}$
0.89	400	2.16	65.98	4.54
	350	3.12	69.38	5.02
	300	4.32	69.98	5.07
	250	5.76	67.34	4.73
	200	7.92	63.17	4.15
	150	14.40	63.88	4.20
2.23	500	18.24	66.10	4.56
	450	23.09	66.84	4.66
	400	31.80	69.84	5.09
	350	38.40	67.18	4.71
			mean	4.69

Table 4.2.11

Chronopotentiometric Data on Ni^{++} Ion in Li, Na, K) NO_3 Eutectic at 423 $\pm$ 2 K (Reverse)

Concentration $C \times 10^6$ mole cm^{-3}	Current $i \times 10^6$ A	Transition time τ_r s	$\frac{i \times \tau_r^{1/2}}{C}$ $A\, s^{-1}$ $mole^{-1}$ cm^3	Diffusion coefficient $(D_o)_r \times 10^6$ $cm^2\ s^{-1}$
0.87	300	1.32	38.73	1.56
	250	1.92	38.80	1.58
	200	3.18	40.07	1.67
	150	5.94	41.08	1.76
2.23	500	6.96	40.84	1.74
	450	9.12	42.07	1.84
	400	11.00	41.07	1.76
	350	14.11	40.73	1.72
				mean 1.70

Table 4.2.12

Chronopotentiometry of Ni^{++} Ion in (Li, Na, K) NO_3 Eutectic at 423 $\pm$ 2 K

Current density = 112.10 $\mu A\ cm^2$

τ = 5.76 s

E V vs Ag/Ag^+	t s	$\log\left[\frac{\tau^{\frac{1}{2}} - t^{\frac{1}{2}}}{t^{\frac{1}{2}}}\right]$	$\log\left[\frac{\tau^{\frac{1}{2}} - t^{\frac{1}{2}}}{\tau^{\frac{1}{2}}}\right]$
-0.64	0.96	+0.161	-0.228
-0.66	1.92	-0.136	-0.374
-0.68	2.88	-0.383	-0.533
-0.70	3.84	-0.648	-0.735
-0.72	4.80	-1.020	-1.060

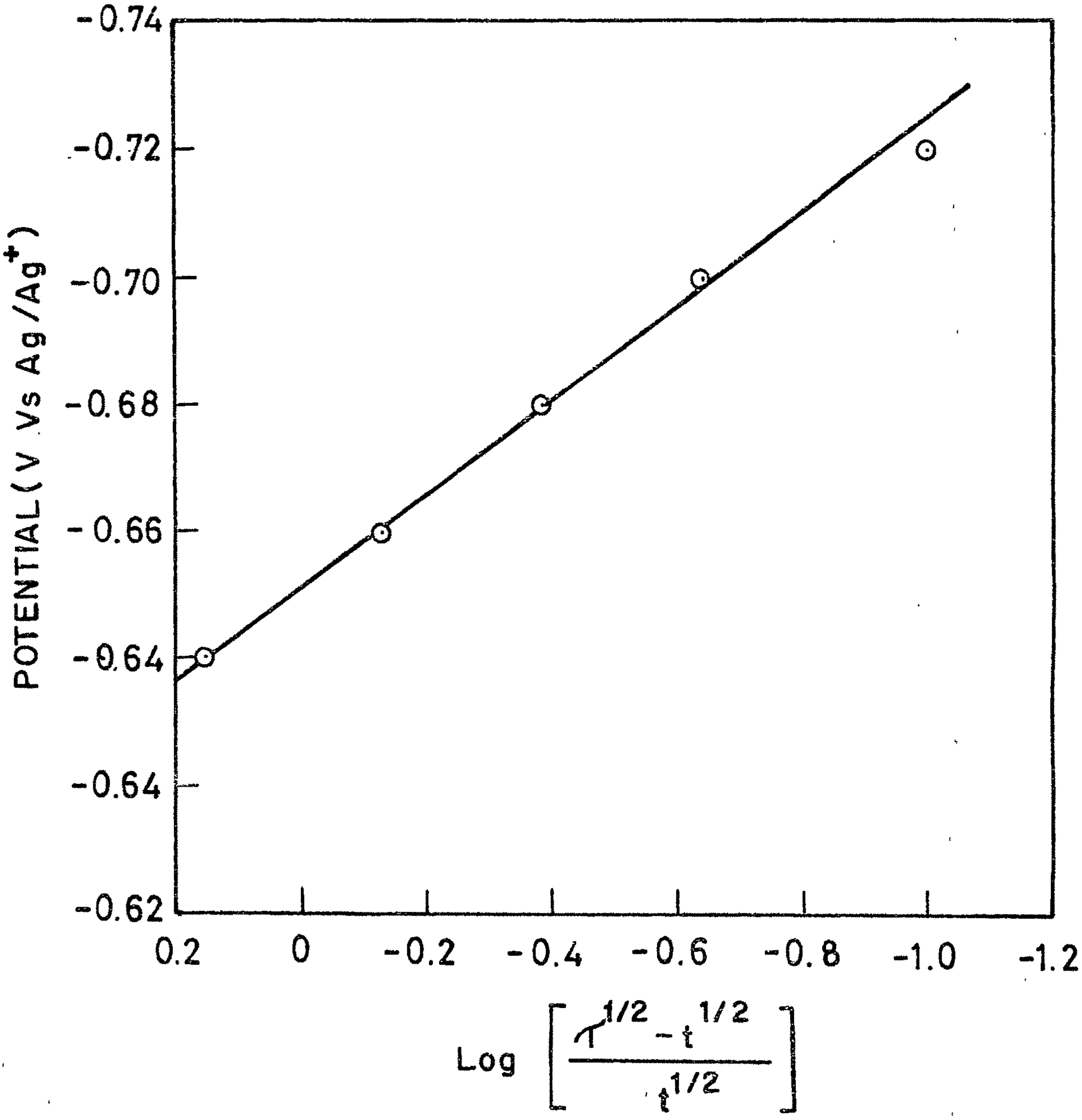

FIG. 4:2.8. LOG PLOT FOR FINDING OUT REVERSIBILITY

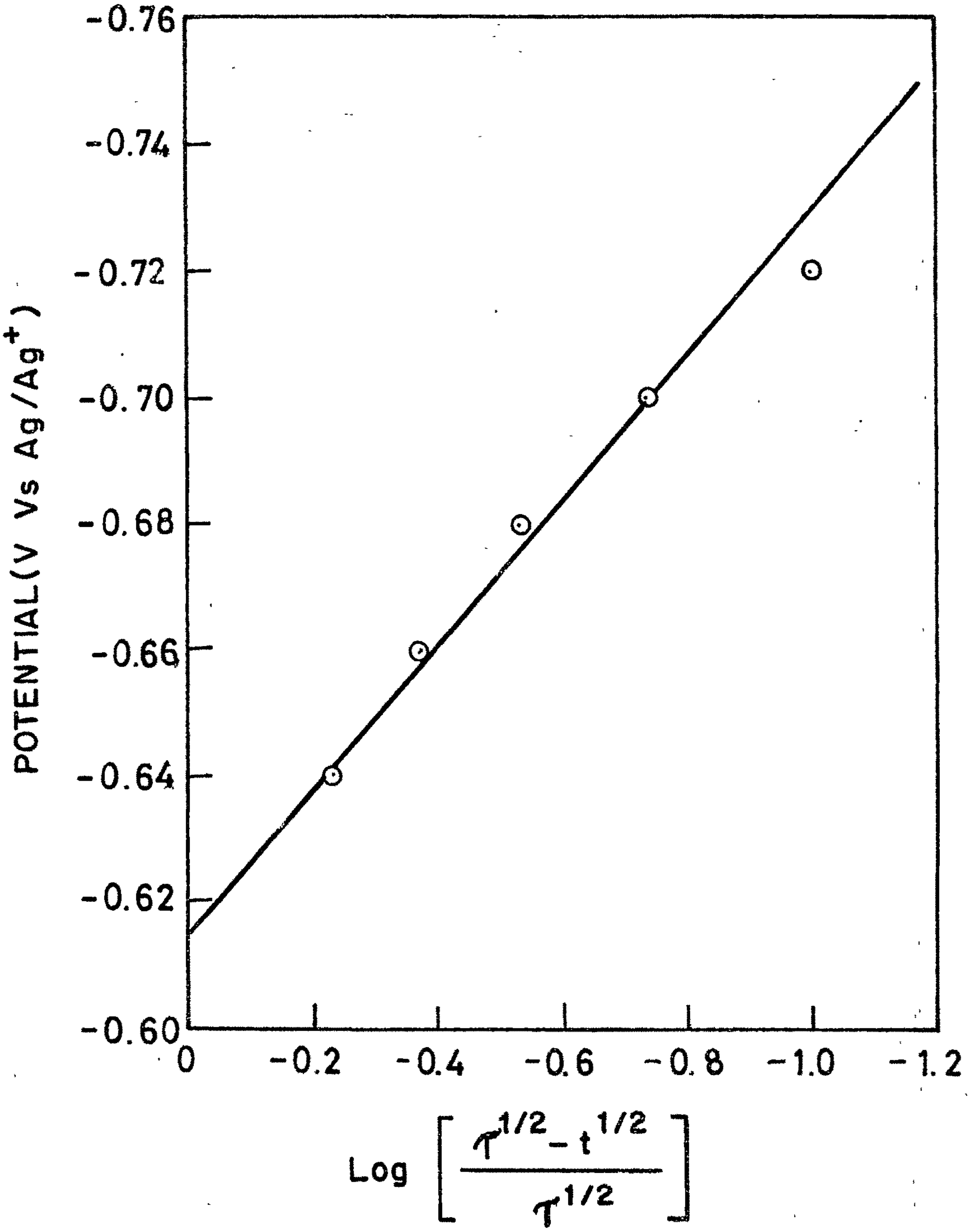

FIG. 4:2.9. LOG PLOT FOR FINDING OUT $\alpha_c n_\alpha$ AND $E_{t=0}$.

did not exceed $\pm$ 5%. The value of the heterogeneous rate constant $k^o_{f,h}$ was then calculated from the intercept of the plot in Fig. 4.2.9.

The relevent data has been summarised in Table 4.2.13.

4.2.4 Irons

In the case of iron, ferric nitrate $Fe(NO_3)_3$ was used as the electroactive solute. Chronopotentiograms, here also, were taken as a function of concentration from 20×10^{6} to 10×10^{-6} mole cm^{-3} and current densities of 4.5 to 2.0 mA cm^{-2} or 4500 to 2000 $\mu A\ cm^{-2}$. The reverse chronopotentiograms were ill shaped at high current densities due to the fact that the transition times were often below one second. Hence, recourse had to be taken to the use of smaller current densities, as under these conditions the transition time will be higher. The mean ratio of τ_f / τ_r was as high as 5.8 approximately and that was the reason for the difficulty of measuring transition times at higher current densities. Fig. 4.2.10 shows a typical forward and reverse chronopotentiogram of the ferric ion in the nitrate melt. Tables 4.2.14 and 4.2.15 list the current strengths used, transition times measured, τ_f and τ_r and $\frac{i \times \tau^{\frac{1}{2}}}{C}$ factors for the forward and reverse reactions. The constancy of the factor $\frac{i \times \tau^{\frac{1}{2}}}{C}$ indicates that the reaction is controlled by diffusion alone. The forward and reverse diffusion coefficients were calculated by Sand's equation and are listed

Table 4.2.13

Electrochemical Chronopotentiometric Constants of Ni^{++} Ion in (Li, Na, K) NO_3 Eutectic at 423 $\pm$ 2 K

1. $E_{\tau/4_f} = -0.650$ vs Ag/Ag^+

2. $E_{\tau/4_r} = +0.275$ V vs Ag/Ag^+

3. Ratio of $\tau_f / \tau_r = 2.48$ (mean)

4. $(D_o)_f = 4.69 \times 10^{-6}\ cm^2\ s^{-1}$

   $(D_o)_r = 1.70 \times 10^{-6}\ cm^2\ s^{-1}$

5. Slope of

   Plot $\log\left[\dfrac{\tau^{\frac{1}{2}} - t^{\frac{1}{2}}}{t^{\frac{1}{2}}}\right]$ vs E = 0.75

6. Slope of

   Plot of $\log\left[\dfrac{\tau^{\frac{1}{2}} - t^{\frac{1}{2}}}{\tau^{\frac{1}{2}}}\right]$ vs E = 0.117

7. $\alpha_c n_\alpha = 0.718$ $E_{t=0} = -0.547$ vs NHE

8. $\log k^o_{f,h} = -8.575$ $k^o_{f,h} = 3.0 \times 10^{-9}$ cm s^{-1}

Table 4.2.14

Chronopotentiometric Data on Fe^{+++} Ion in
(Li, Na, K) NO_3 at 423 $\pm$ 2 K (Forward)

Concentration $C \times 10^6$ mole cm^{-3}	Current $i \times 10^6$ μA	Transition time τ_f s	$\frac{i \times \tau_f^{1/2}}{C}$ A $s^{1/2}$ $mole^{-1}$ cm^3	Diffusion coefficient $(D_o)_f \times 10^6$ cm^2 s^{-1}
20.5	900	3.88	86.48	7.78
	850	4.08	83.78	7.34
	800	5.28	89.68	8.35
	700	8.88	101.80	10.76
	650	12.00	109.83	12.25
	600	14.40	111.07	12.82
	550	17.28	111.50	12.96
	500	19.20	106.88	11.96
				mean 10.53
15.3	650	4.05	105.21	
	600	6.42	107.62	
	500	12.44	115.34	

Table 4.2.15

Chronopotentiometric Data on Fe^{+++} Ion in $(Li, Na, K)NO_3$ at 423 ± 2 K (Reverse)

Concentration $C \times 10^6$ mole cm^{-3}	Current $i \times 10^6$ μA	Transition time τ_f s	$\frac{i \times \tau_f^{1/2}}{C}$ A $s^{1/2}$ $mole^{-1}$ cm^3	Diffusion coefficient $(D_o) \times 10^6$ cm^2 s^{-1}
20.5	700	1.68	44.25	2.04
	650	2.00	44.83	2.10
	600	2.40	45.34	2.25
	550	2.88	45.53	2.25
	500	3.36	44.71	2.08
			mean	2.14
15.3	650	1.18	46.21	
	600	1.31	44.90	
	500	1.91	45.16	
	400	2.72	43.12	

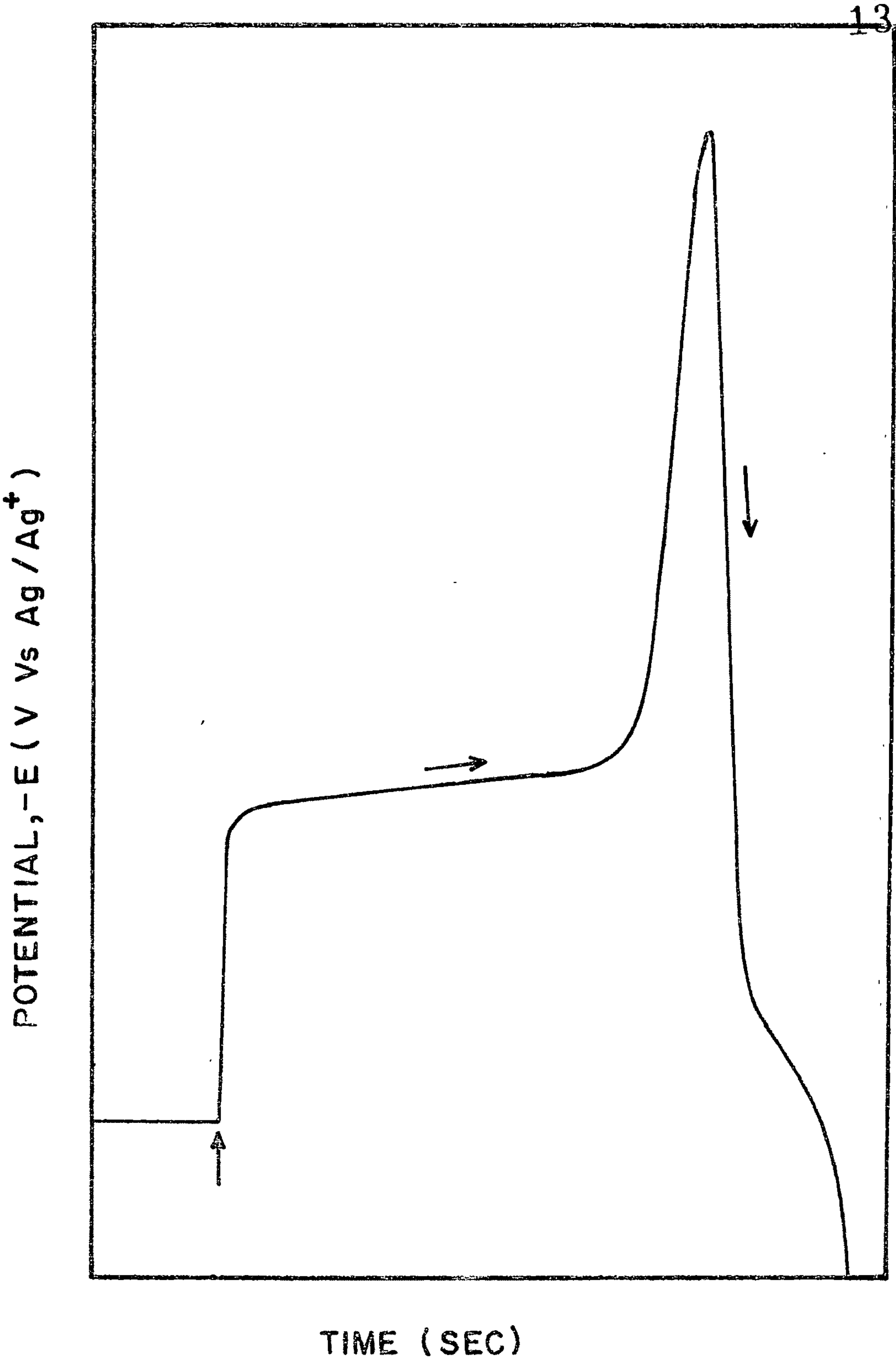

FIG. 4.2.10. A TYPICAL CHRONOPOTENTIOGRAM OF Fe^{+++} ION IN (Li, Na, K) NO_3 AT 423 ± 2K.

in Table 4.2.14. The $E_{\tau/4}$ values were found to vary within a slight margin with concentrations and current densities. The rise in the potential was sharp indicating the irreversible nature of the reaction.

Table 4.2.16 lists the values of the potentials E together with t, $\log\left[\frac{\tau^{1/2} - t^{1/2}}{t^{1/2}}\right]$ and $\log\left[\frac{\tau^{1/2} - t^{1/2}}{\tau^{1/2}}\right]$. The plot of E vs $\log\left[\frac{\tau^{1/2} - t^{1/2}}{t^{1/2}}\right]$ did not show any linear relationship, confirming irreversible nature of the electrode process. This plot is given in Fig. 4.2.11. Fig. 4.2.12 gives the plot of E vs $\log\left[\frac{\tau^{1/2} - t^{1/2}}{\tau^{1/2}}\right]$ and this straight line yielded a slope of 0.683, which is equal to $\frac{2.303\,RT}{\alpha_c n_\alpha}$. Thus the value of $\alpha_c n_\alpha$ works out to be 0.123. The intercept of this graph yielded the first term of the right hand side of the equation 2.8 from which the $k^o_{f,h}$ values were obtained. The relevant values, put in as a summary, are given in Table 4.2.17.

4.2.5 Copper

Chronopotentiograms of Cu^{++} were taken with Copper Nitrate $Cu(NO_3)_2$ as the electroactive solute. The concentrations were varied from 7 to 5×10^{-5} mole cm^{-3} and the current densities from 2.5 to 4.5 mA cm^{-2}. Both forward and reverse chronopotentiograms could be obtained. The cupric ion yielded a double wave at all concentrations in the both forward and reverse direction. The transition times obtained from these curves were nearly equal in magnitude, both in the forward and reverse direction. Tables 4.2.18 and 4.2.19 lists the current

Table 4.2.16

Chronopotentiometry of Fe^{+++} Ion in (Li, Na, K) NO_3 Eutectic at 423 $\pm$ 2 K.

Current density = 3867 $\mu A\ cm^2$

τ = 7.68 s

E V vs Ag/Ag^+	t S	$\log\left[\frac{\tau^{1/2} - t^{1/2}}{t^{1/2}}\right]$	$\log\left[\frac{\tau^{1/2} - t^{1/2}}{\tau^{1/2}}\right]$
-0.350	0.96	0.262	-0.190
-0.400	1.92	0.000	-0.301
-0.435	2.88	-0.199	-0.411
-0.450	3.84	-0.383	-0.533
-0.475	4.80	-0.577	-0.680
-0.500	5.76	-0.811	-0.873
-0.525	6.72	-1.161	-1.187
-0.565	7.44	-1.769	-1.796

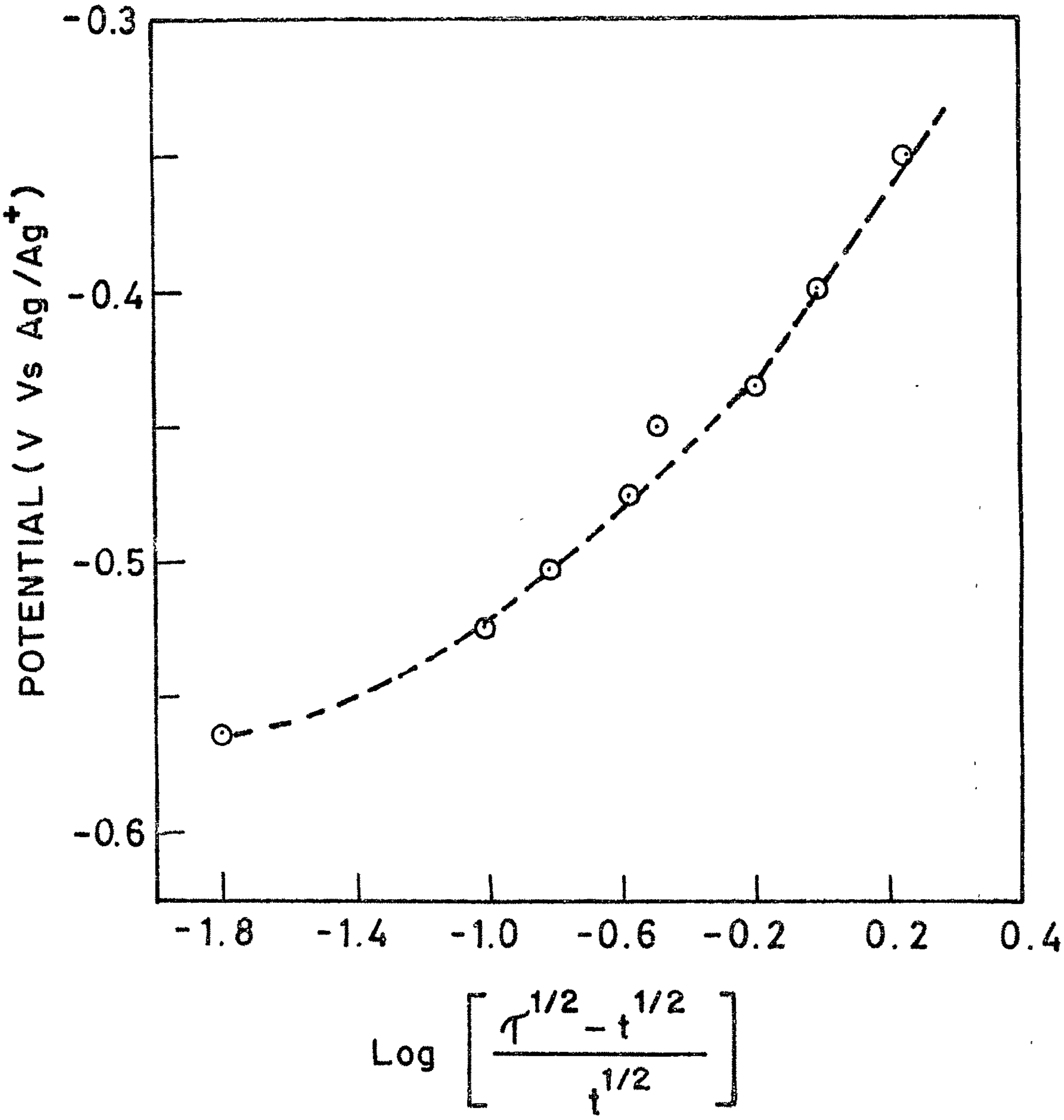

FIG. 4.2.11. LOG PLOT FOR FINDING OUT REVESIBILITY.

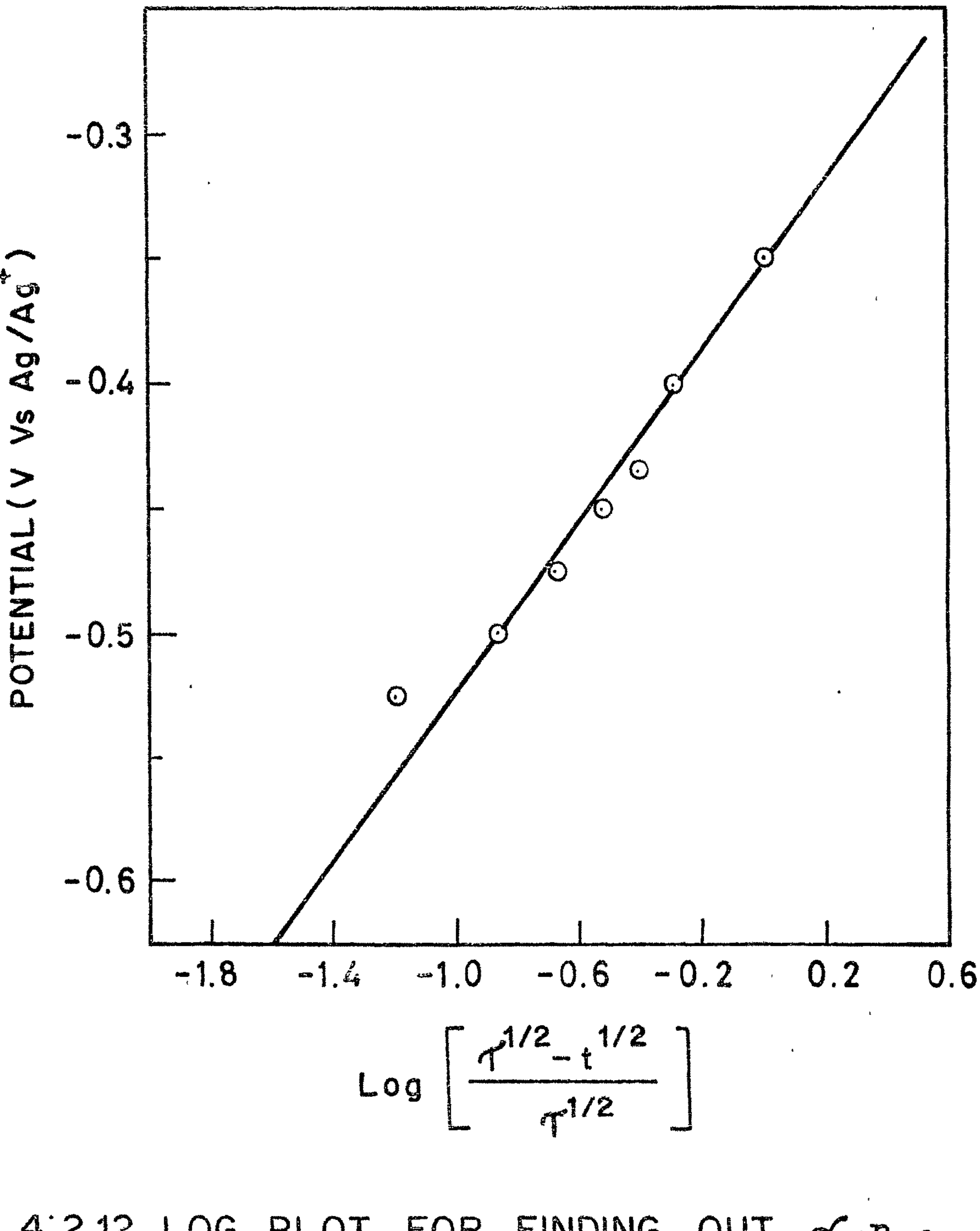

FIG. 4.2.12. LOG PLOT FOR FINDING OUT $\alpha_c n_\alpha$ AND $E_t = 0$

Table 4.2.17

Electrochemical chronopotentiometric constants of Fe^{+++} Ions in (Li, Na, K) NO_3 at 423 $\pm$ 2 K.

1. $E_{\tau/4_f}$ = −0.425 V vs Ag/Ag^+

2. $E_{\tau/4_r}$ = +0.400 V vs Ag/Ag^+

3. Ratio of τ_f/τ_r = 5.8

4. $(D_o)_f$ = 10.53×10^{-6} cm^2 s^{-1}

   $(D_o)_r$ = 2.14×10^{6} cm^2 s^{-1}

5. Slope of plot of $\log \left[\dfrac{\tau^{1/2} - t^{1/2}}{t^{1/2}} \right]$ vs E = Not linear

6. Slope of plot of $\log \left[\dfrac{\tau^{1/2} - t^{1/2}}{\tau^{1/2}} \right]$ vs E = 0.683

7. $\alpha_c n_\alpha$ = 0.123 $E_{t=0}$ = −0.247 V vs NHE

8. $\log k^o_{f,h}$ = −3.07 $k^o_{f,h}$ = 8.50×10^{-4}

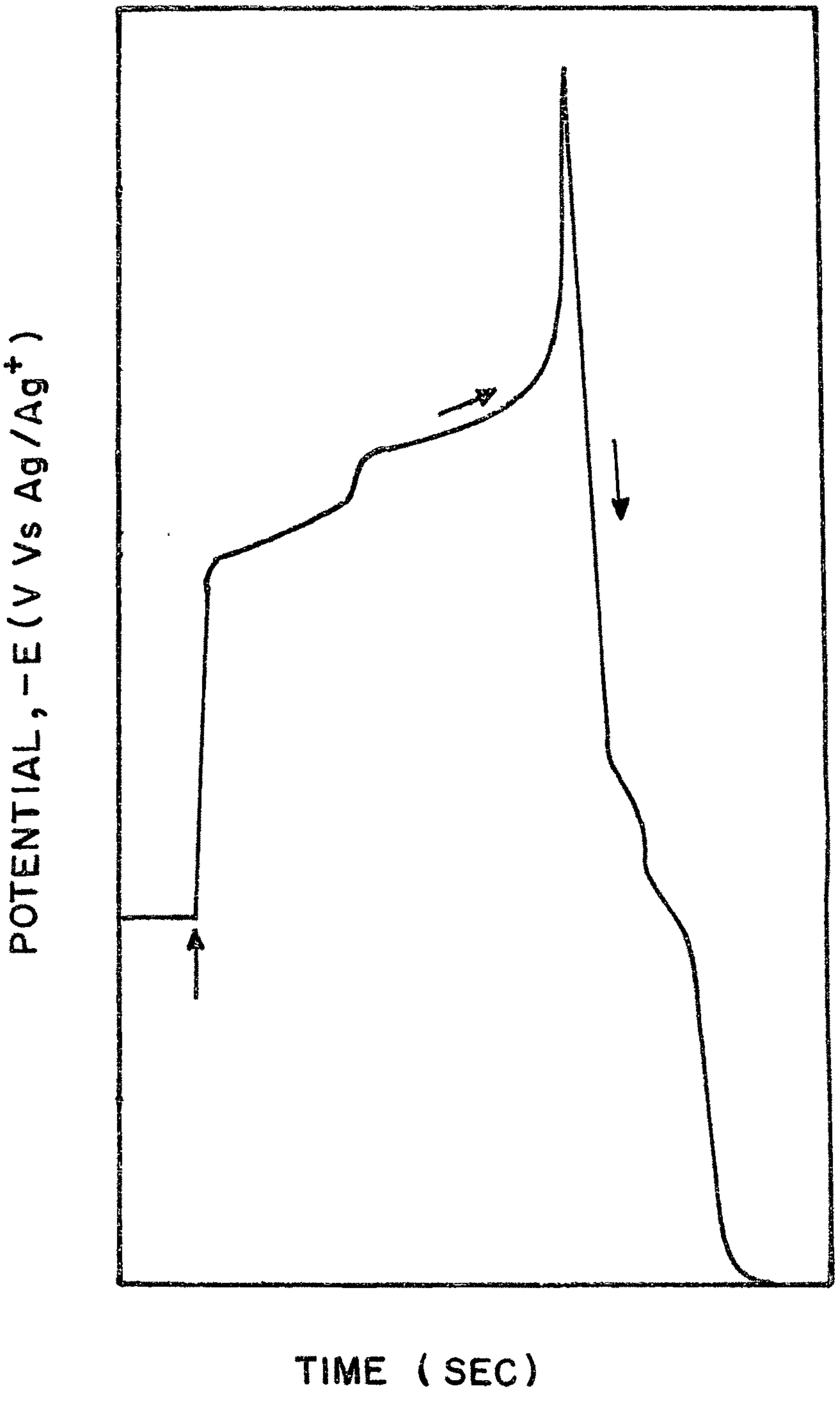

FIG. 4.2.13. A TYPICAL CHRONOPOTENTIOGRAM OF Cu^{++} ION IN (Li, Na, K) NO_3 EUTECTIC AT 423 ± 2K.

strengths, transition times and the factor $\frac{i \times \tau_f^{\frac{1}{2}}}{C}$ and from these Tables it can be seen that $\frac{i \times \tau_{f_1}^{\frac{1}{2}}}{C}$ is $\frac{i \times \tau_{f_2}^{\frac{1}{2}}}{C}$ in both typical concentrations cited. The mean factors τ_{f_1}/τ_{r_1} and τ_{f_2}/τ_{r_2} works out to be 3.1 and 2.9 respectively. Because of this factor difference $\frac{i \times \tau_f^{\frac{1}{2}}}{C}$ was greater in magnitude in comparison with $\frac{i \times \tau_r^{\frac{1}{2}}}{C}$.

The relevant data for the reverse chronopotentiograms is listed in Tables 4.2.20 and 4.2.21. The diffusion coefficients for the waves one and two calculated from Sand's equation are also listed in the relevant Tables and it has been found that the mean diffusion coefficient $(D_o)_f \simeq 2 \times (D_o)_r$.

In order to ascertain the reversibility of the redox reaction the potential E were plotted against $\log\left[\frac{\tau^{\frac{1}{2}} - t^{\frac{1}{2}}}{t^{\frac{1}{2}}}\right]$ and even though this plot was linear it did not yield value of 0.042 for $n = 1$ reduction. The presence of two waves for Cu^{++} indicates strongly that the reduction takes place from cupric to cuprous. The magnitude of the transition times confirms this factor. Even then, it cannot be positively said that the reduction is due to the simple transformation from cupric to cuprous. Fig. 4.2.14 shows the relationship between E and $\log\left[\frac{\tau^{\frac{1}{2}} - t^{\frac{1}{2}}}{t^{\frac{1}{2}}}\right]$ and the relevant details are given in Table 4.2.22. Next a plot of E vs $\log\left[\frac{\tau^{\frac{1}{2}} - t^{\frac{1}{2}}}{\tau^{\frac{1}{2}}}\right]$ was made (Fig. 4.2.15). The data is given in Table 4.2.22. The slope of this line worked out to be 0.207 which gives a value of $\alpha_c n_\alpha = 0.406$. The variation

Table 4.2.18

Chronopotentiometric Data on Cu^{++} Ion in (Li, Na, K) NO_3 Eutectic at 423 ± K (Forward)

Concentration = 7.89 x cm^{-5} mole cm^{-3}

First Wave

Current $i \times 10^6$ A	Transition time τ_{f_1} s	$\frac{i \times \tau_{f_1}^{1/2}}{C}$ A $s^{1/2}$ $mole^{-1}$ cm^3	Diffusion coefficient $(D_o)_{f_1} \times 10^6$ cm^2 s^{-1}
800	10.16	32.31	4.36
750	12.72	33.91	4.80
700	13.44	32.53	4.42
600	16.80	31.18	4.06
		mean	4.41

Second Wave

Current $i \times 10^6$ A	Transition time τ_{f_2} s	$\frac{i \times \tau_{f_2}^{1/2}}{C}$ A $s^{1/2}$ $mole^{-1}$ cm^3	Diffusion coefficient $(D_o)_{f_2}$ cm^2 s^{-1}
800	10.38	33.43	4.64
750	13.20	34.53	4.98
700	14.38	33.64	4.75
600	19.20	33.32	5.44
			4.95

Table 4.2.19

Chronopotentiometric Data on Cu^{++} Ion in (Li, Na, K) NO_3 Eutectic at 423 ± 2 K (Forward)

Concentration = 5.61×10^{-5} mole cm^{-3}

First Wave

Current $i \times 10^6$ A	Transition time τ_{f_1} s	$\frac{i \times \tau_{f_1}^{1/2}}{C}$ A $s^{1/2}$ $mole^{-1}$ cm^3	Diffusion coefficient $(D_o)_{f_1} \times 10^6$ cm^2 s^{-1}
900	4.36	33.50	1.92
850	5.04	34.02	2.20
750	7.64	36.95	2.40
650	9.88	36.42	2.35
		mean	2.22

Second Wave

Current $i \times 10^6$ A	Transition time τ_{f_2} s	$\frac{i \times \tau_{f_2}^{1/2}}{C}$ A $s^{1/2}$ $mole^{-1}$ cm^3	Diffusion coefficient $(D_o)_{f_2} \times 10^6$ cm^2 s^{-1}
900	3.36	29.41	3.60
850	5.52	33.59	5.29
750	6.24	33.38	4.60
650	10.32	37.21	4.78
		mean	4.82

Table 4.2.20

Chronopotentiometric Data on Cu^{++} Ion in (Li, Na, K) NO_3 Eutectic at 423 ± 2 K (Reverse)

Concentration 5.61×10^{-5} mole cm^{-3}

Frist Wave

Current $i \times 10^6$ A	Transition time τ_{r_1} S^-	$\frac{i \times \tau_{r_1}^{1/2}}{C}$ $A\,s^{-1}$ $mole^{-1}$ cm^3	Diffusion coefficient $(D_o)_{r_1} \times 10^6$ $cm^2\ s^{-1}$
850	1.30	17.27	1.25
700	1.92	17.29	1.25
650	2.40	17.94	1.35
600	2.60	17.25	1.25
		mean	1.28

Second Wave

Current $i \times 10^6$ A	Transition time τ_{r_2} S	$\frac{i \times \tau_{r_2}^{1/2}}{C}$ $A\,s^{-1}$ $mole^{-1}$ cm^3	Diffusion coefficient $(D_o)_{r_2} \times 10^6$ $cm^2\ s^{-1}$
850	1.90	20.88	1.82
700	3.36	22.87	2.19
650	3.60	21.97	2.02
600	4.32	22.22	2.06
		mean	2.03

Table 4.2.21

Chronopotentiometric Data on Cu^{++} Ion in (La, Na, K) NO_3 Eutectic at 423 $\pm$ 2 K (reverse)

Concentration 7.89×10^{-5} mole cm^{-3}

First Wave

Current $i \times 10^6$ A	Transition time τ_{r_1} s	$\frac{i \times \tau_{r_1}^{1/2}}{C}$ A $s^{-1/2}$ $mole^{-1}$ cm^3	Diffusion coefficient $(D_o)_{r_1} \times 10^6$ cm^2 s^{-1}
800	2.64	16.45	1.13
750	4.00	17.01	1.51
700	4.51	18.82	1.45
600	5.01	17.00	1.21
500	6.00	15.52	1.01
		mean	1.26

Second Wave

Current $i \times 10^6$ A	Transition time τ_{r_2} s	$\frac{i \times \tau_{r_2}^{1/2}}{C}$ A $s^{-1/2}$ $mole^{-1}$ cm^3	Diffusion coefficient $(D_o)_{r_2} \times 10^6$ cm^2 s^{-1}
800	3.52	19.02	1.51
750	4.22	19.52	1.59
700	5.40	20.61	1.78
600	8.02	21.53	1.94
500	10.23	20.26	1.72
		mean	1.71

Table 4.2.22

Chronopotentiometry of Cu^{++} Ion in (Li, Na, K) NO_3 Eutectic at 423 ± 2 K

Current density = 3867 μA cm^2

τ = 11.28 s

E V vs Ag/Ag^+	t s	$\log\left[\frac{\tau^{\frac{1}{2}} - t^{\frac{1}{2}}}{t^{\frac{1}{2}}}\right]$	$\log\left[\frac{\tau^{\frac{1}{2}} - t^{\frac{1}{2}}}{\tau^{\frac{1}{2}}}\right]$
-0.653	1.46	+0.180	-0.194
-0.693	2.87	-0.979	-0.308
-0.718	4.31	-0.616	-0.419
-0.728	5.76	-0.399	-0.545
-0.768	7.19	-0.252	-0.697
-0.803	8.62	-0.143	-0.903
-0.853	10.06	-0.058	-1.260

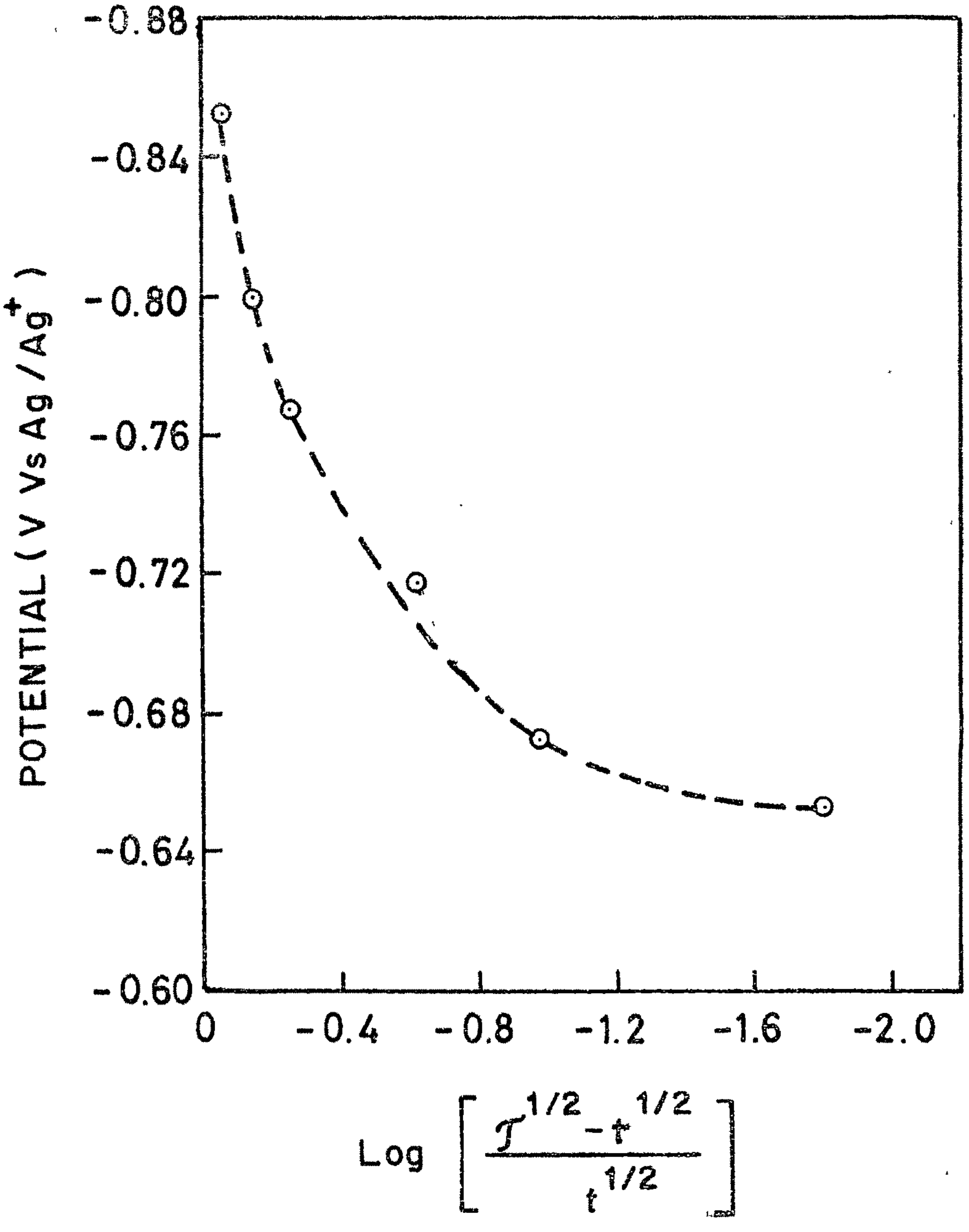

FIG. 4:2.14. LOG PLOT FOR FINDING OUT REVERSIBILITY.

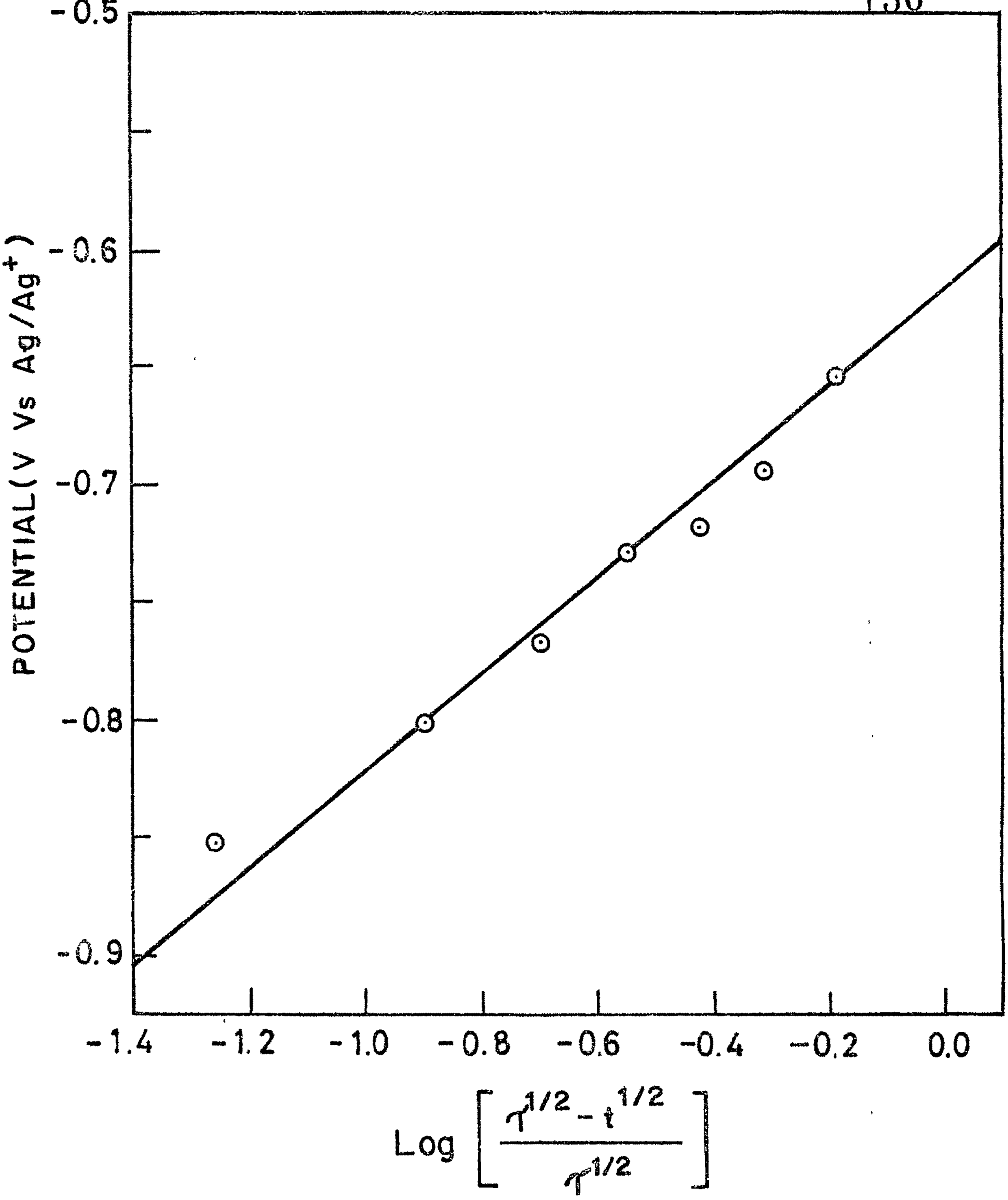

FIG. 4.2.15. LOG PLOT FOR FINDING OUT $\alpha_c n_\alpha$ AND $E_{t=0}$.

Table 4.2.23

Electrochemical Chronopotentiometric Constants of Cu^{++} Ions in (Li, Na, K) NO_3 Eutectic at 423 $\pm$ 2 K

1. $E_{\tau/4\,f}$ = -0.703 V vs Ag/Ag^{+}

2. Ratio of τ_{f_1}/τ_{r_1} = 3.31 τ_{f_2}/τ_{r_2} = 2.9

3. Diffusion coefficient $(D_o)_f$ = 1^{st} wave = 3.32×10^{-6} $cm^2\,s^{-1}$
   2^{nd} wave = 4.89×10^{-6} " "

   Diffusion coefficient $(D_o)_r$ = 1^{st} wave = 1.27×10^{-6} " "
   2^{nd} wave = 1.87×10^{-6} " "

4. Slope of plot of $\log\left[\frac{\tau^{1/2} - t^{1/2}}{t^{1/2}}\right]$ vs E = 0.131

5. Slope of plot of $\log\left[\frac{\tau^{1/2} - t^{1/2}}{\tau^{1/2}}\right]$ vs E = 0.207

6. $\alpha_c n_\alpha$ = 0.406 , $E_{t=0}$ = -0.512 vs NHE

7 $\log k^o_{f,h}$ - 5.71 $k^o_{f,h}$ = 1.95×10^{-6} cm s^{-1}

in this quantity with different current densities was found to be minimal and $k^{o}_{f,h}$ values calculated using the equation 2.8 was found to be 1.95×10^{-6}. All the relevant data which could be obtained from the chronopotentiometric waves are listed in Table 4.2.23.

4.3 CYCLIC VOLTAMMETRY

In the next few pages are given the data of cyclic voltammetric experiments conducted on Pb^{++}, Co^{++}, Ni^{++}, Fe^{+++} and Cu^{++} ions in the (Li, Na, K) NO_3 melt at 423 K. The details of calculation are given only for lead, as the calculations are only repetitions for the other elements. The parameters, which have been changed, are the concentration of the solute and the scan rate.

4.3.1 Lead

Experiments on the cyclic voltammetry of Pb^{++} ions were conducted as described in the earlier chapter. The solute used was $Pb(NO_3)_2$ which was dried and dehydrated before weighing. The mechanism of dehydration and so the complete absence of moisture was explained in the earlier chapter. The weight of solvent taken was kept constant through the series of experiments as the solvent was not disturbed and the solute was added to the same solvent to increase the concentration. The volume of the solvent was calculated using equation 3.1. The same solution could seldom be used for cyclic voltammetry as the ones used in chronopotentiometry. This was deliberately followed because of the fear of coatings on the working electrode due to adsorption.

Fig. 4.3.1 gives a typical voltammogram of Pb^{++} ions (concentration 2.88 mM) in the nitrate melt. The first run yielded a wave the shape and magnitude of which changed on the second run. The runs were repeated until successive runs yielded reproducible waves. Reproducibility of the waves resulted from the conditioning of the working electrode and was finally lost, presumably, due to adsorption of oxides on the electrode. The peaks started shifting to more negative values.

The concentrations were varied from 2 - 10 mM. However, only certain values, representative of the experiments, are quoted here. These typical values for 3 concentrations, viz., 2.88, 5.54 and 8.02 mM are given in Table 4.3.1. The various scan rates used for various concentrations, the peak potential E_p^c vs Ag/Ag^+ and the half - peak potential, $E_{p/2}^c$, at which the current is half of the peak current I_p^c, are given in this Table. It can be seen from this Table that E_p^c values not independent of the scan rates, but show a trend towards higher negative values with increase in scan rates. Though marginal E_p^c shows some variation with concentration, also.

The curves obtained were marked by the conspicuous absence of an anodic peak. As explained earlier the most marked

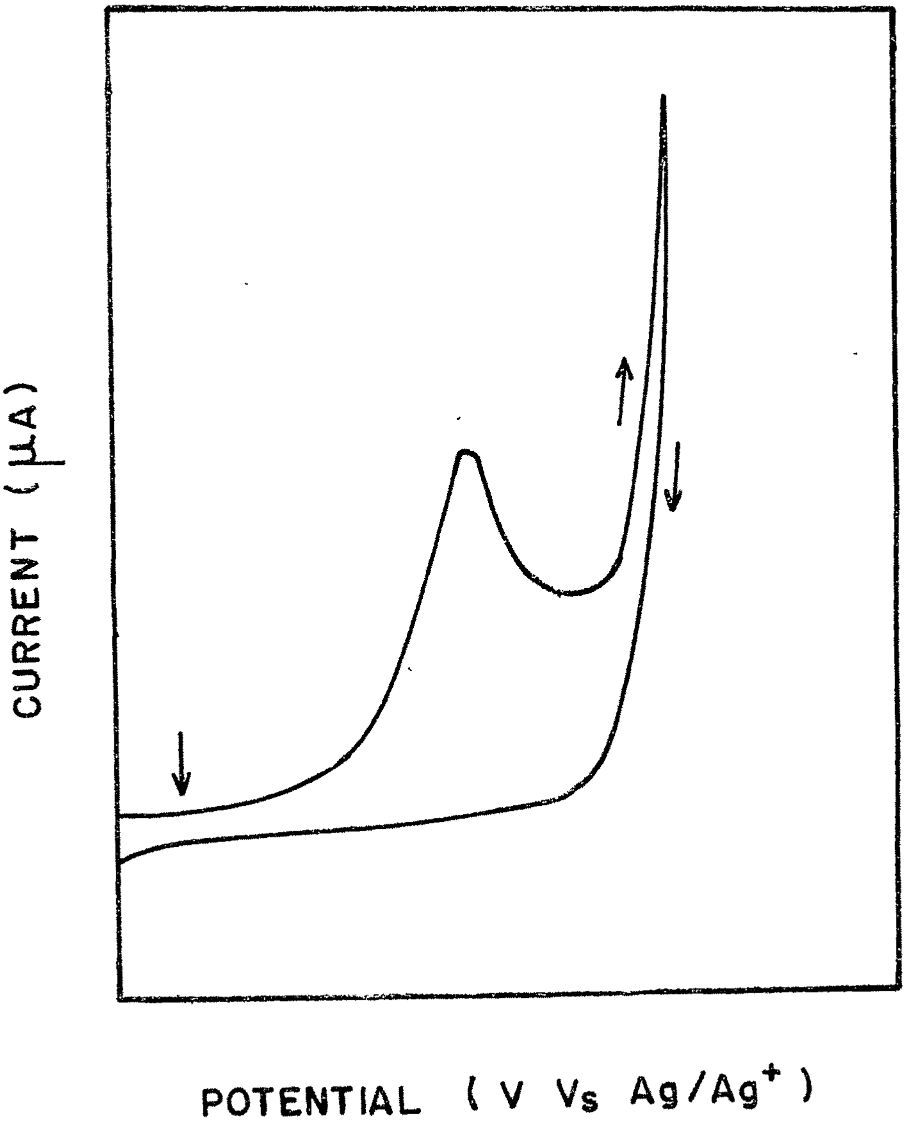

FIG. 4.3.1. A TYPICAL CYCLIC VOLTAMMOGRAM OF Pb^{++} ION IN (Li, Na, K)NO_3 EUTECTIC AT 423±2K.

Table 4.3.1

Cyclic Voltammetric Data on Pb^{++} Ion in (Li, Na, K) NO_3 Eutectic at 423 ± 2 K

Concentration C mM	Voltage sweep rate ν mV s^{-1}	E_p^c V vs Ag/Ag^+	$E_{p/2}^c$ V vs Ag/Ag^+
2.88	40	−0.623	−0.485
	50	−0.626	−0.474
5.54	30	−0.581	−0.470
	40	−0.581	−0.471
	50	−0.609	−0.468
8.02	20	−0.509	−0.427
	30	−0.515	−0.416
	40	−0.552	−0.442
	50	−0.663	−0.527

Table 4.3.2

Cyclic Voltammetry of Pb^{++} Ion in (Li, Na, K) NO_3 at 423 ± 2 K. Relationship between Cathodic Peak Current and Voltage Sweep Rate

Concentration C mM	i_p^c µA	Voltage sweep rate γ mV s^{-1}	$i_p^c/\gamma^{\frac{1}{2}}$ µA mV$^{-\frac{1}{2}}$ s$^{\frac{1}{2}}$	$i_p^c/C \times \gamma^{\frac{1}{2}}$ µA mM^{-1} mV$^{-\frac{1}{2}}$ s$^{\frac{1}{2}}$
2.88	65.4	40	10.34	3.59
	69.4	50	9.82	3.41
5.54	106.2	30	19.39	3.50
	112.3	40	17.76	3.20
	122.6	50	17.34	3.13
8.02	120.5	20	26.95	3.36
	153.2	30	27.97	3.49
	157.3	40	24.87	3.10
	181.8	50	25.71	3.21

feature of a cyclic voltammogram of a totally irreversible system is the absence of a reverse peak. Such a feature on its own does not necessarily imply an irreversible electron transfer process, but could be due to a fast following chemical reaction. The test of the magnitude of the irreversibility of the reaction is to verify the linearity of the plot of I_p^c vs $\nu^{\frac{1}{2}}$ and also to see whether the straight line passes through the origin. Alternatively the function $\frac{I_p^c}{C\,\nu^{\frac{1}{2}}}$ should be a constant within a reasonable limit of concentrations and scan rates. Table 4.3.2 lists the values of the peak current i_p^c, $i_p^c/\nu^{\frac{1}{2}}$ and $i_p^c/C\,\nu^{\frac{1}{2}}$ where C is the concentration in millimoles. It can be seen from this Table that the values of $i_p^c/C\,\nu^{\frac{1}{2}}$ are reasonably constant in the concentration range studied.

The variation of E_p^c with scan rates can be quantified by the equation

$$E_p^c = K - \frac{2.303\ RT}{2\alpha_c n_\alpha F} \log \nu \qquad 2.32$$

A fuller discussion of the calculation $\alpha_c n_\alpha$, the transfer coefficient, will be given in the chapter on Discussion, but it can be shown that the shift in E_p^c at 298 K with scan rate will be equal to $\frac{30}{\alpha_c n_\alpha}$ for each decade change in . In effect it becomes more negative as ν is increased. The shape factor $\left| E_p^c - E_{p/2}^c \right|$ for an irreversible case is given by

$$\left| E_p^c - E_{p/2}^c \right| = \frac{48.0}{\alpha_c n_\alpha} \text{ mV at } 298\,K \qquad 2.34$$

In all the above equations corrections for the temperature becomes necessary as the experimental temperature was 423 K. Thus the above equation 2.34 will be converted into the form

$$\left| E_p^c - E_{p/2}^c \right| = \frac{68.1}{\alpha_c n_\alpha} \text{ mV at } 423\,K \qquad 4.2$$

The above equation permits the calculation of the transfer coefficient required for the calculation of the diffusion coefficient D_o and the electron transfer rate constant $k_{s,h}$. In the present case the scan rates have been varied only from 20 - 50 mV s^{-1} and hence the shift in E_p^c, which changes by $\frac{42.58}{\alpha_c n_\alpha}$ mV/decade change in ν, could not be calculated directly. However equation 4.2 has been used to calculate the transfer coefficients. These values together with the factor $\left| E_p^c - E_{p/2}^c \right|$ are listed in Table 4.3.3. The variation of the transfer coefficient values was found to be within limits with a mean value of 0.431.

The shape of the voltammogram does not satisfy the conditions of reversible nature of the electrode reaction.

Thus the peak current density can be equated as per Randles - Sevcik equation[72,73] in the following manner,

$$I_p^c = (2.99 \times 10^5) n \, (\alpha_c n_\alpha)^{\frac{1}{2}} C_o^\infty D_o^{\frac{1}{2}} \nu^{\frac{1}{2}} \qquad 2.31$$

Table 4.3.3

Cyclic Voltammetric Data on Pb^{++} Ions in (Li, Na, K) NO_3 Eutectic at 423 $\pm$ 2 K. Calculated Values of Transfer Coefficient $\alpha_c n_\alpha$ and Diffusion Coefficient D_o

$\left\lvert E_p^c - E_{p/2}^c \right\rvert$ V	Transfer coefficient $\alpha_c n_\alpha$	Diffusion coefficient $D_o \times 10^6$ cm^2 s^{-1}
0.138	0.494	2.59
0.152	0.448	2.64
0.140	0.487	2.61
0.110	0.619	1.64
0.141	0.483	2.06
0.082	0.831	1.35
0.099	0.688	1.83
0.110	0.619	1.61
0.136	0.501	2.18
	mean	mean
	0.431	2.06

at 298 K. As the Randles - Sevcik constant is inversely proportional to temperature, the equation takes the shape

$$I_p^c = (2.53 \times 10^5) n \ (\alpha_c n_\alpha)^{\frac{1}{2}} C_O^{\infty} D_O^{\frac{1}{2}} \nu^{\frac{1}{2}} \qquad 4.3$$

where I_p^c is the current density in A cm^{-2}, n is the number of electrons involved in the reaction, C_O^{∞} the bulk concentration in moles cm^{-3}, ν is the voltage sweep rate in V s^{-1}, and D_O the diffusion coefficient in cm^2 s^{-1}. Thus in the above equation all values except D_O are known. The area of the electrode was taken as 0.181 cm^2. The values of D_O so calculated are also listed in Table 4.3.3.

The extent of irreversibility or reversibility can be determined from the calculation of the standard rate constants $k_{s,h}$ from the data already obtained. As discussed earlier the empirical constant K in equation 2.32 can be calculated[76] with the knowledge of ν and $\alpha_c n_\alpha$. The values of K so calculated are listed in Table 4.3.4. K can now be equated to

$$K = E_e^o - \frac{RT}{\alpha_c n_\alpha F}\left[0.78 - \frac{2.303}{2}\log\left(\frac{\alpha_c n_\alpha F D_o}{k_{s,h}^2 RT}\right)\right] \qquad 2.33$$

This equation enables one to calculate $k_{s,h}$, once K, $\alpha_c n_\alpha$, D_o and E_e^o are known. Here D_o is the diffusion coefficient in cm^2 s^{-1}. The significance of the values of $k_{s,h}$ so calculated from the mean value of K is discussed in the next chapter.

Table 4.3.4

The Values of K, the Empirical Constant of Pb^{++} Ions in (Li, Na, K) NO_3 Eutectic at 423 ± 2 K

$$E_p^c = K - \frac{2.303\ RT}{2\alpha_c n_\alpha F} \log \nu$$

E_p^c corrected to NHE V	Voltage sweep rate ν Vs^{-1}	K
-0.520	0.04	-0.640
-0.523	0.05	-0.646
-0.478	0.03	-0.611
-0.478	0.04	-0.551
-0.506	0.05	-0.621
-0.406	0.02	-0.493
-0.412	0.03	-0.506
-0.449	0.04	-0.545
-0.560	0.05	-0.670
	mean	-0.587

Yet another equation[142] which can be used for calculating $k^{o}_{f,h}$, the forward electron transfer rate constant and therefrom $k_{s,h}$ the standard electron transfer rate constant is given by

$$E_p^c = -1.14 \frac{RT}{\alpha_c n_\alpha F} + \frac{RT}{\alpha_c n_\alpha F} \ln\left(\frac{k^{o}_{f,h}}{D_o^{1/2}}\right) - \frac{RT}{2_c n F} \ln \alpha_c n_\alpha \nu \qquad \ldots\ldots\ldots \quad 4.4$$

and $$k_{s,h} = k^{o}_{f,h} \exp.\left[\frac{-\alpha_c n_\alpha F E_e^{o}}{RT}\right] \qquad 4.5$$

From the first of the above equations $k^{o}_{f,h}$ can be calculated with the knowledge of E_p, $\alpha_c n_\alpha$, D_o and ν. The values of $k^{o}_{f,h}$ and log $k^{o}_{f,h}$ so calculated are listed in Table 4.3.5.

For the determination of $k_{s,h}$ from $k^{o}_{f,h}$ additional information of E_e^{o} is required. This is true for the solution of equation for K in the first instance, too. E_e^{o} is the formal redox potential of the reaction taking place. As it is difficult to determine this quantity directly, the same has been approximated to $E_{\tau/4}$, which is the potential at ¼ of the transition time τ in chronopotentiometry. The justification for the same has been given in Chapter 2 of the thesis and the $E_{\tau/4}$ values are mentioned in Table 4.2.3. The value of $k_{s,h}$ so calculated is discussed in the next chapter.

Table 4.3.5

The Values of Forward Electron Transfer Rate Constant $K^{o}_{f,h}$ of Pb^{++} Ion in (Li,Na, K) NO_3 Eutectic at 423 ± 2 K

$$E_p^c = 1.14 \frac{RT}{\alpha_c n_\alpha F} + \frac{RT}{\alpha_c n_\alpha F} \ln \left(\frac{k^o_{f,h}}{D_o^{\frac{1}{2}}} \right) - \frac{RT}{2\alpha_c n_\alpha F} \ln \alpha_c n_\alpha \gamma$$

E_p^c corrected to NHE V	$\log k^o_{f,h}$	$k^o_{f,h}$ x 10^7 cm s^{-1}
-0.520	-6.03	9.07
-0.523	-5.89	12.95
-0.478	-7.31	0.49
-0.478	-6.42	3.76
-0.506	-6.04	9.04
-0.406	-7.31	0.49
-0.412	-6.56	2.76
-0.449	-6.23	5.99
-0.560	-6.45	3.56
		mean 5.35

The foregoing calculations have been based on the value of n, the number of electrons involved being taken as 2 and may not give a true picture of the actual reaction taking place, i.e., whether electrode position of the metal is taking place or the reduction of the nitrate complex. A full discussion of the ambiguity of these reactions as well as the significance of the values of $\alpha_c n_\alpha$, D_o, $k^o_{f,h}$ and $k_{s,h}$ are given in the chapter on discussion of the results.

4.3.2 Cobalt

Experiments on the cyclic voltammetry of Co^{++} ions were conducted in a manner similar to Pb^{++} ions. $Co(NO_3)_2$ was dehydrated before use as described earlier.

Fig. 4.3.2 gives a typical voltammogram of Co^{++} ion in the nitrate melt. Here also the curves were run until successive runs gave reproducible curves. The concentrations were varied only in a limited range due to the low solubility of $Co(NO_3)_2$ in the eutectic. It was found that above 0.5 mM the kinetics of the solubility process was increased and hence higher concentrations did not yield reproducible results.

Table 4.3.6 lists the values of the peak potentials E_p^c and half peak potentials $E_{p/2}^c$ as a function of the scan rate and concentration. E_p^c values were not independent of scan rate and showed slight deviations with concentrations. These factors together with the absence of a reverse peak and

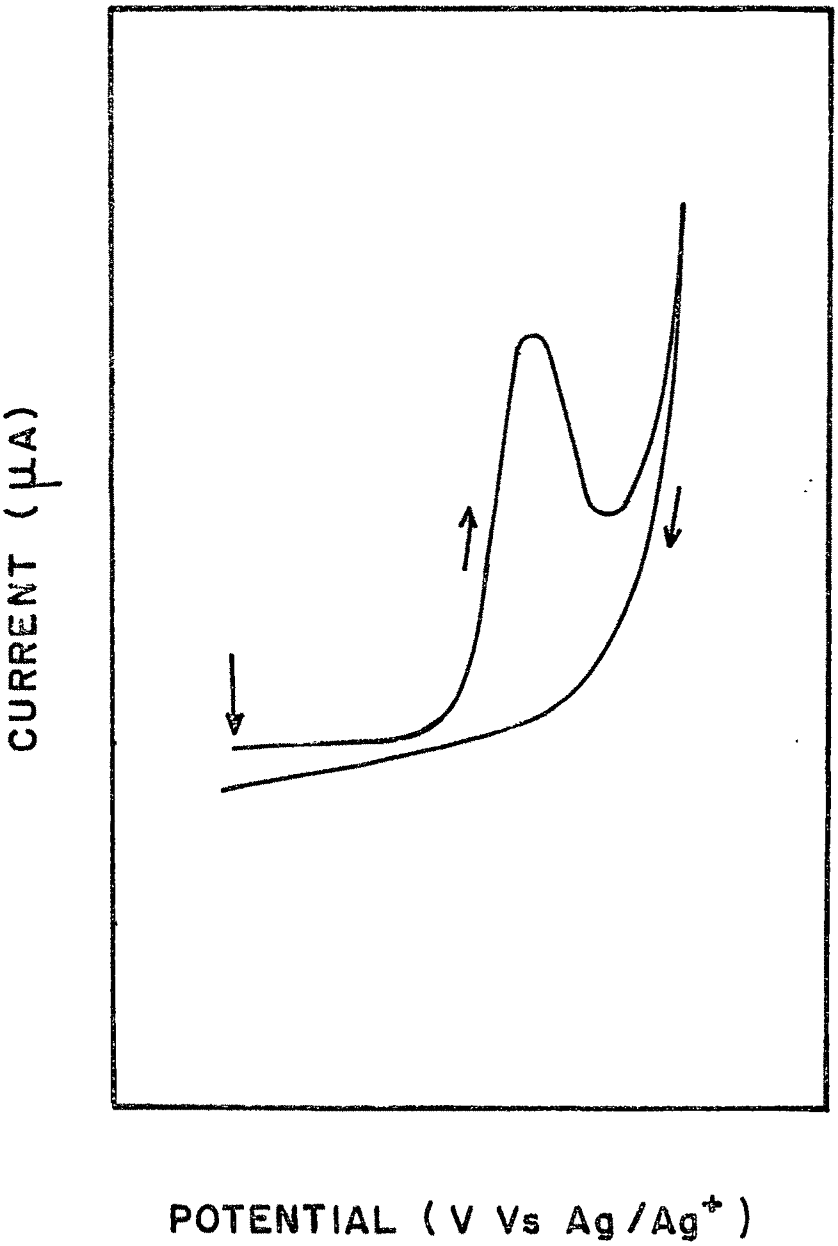

FIG. 4.3.2. A TYPICAL CYCLIC VOLTAMMOGRAM OF Co^{++} ION IN $(Li,Na,K)NO_3$ EUTECTIC AT 423 ± 2K.

Table 4.3.6

Cyclic Voltammetric Data on Co^{++} in (Li, Na, K) NO_3 Eutectic at 423 $\pm$ 2 K

Concentration C mM	Voltage sweep rate ν mV s^{-1}	E_p^c V vs Ag/Ag^+	$E_{p/2}^c$ V vs Ag/Ag^+
0.138	20	-0.471	-0.402
	30	-0.489	-0.414
	40	-0.499	-0.425
	50	-0.512	-0.437
0.430	20	-0.471	-0.402
	30	-0.489	-0.414
	40	-0.487	-0.425
	50	-0.506	-0.442

the shape of the curve indicated an irreversible process for the redox reaction of Co^{++}. Table 4.3.7 gives the peak current i_p^c again as a function of voltage sweep rates and concentration. It was found that i_p^c increased with $\gamma^{\frac{1}{2}}$ but was not proportional to it. The shape factor $\left| E_p^c - E_{p/2}^c \right|$ was utilised for calculating $\alpha_c n_\alpha$ which yielded a mean value of 0.972, an unusually large value. The significance of this value is discussed in Chapter 5. The diffusion coefficient of Co^{++} in the nitrate melt was obtained from Randle - Sevcik equation to be 4.43×10^{-6} cm^2 s^{-1}. The values of $\alpha_c n_\alpha$ and D_o are quoted in Table 4.3.8. The values of the empirical constant K are given in Table 4.3.9 as a function of voltage sweep rates. These values were obtained using equation 2.32. The values of K were utilised for calculating $k_{s,h}$ which are given in Chapter V. Using equation the values of $k^o_{f,h}$ and log $k^o_{f,h}$ have been calculated and are given in Table 4.3.10.

4.3.3 Nickel

Fig. 4.3.3 gives a typical voltammogram of Ni^{++} ions in the nitrate melt (concentration 0.176 mM) and as can be seen from this figure the anodic peak is conspicuously absent. Table 4.3.11 lists the peak potentials E_p^c and the half - peak potentials $E_{p/2}^c$ as a function of scan rates and concentration which was varied upto 0.236 mM only. The variation in E_p^c with concentration scan rate was minimal. Peak currents i_p^c showed a near linear relationship with C $\gamma^{\frac{1}{2}}$, thus confirming the

Table 4.3.7

Cyclic Voltammetric Data on Co^{++} Ion in (Li, Na, K) NO_3 Eutectic at 423 $\pm$ 2 K. Relationship between Cathodic Peak Current and Voltage Sweep Rate

Concentration C mM	Voltage sweep rate γ mV s^{-1}	i_p^c µA	$i_p^c/\gamma^{1/2}$ µA $mV^{-1/2}$ $s^{1/2}$	$i_p^c/C\gamma^{1/2}$ µA mM^{-1} $mV^{-1/2}$ $s^{1/2}$
0.138	50	7.07	1.99	0.14
	40	6.33	1.86	0.14
	30	5.48	1.64	0.12
	20	4.47	1.37	0.10
0.430	50	20.02	2.75	0.06
	40	11.74	1.81	0.04
	30	8.99	1.64	0.04
	20	6.13	1.34	0.03

Table 4.3.8

Cyclic Voltammetric Data on Co^{++} Ion in (Li, Na, K) NO_3 Eutectic at 423 $\pm$ 2 K. Calculated Values of Transfer Coefficient $\alpha_c n_\alpha$ and Diffusion Coefficient D_o

$\lvert E_p^c - E_{p/2}^c \rvert$ V	Transfer coefficient $\alpha_c n_\alpha$	Diffusion coefficient $D_o \times 10^6$ $cm^2\ s^{-1}$
0.069	0.986	6.03
0.075	0.908	6.81
0.074	0.920	6.41
0.075	0.908	6.86
0.069	0.986	1.16
0.075	0.908	1.81
0.063	1.081	1.95
0.063	1.081	4.44
	mean 0.972	mean 4.43

Table 4.3.9

The Values of K, the Empirical Constant of Co^{++} Ion in (Li, Na, K) NO_3 Eutectic of 423 ± 2 K

$$E_p^c = K - \frac{2.303\,R\,T}{2\,\alpha_c\,n_\alpha F} \log \nu$$

E_p^c corrected to NHE V	Voltage sweep rate ν $V\,s^{-1}$	K
-0.368	0.02	-0.441
-0.386	0.03	-0.457
-0.396	0.04	-0.461
-0.409	0.05	-0.470
-0.368	0.02	-0.441
-0.386	0.03	-0.457
-0.384	0.04	-0.439
-0.403	0.05	-0.454
	mean	-0.452

Table 4.3.10

The Value of Forward Electron Transfer Rate Constant $k^{o}_{f,h}$ of Co^{++} Ion in (Li, Na, K) NO_3 at 423 ± 2 K

E_p^c V corrected to NHE	log $k^{o}_{f,h}$	$k^{o}_{f,h}$ x 10^8 cm s^{-1}
-0.368	-7.10	7.9
-0.386	-7.01	9.9
-0.396	-7.13	7.4
-0.409	-7.13	7.4
-0.368	-7.54	2.9
-0.386	-7.30	5.1
-0.384	-7.96	1.1
-0.403	-7.96	1.1
	mean	5.3

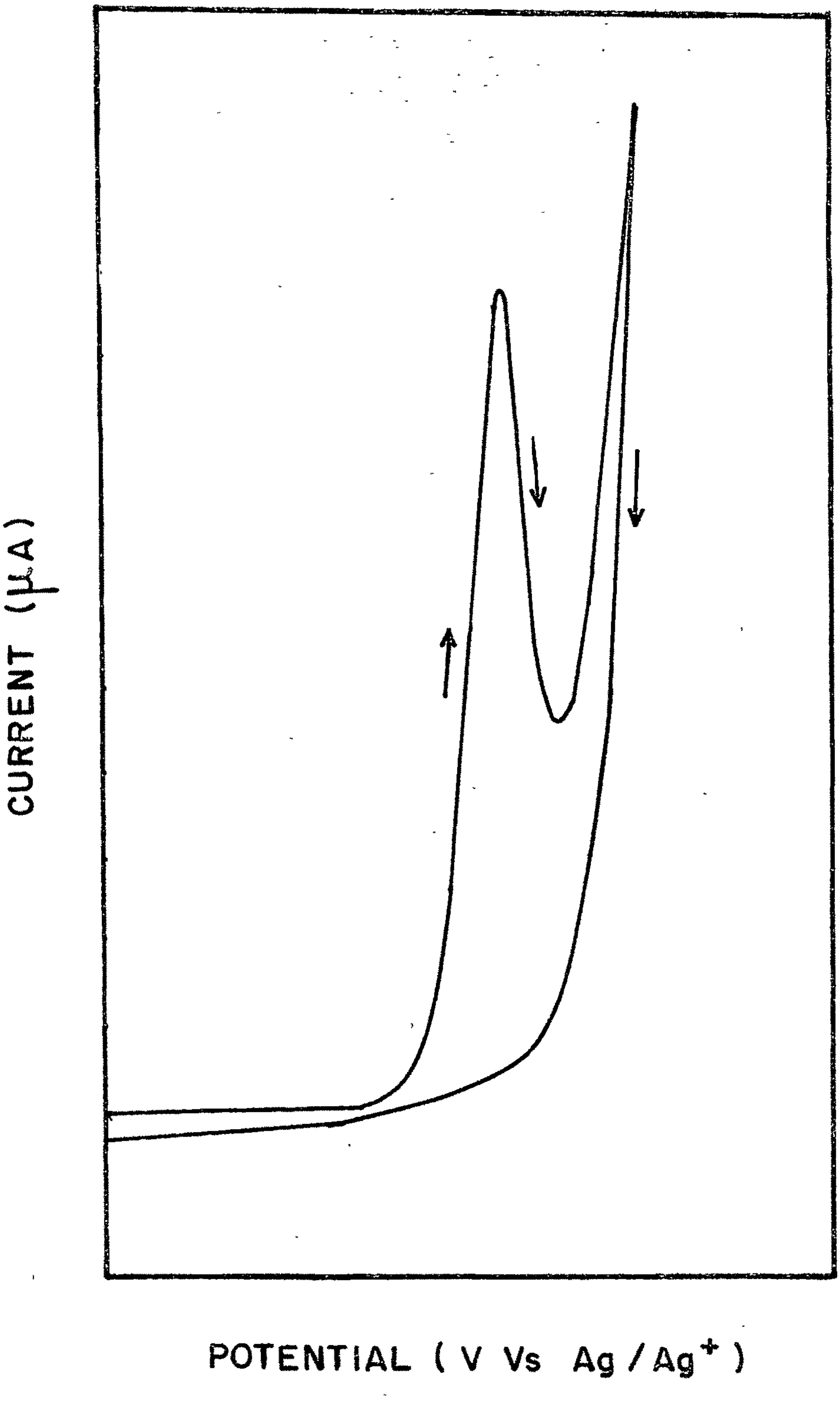

FIG. 4.3.3. A TYPICAL CYCLIC VOLTAMMOGRAM OF Ni^{++} ION IN (Li, Na, K) NO_3 EUTECTIC AT 423 ± 2K.

Table 4.3.11

Cyclic Voltammetric Data on Ni^{++} Ion in (Li, Na, K) NO_3 Eutectic at 423 ± 2 K

Concentration C mM	Voltage scan rate ν mV s^{-1}	E_p^c V vs Ag/Ag^+	$E_{p/2}^c$ V vs Ag/Ag^+
0.176	20	-0.456	-0.397
	30	-0.452	-0.397
	40	-0.450	-0.390
	50	-0.440	-0.379
0.236	20	-0.470	-0.409
	30	-0.465	-0.404
	40	-0.461	-0.403
	50	-0.456	-0.398

irreversibility of the reaction. This data is given in Table 4.3.12. The shape factor $\left|E_p^c - E_{p/2}^c\right|$ was utilised for calculating $\alpha_c n_\alpha$ and the transfer coefficients were found to yield values above unity which has been found to be a peculiar factor with nickel. The values of $\alpha_c n_\alpha$ together with the diffusion coefficients are given in Table 4.3.13. The values of the empirical constant K and $k^o_{f,h}$ calculated from equations 2.32 and 4.4 are listed in Table 4.3.14 and Table 4.3.15 respectively.

4.3.4 Iron

Fig. 4.3.4 gives a typical voltammogram of Fe^{+++} ions in the nitrate melt (concentration 0.63 mM). Table 4.3.16 lists the peak potentials E_p^c and the half-peak potentials $E_{p/2}^c$ as a function of scan rates and concentration. On the anodic side a small anodic peak was observed near +0.0 V vs Ag/Ag^+ which could have resulted from the reduced ferrous form of ion getting oxidised to Fe^{+++}. However the shape of the wave was irregular and difficult to repeat. With higher concentrations of the Fe^{+++} ion, the peak current was found to decrease. ΔE_p, the difference between E_p^c and E_p^a was found to be of the order of 400 mV, a value which could not be reasoned out for such scan rates as 0.05 V s^{-1}. The anodic peak is not due to the electrolyte, however, as it was not noticed in other cases. Under these circumstances the anodic peak was ignored and the data on the cathodic peak alone was taken.

Table 4.3.12

Cyclic Voltammetric Data on Ni^{++} Ion in (Li, Na, K) NO_3 Eutectic at 423 $\pm$ 2 K. The Relationship between Cathodic Peak Current and Voltage Sweep Rate

Concentration C mM	Voltage sweep rate γ mV s^{-1}	i_p^c µA	$i_p^c/\gamma^{1/2}$ µA $mV^{-1/2}$ $s^{1/2}$	$i_p^c/C\gamma^{1/2}$ µA mM^{-1} $mV^{-1/2}$ $s^{1/2}$
0.176	20	7.20	1.826	0.092
	30	8.17	1.491	0.085
	40	10.40	1.644	0.094
	50	11.03	1.598	0.091
0.236	20	9.02	2.017	0.086
	30	9.87	1.802	0.078
	40	13.3	2.102	0.089
	50	15.0	2.121	0.090
0.359	20	15.93	3.562	0.099
	30	20.22	3.691	0.103
	40	21.04	3.326	0.093
	50	21.86	2.838	0.080

Table 4.3.13

Cyclic Voltammetric Data on Ni^{++} in (Li, Na, K) NO_3 Eutectic at 423 ± 2 K Calculated Values of Transfer Coefficient $\alpha_c n_\alpha$ and Diffusion Coefficient D_o

$\lvert E_p^c - E_{p/2}^c \rvert$ V	Transfer coefficient $\alpha_c n_\alpha$	Diffusion coefficient $D_o \times 10^6$ $cm^2\ s^{-1}$
0.059	1.156	8.29
0.059	1.156	8.00
0.060	1.135	8.35
0.061	1.116	7.84
0.061	1.116	0.33
0.061	1.116	6.57
0.058	1.174	11.14
0.058	1.174	7.18
	mean 1.143	mean 7.21

Table 4.3.14

Values of K, the Empirical Constant of Ni^{++} Ions in (Li, Na, K) NO_3 Eutectic at 423 $\pm$ 2 K.

$$E_p^c = K - \frac{2.303\,R\,T}{2\alpha_c\, n_\alpha F} \log \gamma$$

E_p^c corrected to NHE V	Voltage sweep rate γ V s^{-1}	K
-0.353	0.02	-0.415
-0.349	0.03	-0.405
-0.347	0.04	-0.400
-0.337	0.05	-0.387
-0.367	0.02	-0.432
-0.362	0.03	-0.420
-0.358	0.04	-0.409
-0.353	0.05	-0.400
	mean	-0.409

Table 4.3.15

Values of Forward Electron Transfer Rate Constant $k^{o}_{f,h}$ of Ni^{++} Ion (Li, Na, K) NO_3 Eutectic at 423 ± 2 K.

E_p^c corrected to NHE V	$\log k_{f,h}$	$k^{o}_{f,h}$ x 10^{10} cm s^{-1}
-0.353	-9.62	2.4
-0.349	-9.60	2.5
-0.347	-9.37	4.3
-0.337	-9.12	7.6
-0.367	-9.77	1.7
-0.362	-9.60	2.5
-0.358	-9.72	1.9
-0.353	-9.59	2.6
		mean 3.2

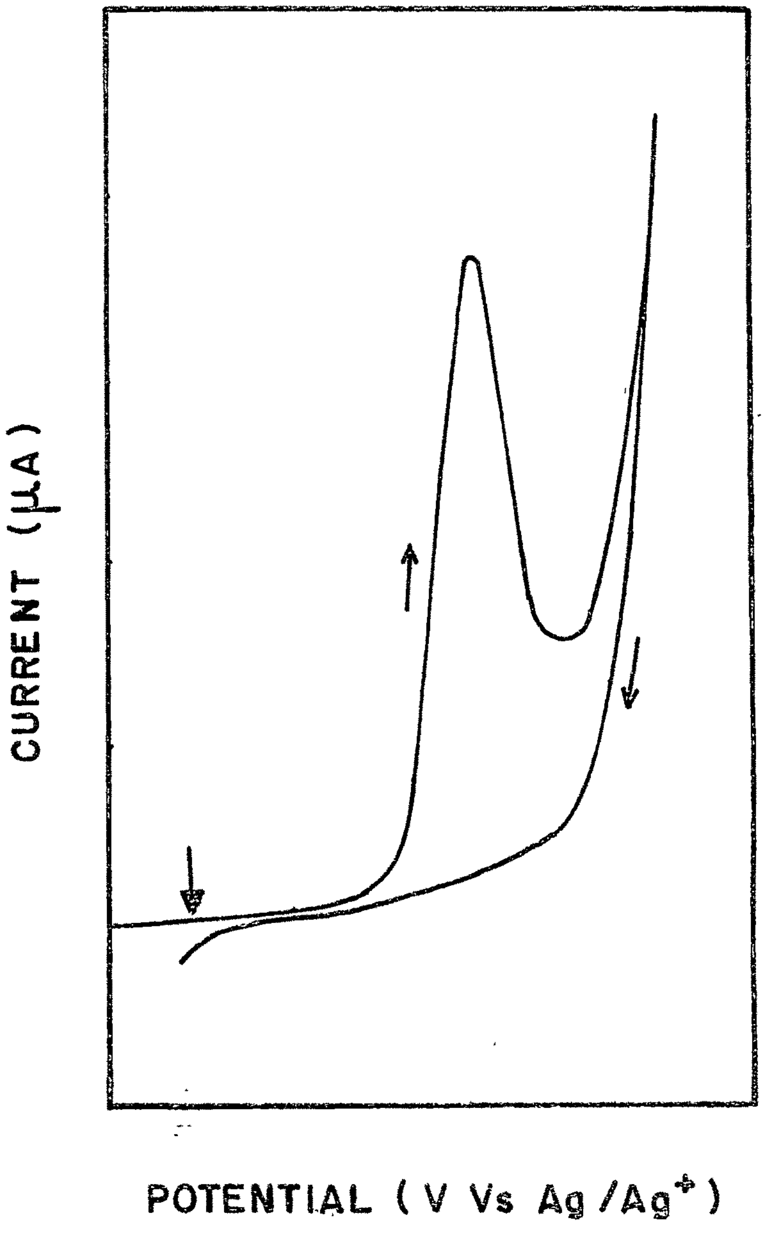

FIG. 4.3.4. A TYPICAL CYCLIC VOLTAMMOGRAM OF Fe^{+++} ION IN (Li, Na, K) NO_3 EUTECTIC AT 423 ± 2K.

Table 4.3.16

Cyclic Voltammetric Data on Fe^{+++} Ion in (La, Na, K) NO_3 Eutectic at 423 ± 2 K.

Concentration C mM	Voltage sweep rate ν mV s^{-1}	E_p^c V vs Ag/Ag$^+$	$E_{p/2}^c$ V vs Ag/Ag$^+$
0.63	30	-0.505	-0.450
	40	-0.512	-0.456
	50	-0.512	-0.449
1.21	30	-0.560	-0.509
	40	-0.579	-0.521
	50	-0.583	-0.531

Table 4.3.17

Cyclic Voltammetric Data on Fe^{+++} in (Li, Na, K) NO_3 Eutectic at 423 ± 2 K. Relationship between Cathodic Peak Current and Voltage Sweep Rate

Concentration C mM	Voltage sweep rate ν mV s^{-1}	i_p^c μA	$i_p^c/\nu^{\frac{1}{2}}$ μA $mV^{-\frac{1}{2}}$ $s^{\frac{1}{2}}$	$i_p^c/C\,\nu^{\frac{1}{2}}$ μA mM^{-1} $mV^{-\frac{1}{2}}$ $s^{\frac{1}{2}}$
0.63	30	11.15	2.035	3.23
	40	13.0	2.055	3.26
	50	14.8	2.093	3.32
1.213	30	22.0	4.02	3.32
	40	25.35	4.01	3.31
	50	30.21	4.27	3.52

Table 4.3.18

Cyclic Voltammetric Data on Fe^{+++} Ion in (Li, Na, K) NO_3 Eutectic at 423 ± 2 K.

Calculated Values of Transfer Coefficients $\alpha_c n_\alpha$ and Diffusion Coefficient D_o

$\lvert E_p^c - E_{p/2}^c \rvert$ V	Transfer coefficient $\alpha_c n_\alpha$	Diffusion coefficient $D_o \times 10^6$ $cm^2\ s^{-1}$
0.055	1.239	1.19
0.056	1.217	1.23
0.063	1.081	1.43
0.051	1.325	1.17
0.058	1.181	1.29
0.053	1.285	1.35
	mean 1.221	mean 1.28

Table 4.3.19

The Values of K, the Empirical Constant of Fe^{+++} Ions in (Li, Na, K) NO_3 Eutectic at 423 ± 2 K

$$E_p^c = K - \frac{2.303\,R\,T}{2\alpha_c\,n_\alpha F}\log \nu$$

E_p^c corrected to NHE V	Voltage sweep rate ν V s^{-1}	K
-0.402	0.03	-0.454
-0.409	0.04	-0.458
-0.412	0.05	-0.463
-0.475	0.03	-0.506
-0.476	0.04	-0.526
-0.480	0.05	-0.523
	mean	-0.488

Table 4.3.20

The Values of Forward Electron Transfer Rate Constant $k^{o}_{f,h}$ of Fe^{+++} Ions in (Li, Na, K) NO_3 Eutectic at 423 ± 2 K

E_p^c corrected to NHE V	$\log k^{o}_{f,h}$	$k^{o}_{f,h}$ x 10^{10} cm s^{-1}
-0.402	-9.06	8.8
-0.409	-9.00	10.0
-0.412	-8.40	4.0
-0.475	-10.31	0.49
-0.476	-9.75	1.8
-0.480	-10.31	0.49
		mean 1.26

In this case, too, i_p^c showed a near linear relationship with the square root of scan rates and concentration. This data is shown in Table 4.3.17 while the parameters $\left| E_p^c - E_{p/2}^c \right|$ was used for calculating $\alpha_c n_\alpha$. These values together with the diffusion coefficient values are given in Table 4.3.18. The values of the empirical constant K and $k^o_{f.h}$ calculated from equations 2.32 and 4.4 are listed in Tables 4.3.19 and 4.3.20 respectively.

4.3.5 Copper

For the cyclic voltammetric investigation of copper cupric nitrate was taken. At least two concentrations are given in the present text, viz., 6.6 mM and 13.8 mM.

Fig. 4.3.5 gives a typical voltammogram of Cu^{++} ions in the nitrate melt. The voltammogram shows a clear cut cathodic and anodic wave showing the probability of this reaction being reversible. E_p^c and E_p^a values were found to be nearly constant, but there was a decrease in the E_p^c and E_p^a values with scan rate, the values becoming more negative with the increase in scan rate. Table 4.3.21 shows the values of E_p^c and $E_{p/2}^c$ together with the concentration. For a reversible reaction it is expected that the shape factor $\left| E_p^c - E_{p/2}^c \right|$ should be equal to $\frac{0.059}{n}$ at 298 K. On conversion to 423 K this value will be $\frac{0.084}{n}$ and hence if it is a 2 - electron reduction leading to the deposition or formation of metallic

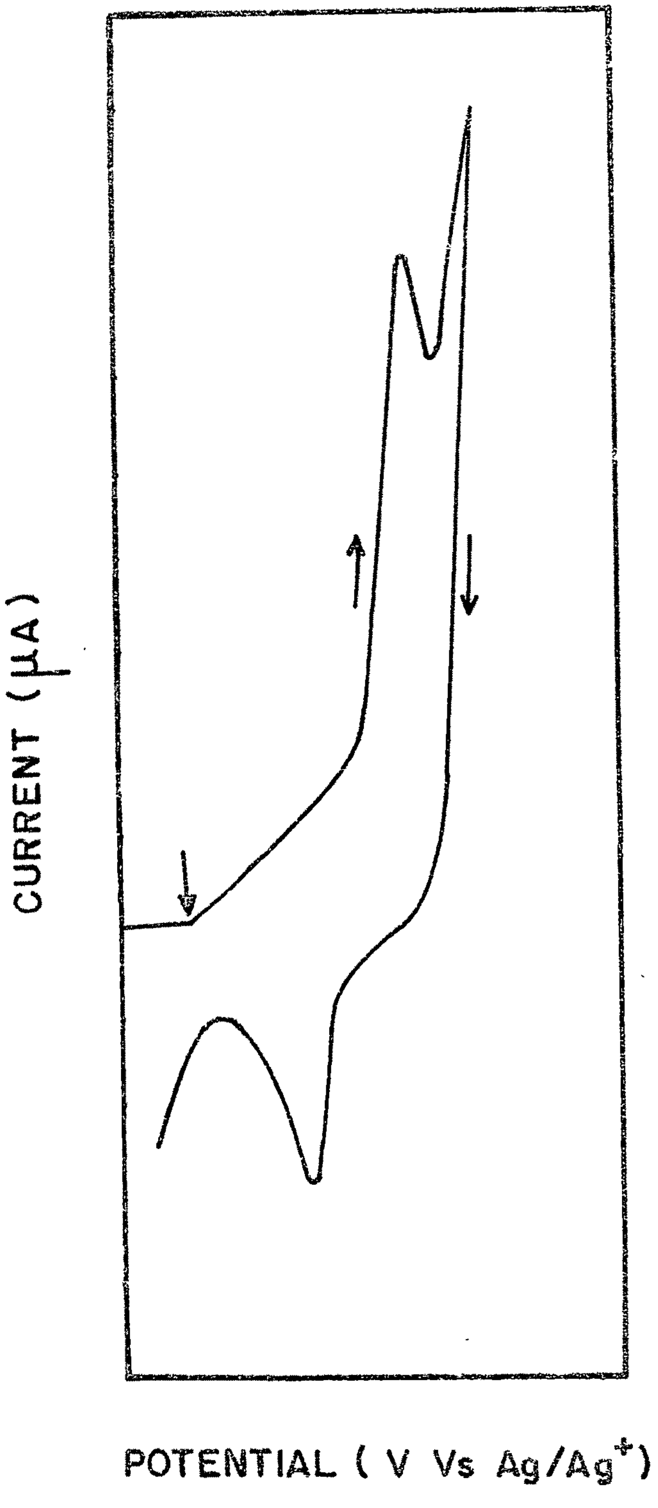

FIG. 4.3.5. A TYPICAL CYCLIC VOLTAMMOGRAM OF Cu^{++} ION IN (Li, Na, K)NO_3 EUTECTIC AT 423±2K.

Table 4.3.21

Cyclic Voltammetric Data on Cu^{++} Ion in (Li, Na, K) NO_3 Eutectic at 423 $\pm$ 2 K

Concentration C mM	Voltage sweep rate γ mV s^{-1}	E_p^c V vs Ag/Ag^+	$E_{p/2}^c$ V vs Ag/Ag^+
6.6	20	0.818	0.725
	30	0.823	0.746
	40	0.825	0.745
	50	0.830	0.745
13.8	20	0.828	0.741
	30	0.830	0.733
	40	0.840	0.742
	50	0.845	0.745

Table 4.3.22

Cyclic Voltammetric Data on Cu^{++} Ion in (Li, Na, K) NO_3 Eutectic at 423 ± 2 K.

Concentration C mM	Voltage sweep rate ν mV s^{-1}	E_p^a V vs Ag/Ag^+	$E^a_{p/2}$ V vs Ag/Ag^+
6.6	20	-0.527	-0.462
	30	-0.529	-0.475
	40	-0.530	-0.465
	50	-0.531	-0.464
13.48	20	-0.537	-0.462
	30	-0.537	-0.460
	40	-0.540	-0.462
	50	-0.545	-0.469

copper the shape factor should be equal to 0.042 V. Table 4.3.23 lists the values of the shape factor and it is seen that the values approximate to 0.090 V which is indicative of a one electron reduction. Similarly Table 4.3.22 lists the values of the peak anodic potential E_p^a and the half-peak potential $E_{p/2}^a$. Here, too, the peak potentials are negative and are not independent of ν. There is a marginal variation with ν in E_p^a, the values showing a tendency to become more negative with the scan rate. The shape factor $\left| E_p^a - E_{p/2}^a \right|$ is nearly equal to $\left| E_p^c - E_{p/2}^c \right|$, pointing out to a one electron reduction. The values of $\left| E_p^a - E_{p/2}^a \right|$ are listed in Table 4.3.24. Tables 4.3.25 and 4.3.26 list the current relationships between voltage sweep rates. As can be seen the peak currents I_p^c and I_p^a are proportional to $C\,\nu^{\frac{1}{2}}$.

On the other hand, some indication of irreversibility is given by the values of the peak potential difference ΔE_p which is defined as $E_p^a - E_p^c$. This gives a mean difference of 295 mV which is too high a value. ΔE_p for a reversible case should be equal to $\frac{0.084}{n}$ at 423 K. Even for a one electron reduction this value is too high. For a quasi-reversible system ΔE_p can be greater than $\frac{0.084}{n}$ V and increases with ν. A perusal of the Table 4.3.27 shows that this is the case and a marginal increase of 0.005 V is noticed when ν is changed from 20 – 50 mV s^{-1}. For a

Table 4.3.23

Cyclic Voltammetric Data on Cu^{++} Ion in (Li, Na, K) NO_3 Eutectic at 423 ± 2 K. Calculated Values for Transfer Coefficient $(\alpha_c n_\alpha)_c$ and Diffusion Coefficient $(D_o)_c$

$\left\lvert E_p^c - E_{p/2}^c \right\rvert$ V	Transfer coefficient $(\alpha_c n_\alpha)_c$	Diffusion coefficient $(D_o)_c \times 10^6$ $cm^2\ s^{-1}$
0.093	0.792	1.69
0.077	0.868	1.40
0.080	0.850	1.40
0.085	0.801	1.47
0.087	0.783	1.46
0.097	0.702	1.48
0.098	0.695	1.83
0.100	0.681	1.66
	mean 0.772	mean 1.55

Table 4.3.24

Cyclic Voltammetric Data on Cu^{++} Ion in (La, Na, K) NO_3 Eutectic at 423 ± 2 K Calculated Values of Transfer Coefficient $(\alpha_c n_\alpha)_a$ and Diffusion Coefficient $(D_o)_a$

$\lvert E_p^a - E_{p/2}^a \rvert$ V	$(\alpha_c n_\alpha)_a$	Diffusion coefficient $(D_o)_a \times 10^7$
0.065	1.048	0.24
0.054	1.260	0.15
0.065	1.048	0.18
0.067	1.016	0.18
0.075	0.908	0.19
0.077	0.884	0.19
0.078	0.873	0.20
0.076	0.896	0.18
	mean 0.992	mean 0.19

Table 4.3.25

Cyclic Voltammetric Data on Cu^{++} Ion in (Li, Na, K) NO_3 Eutectic at 423 ± 2 K. Relationship of Cathodic Peak Current with Voltage Sweep Rate

Concentration C mM	Voltage sweep rate γ mV s^{-1}	$\gamma^{1/2}$	i_p^c µA	$i_p^c/\gamma^{1/2}$ µA $mV^{-1/2}$ $s^{1/2}$	$i_p^c/C\,\gamma^{1/2}$ µA mM^{-1} $mV^{-1/2}$ $s^{1/2}$
6.6	20	4.47	9.79	2.19	0.315
	30	5.48	11.83	2.16	0.315
	40	6.33	13.16	2.08	0.315
	50	7.07	15.17	2.15	0.325
13.5	20	4.47	19.20	4.29	0.318
	30	5.48	23.44	4.27	0.317
	40	6.33	28.69	4.53	0.336
	50	7.07	30.31	4.29	0.318

Table 4.3.26

Cyclic Voltammetric Data on Cu^{++} Ion in (Li, Na, K) NO_3 Eutectic at 423 ± 2 K

Relationship of Anodic Peak Current with Voltage Sweep Rate

Concentration C mM	Voltage sweep rate γ mV s^{-1}	i_p^a µA	$i_p^a/\gamma^{1/2}$ µA $mV^{-1/2}$ $s^{1/2}$	$i_p^a/C\gamma^{1/2}$ µA mM^{-1} $mV^{-1/2}$ $s^{1/2}$
6.6	20	6.02	1.35	0.204
	30	7.34	1.33	0.200
	40	8.38	1.32	0.200
	50	9.38	1.33	0.202
13.5	20	11.62	2.59	0.193
	30	14.16	2.58	0.191
	40	16.32	2.58	0.191
	50	18.00	2.55	0.189

Table 4.3.27

Cyclic Voltammetric Data on Cu^{++} Ion in (Li, Na, K) NO_3 Eutectic at 423 $\pm$ 2 K

Concentration C mM	Voltage sweep rate ν mV s^{-1}	$\Delta E_p = \left| E_p^a - E_p^c \right|$ V	$\frac{I_p^a}{I_p^c}$
6.6	20	0.291	0.62
	30	0.294	0.62
	40	0.295	0.64
	50	0.296	0.62
13.8	20	0.291	0.61
	30	0.293	0.60
	40	0.300	0.57
	50	0.300	0.60
		mean 0.295	

reversible system $I_p^a = I_p^c$. This relationship is also given in Table 4.2.27 from where it is seen that I_p^a / I_p^c is approximately 0.6 only. For a quasi-reversible system I_p^a / I_p^c is equal to unity only provided $\alpha_c = \alpha_a = 0.5$. The ratio of 0.6 obtained for I_p^a / I_p^c shows that $\alpha_c \neq \alpha_a \neq 0.5$.

Under these conditions it was thought best to consider the system as quasi-reversible and hence Randle-Sevick's equation with the modifications for an irreversible system was utilised to find the diffusion coefficient$(D_o)_c$ of the forward reaction. This was done after calculating the transfer coefficient values $(\alpha_c n_\alpha)_c$ and $(\alpha_c n_\alpha)_a$ of the system. These values are given in Tables 4.3.23 and 4.3.24 together with the diffusion coefficients $(D_O)_c$ and $(D_O)_a$ respectively.

The values of the empirical constants K_c and K_a for both cathodic and anodic reactions are given in Table 4.3.28. These have been calculated using equation 2.32. The values of $k^o_{f,h}$ and $k^o_{b,h}$ are listed in Table 4.3.29 and Table 4.3.30 respectively.

4.4 CHRONOAMPEROMETRY

In chronoamperometry the experiments involve instantaneous change in potential from a value where no electrolysis occurs to a value in the mass-transfer-controlled region for the redox reaction or more accurately a reduction and grasp the current-time response. As described in Chapter 3 of the present

Table 4.3.28

The value of K, the Empirical Constant of Cu^{++} Ion in (Li, Na, K) NO_3 Eutectic at 423 ± 2 K (Cathodic and Anodic)

$$E_p^{c\ or\ a} = K - \frac{2.303\,R\,T}{2\,(\alpha_c\, n_\alpha)\,F_{a\ or\ c}} \log \gamma$$

Voltage sweep rate γ V s^{-1}	E_p^c corrected to NHE V	E_p^a corrected to NHE V	K_c	K_a
0.02	-0.715	-0.424	-0.814	-0.493
0.03	-0.720	-0.426	-0.795	-0.477
0.04	-0.722	-0.427	-0.792	-0.484
0.05	-0.727	-0.428	-0.800	-0.482
0.02	-0.725	-0.434	-0.817	-0.514
0.03	-0.727	-0.434	-0.819	-0.507
0.04	-0.737	-0.437	-0.822	-0.505
0.05	-0.742	-0.442	-0.823	-0.504
			mean -0.810	mean -0.496

Table 4.3.29

The Values of Forward Electron Transfer Rate Constant $k^o_{f,h}$ of Cu^{++} Ion in (Li, Na, K) NO_3 Eutectic at 423 ± 2 K

E_p^c corrected to NHE V	log $k^o_{f,h}$	$k^o_{f,h} \times 10^{10}$ cm s^{-1}
-0.715	-9.48	3.30
-0.720	-10.60	0.25
-0.722	-10.42	0.38
-0.727	-9.24	5.80
-0.725	-10.02	0.96
-0.727	-9.28	5.20
-0.737	-9.31	4.90
-0.742	-9.06	8.90
	mean	3.72

Table 4.3.30

The Values of Backward Electron Transfer Rate Constant $k^o_{b,h}$ of Cu^{++} Ion in (Li, Na, K) NO_3 Eutectic at 423 $\pm$ 2 K.

E_p^a corrected to NHE V	$\log k^o_{b,h}$	$k^o_{b,h} \times 10^{10}$ cm s^{-1}
-0.424	-9.39	4.07
-0.426	-9.45	4.35
-0.427	-9.35	4.50
-0.428	-9.14	7.20
-0.434	-9.08	8.39
-0.434	-8.52	30.00
-0.437	-8.52	30.00
-0.442	-8.70	20.00
	mean	13.06

work the apparatus fabricated in our laboratory was capable of switching on from any one potential to another potential. The cell system used was the same and hence in the experiments on chronoamperometry were performed using the same set-up. The potential of the working electrode was changed from 0 to a known voltage with respect to the reference electrode which are specified in the tables.

In the following pages are given full details of the data obtained for lead. Like in other sections of this chapter, full description is given only for lead, as for the other elements the details are the same.

4.4.1 Lead

As in the case of cyclic voltammetry and chronopotentiometry $Pb(NO_3)_2$ was used as the electroactive solute. The concentrations are expressed in mole cm^{-3} and the solvant taken was 50 gm, the volume of which was calculated using equation 3.1. The same working, reference and auxiliary electrodes as were used in cyclic voltammetry, were used in this technique also.

After arranging the cell set-up and after thermal equilibrium was established, a voltage of -0.191 V was impressed on the cell. The current shifted to a very high value, steadily decreasing to a limiting value, indicating the establishment of steady conditions. After the establishment of this equilibrium, the apparatus was switched off and the next impressed voltage was increased to -0.240 V and the current-time relationship recorded. Similarly the potential step was increased in stages to -0.306, -0.472, -0.520, -0.613 and -0.718 V. More steps were taken, but they are not quoted here. In the next section these are mentioned, because such steps are more useful for sampled current voltammetry than in chronoamperometry. The series of curves obtained in the various potential steps are given in Fig. 4.4.1. The data on the current-time in these potential steps are listed in Tab. 4.4.1.

Now if the current is either controlled by mass transport or a steady state process, it may be determined from the flux associated with the slope of the concentration profile :

$$i\ (t) = n F A D \left. \frac{\partial C\ (x,t)}{\partial x} \right|_{\lambda = 0} \qquad 4.6$$

where n is the " number of electrons ", otherwise expressed as faradays mol^{-1}, A is the area of the electrode and F = 96,500 C $faraday^{-1}$. The slope and the current corresponding to this equation falls off in proportion to $t^{-\frac{1}{2}}$. As discussed earlier, this fundamental relationship is known as the Cottrell equation :

$$i\ (t) = \frac{n F A D_o^{\frac{1}{2}} C}{\pi^{\frac{1}{2}}\ t^{\frac{1}{2}}} \qquad 4.7$$

where i (t) is the current in amperes, C the concentration in

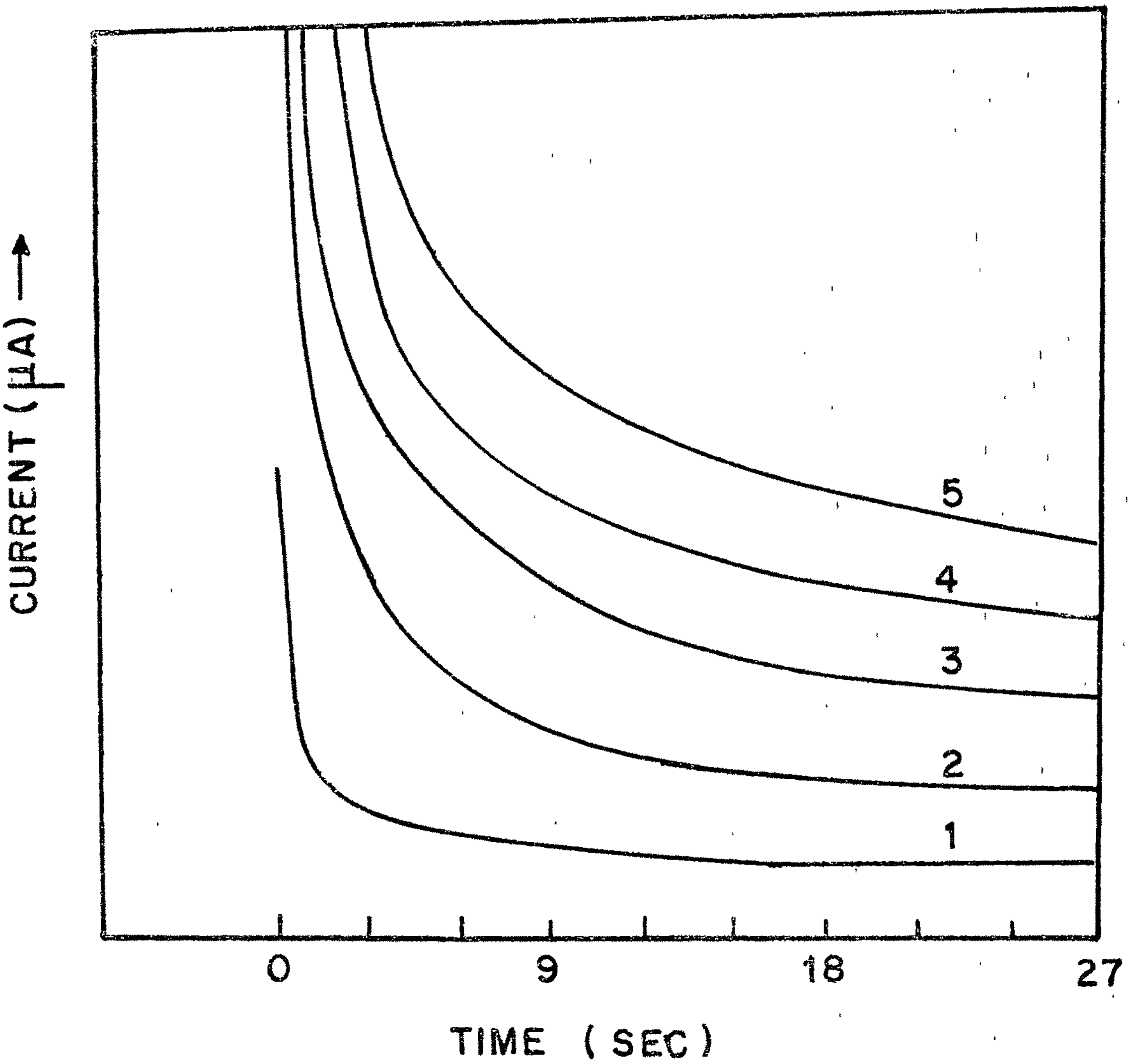

FIG. 4.4.1. CHRONOAMPEROGRAMS OF 2.02×10^{-6} mole cm^{-3} Pb^{++} ION RECORDED AT POTENTIAL STEPS FROM 0.0 V TO (1) -0.306, (2) -0.472, (3) -0.613, (4) -0.718 AND (5) -0.766 V Vs Ag/Ag^{+} ELECTRODE.

Table 4.4.1

Chronoamperometric Data of Pb^{++} Ions in (Li, Na, K) NO_3 Eutectic at 423 $\pm$ 2 K

Concentration of Pb^{++} = 2.02×10^{-6} mole cm^3

Potential step V vs Ag/Ag^+	Time t s	Current $i_{(t)}$ µA	$i_{(t)} \times t^{\frac{1}{2}}$ µA $s^{\frac{1}{2}}$
0 to -0.191	0.30	7.45	4.08
	0.45	5.32	3.57
	0.60	4.47	3.46
	0.90	3.40	3.26
	1.20	2.87	3.14
	1.80	2.45	3.29
	2.40	2.18	3.37
	3.00	2.02	3.50
	4.20	1.76	3.60
	6.00	1.60	3.91
0 to -0.240	0.60	7.45	5.77
	0.90	5.11	4.85
	1.20	4.26	4.67
	1.50	3.72	4.55
	1.80	3.40	4.56
	2.40	3.09	4.79
	3.00	2.87	4.97
	3.60	2.71	5.14
	4.20	2.50	5.12

Contd

Table 4.4.1 (Contd.)

Potential step V vs Ag/Ag^+	Time t s	Current $i_{(t)}$ μA	$i_{(t)} \times t^{\frac{1}{2}}$ μA $s^{\frac{1}{2}}$
0 to -0.306	0.30	18.08	9.90
	0.45	14.89	9.98
	0.60	11.70	9.06
	0.90	8.94	8.48
	1.20	7.87	8.62
	1.50	7.23	8.85
	1.80	6.81	8.55
	2.10	6.38	9.24
	2.40	6.17	9.55
	3.00	5.75	9.96
	3.60	5.32	10.09
	4.20	5.04	9.56
	5.40	4.68	10.50
	6.00	4.47	10.94
0 to -0.472	0.30	58.51	32.05
	0.45	56.38	37.91
	0.60	47.87	37.07
	0.90	40.44	38.36
	1.20	36.17	39.62
	1.50	31.92	39.09
	1.80	28.72	38.53
	2.10	26.59	38.53
	2.40	24.47	37.90
	2.70	23.40	38.45

Contd.

Table 4.4.1 (Contd.)

Potential step V vs Ag/Ag^+	Time t s	Current $i_{(t)}$ μA	$i_{(t)} \times t^{\frac{1}{2}}$ $\mu A\ s^{\frac{1}{2}}$
0 to -0.472	3.00	22.34	38.69
	3.30	21.08	38.29
	3.60	20.21	38.34
	4.20	18.62	38.15
	4.80	17.02	37.29
	5.40	16.17	37.57
0 to -0.520	0.30	42.55	23.30
	0.45	37.23	24.97
	0.60	31.91	24.71
	0.90	26.59	25.22
	1.20	25.00	27.38
	1.50	23.40	28.66
	1.80	21.80	29.24
	2.40	20.21	31.31
	3.00	19.15	33.16
	3.60	18.08	34.30
	4.60	15.42	33.07
	4.80	16.49	36.13
	5.40	15.95	37.06
0 to -0.613	0.60	56.38	43.67
	1.20	45.74	50.10
	1.80	39.36	52.80
	2.40	35.10	54.38
	3.00	31.91	55.27
	3.60	29.79	56.52

Contd.

Table 4.4.1 (Contd.)

Potential step V vs Ag/Ag^{+}	Time t S	Current $i_{(t)}$ µA	$i_{(t)} \times t^{\frac{1}{2}}$ µA $s^{\frac{1}{2}}$
0 to -0.613	3.60	29.79	56.52
	4.20	27.66	56.68
	4.80	26.59	58.26
	5.40	25.53	54.68
	6.00	24.46	59.91
	6.60	23.94	61.50
	7.20	22.87	61.37
0 to -0.718	2.40	47.87	74.16
	3.00	42.55	73.70
	3.60	38.30	72.67
	4.20	35.10	71.93
	4.80	33.51	73.42
	5.40	31.91	74.15
	6.00	29.78	72.94
	6.60	28.72	72.42
	7.20	28.19	75.64
	7.80	27.65	77.22
	8.40	26.59	77.06
	9.00	26.06	78.18
	9.60	25.53	79.10

moles cm^{-3}. In the absence of convection and migration effects the diffusion layer would expand in this manner, i.e., such that the concentration gradient decreases with $t^{-\frac{1}{2}}$. Normally currents which obey this $t^{-\frac{1}{2}}$ relationship are called diffusion currents.

According to the Cottrell equation, at the same concentration of the solute, $2(t) \times t^{\frac{1}{2}}$ is a constant. As can be seen from Table 4.4.1, the values of $i(t) \times t^{\frac{1}{2}}$ are reasonably constant for every potential step. Further the plot of $i(t)$ against $\frac{1}{t^{\frac{1}{2}}}$ should be a straight line. This linear relationship was exhibited for all the potential steps, but in certain cases the straight line did not pass through the origin. The calculated current for a reversible process is infinite for $t = 0$ as per the equations

$$i = i_d \frac{1}{1 + (D_R + D_O)^{\frac{1}{2}} (f_O f_R) \exp (nF/_{RT}) (E - E^O)} \qquad \ldots\ldots\ldots \quad 2.48$$

and

$$i_d = \left[\frac{n F A D_O^{\frac{1}{2}}}{\pi^{\frac{1}{2}} t^{\frac{1}{2}}} \right] C \qquad 2.49$$

whereas the current for an irreversible process is finite at $t = 0$. This result is consistent with the assumptions that were made in the derivation. For reverse processes it is assumed that diffusion is the sole rate-determining factor. In the time $t = 0$ to $t = \triangle t$ the concentration C_O at the electrode surface must vary from C to another value prescribed by the Nernst equation. This change in concentration corresponds to an infinite current as Δt approaches 0. Conversely the current density at time $t = 0$ for irreversible processes is simply $n F k_{f,h} C$ or more precisely $\alpha_c n_\alpha F k_{f,h} C$ where C, as usual, is the bulk concentration of substance O. This usage is particularly pertinent as there is no depletion of the electroactive substance at $t = 0$.

Having thus ascertained that the reaction is diffusion controlled, the diffusion coefficient was calculated using the Cottrell's equation mentioned above. The average value of the diffusion coefficient was found to be 2.01×10^{-6} $cm^2\ s^{-1}$. Fig. 4.4.2 gives a typical relationship between $t^{-\frac{1}{2}}$ and $i(t)$ for the potential step 0 to -0.472 V. In this case however, the straight line passes through the origin showing that when $t = 0$, $i(t)$ also is equal to 0. In some cases in the 10 potential step experiments, a small intercept was obtained.

4.4.2 Cobalt

Chronoamperometry of Co^{++} ions was done using $Co(NO_3)_2$ as the electroactive solvent. As usual a known weight of solvent was used and its volume calculated from equation 3.1. Various potential steps were taken and each of the curve so obtained were analysed for the time - current relationships.

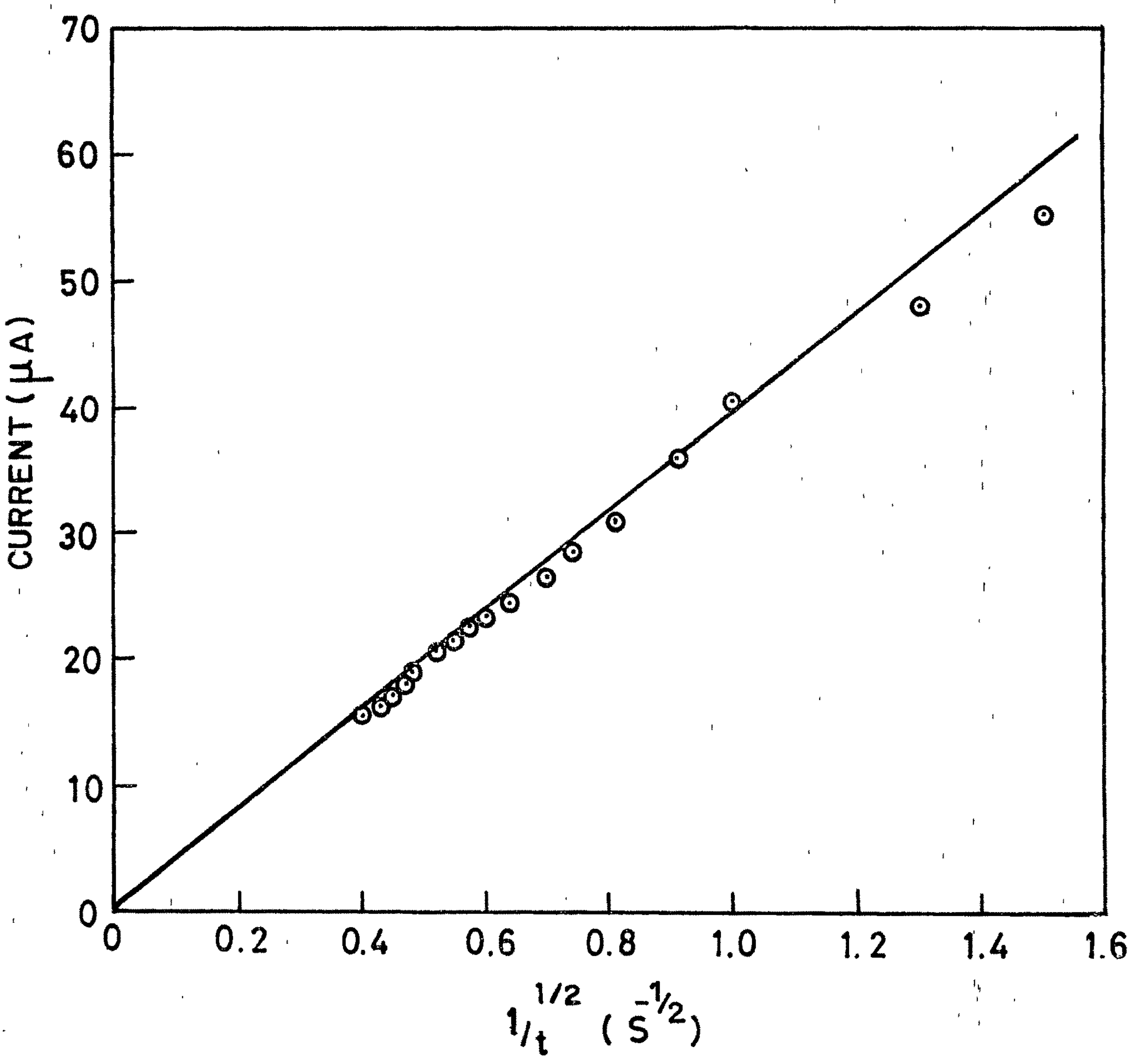

FIG.4.4.2. A TYPICAL PLOT OF RELATIONSHIP BETWEEN $1/t^{1/2}$ AND $i_{(t)}$ FOR Pb^{++} ION, POTENTIAL STEP 0 TO −0.472 V Vs Ag/Ag^{+}.

Table 4.4.2

Chronoamperometric Data of Co^{++} Ion in $(Li, Na, K)NO_3$ Eutectic at 423 ± 2 K

Concentration of $Co^{++} = 2.054 \times 10^{-6}$ mole cm^{-3}

Potential step V vs Ag/Ag^+	Time t s	Current $i_{(t)}$ µA	$i_{(t)}\ t^{\frac{1}{2}}$ µA $s^{\frac{1}{2}}$
0 to −0.143	0.60	10.63	8.23
	0.90	4.25	4.03
	1.05	3.40	3.48
	1.20	2.76	3.02
	1.50	2.34	2.86
	1.80	2.02	2.71
	2.40	1.64	2.54
	3.00	1.43	2.47
	3.60	1.33	2.52
	4.20	1.22	2.50
	4.80	1.17	2.56
0 to −0.241	0.60	21.28	16.48
	0.90	10.63	10.08
	1.20	7.44	8.15
	1.80	5.31	7.12
	2.40	4.25	6.58
	3.00	3.72	6.44
	4.20	3.19	6.54
	6.00	2.66	6.52
0 to −0.341	0.60	26.59	20.60
	0.90	17.02	16.15
	1.20	13.23	14.49

Contd.

Table 4.4.2 (Contd.)

Potential step V vs Ag/Ag^+	Time t s	Current $i_{(t)}$ μA	$i_{(t)}\ t^{\frac{1}{2}}$ μA $s^{\frac{1}{2}}$
0 to -0.341	1.80	10.11	13.56
	2.40	8.51	13.18
	3.00	7.44	12.88
	3.60	6.91	13.11
	4.20	6.38	13.07
	6.00	5.31	13.00
0 to -0.444	0.60	53.19	41.20
	0.90	39.36	37.34
	1.20	31.91	34.95
	1.50	27.66	33.88
	1.80	24.47	32.83
	2.10	22.34	32.37
	2.40	20.21	31.31
	3.00	18.29	31.68
	3.60	16.49	31.28
	4.20	15.42	31.60
	4.80	14.36	31.46
	5.40	13.83	32.14
	6.00	13.03	31.91
0 to -0.490	2.40	31.91	49.43
	3.00	27.66	47.90
	3.60	24.47	46.43
	4.20	22.34	45.78
	4.80	20.74	45.44
	5.40	19.68	45.44
	6.00	18.35	45.73
	7.20	17.02	45.67
	8.40	15.42	44.69

Contd.

Table 4.4.2 (Contd.)

Potential step V vs Ag/Ag^+	Time t s	Current $i_{(t)}$ μA	$i_{(t)}$ $t^{\frac{1}{2}}$ $\mu A\ s^{\frac{1}{2}}$
0 to -0.581	2.40	47.87	74.16
	3.00	42.55	73.70
	3.60	38.29	72.65
	4.20	35.37	72.49
	4.80	33.51	73.42
	5.40	31.91	74.15
	6.00	30.30	74.21
	6.60	29.25	75.14
	7.40	27.65	75.22
	8.40	26.59	77.06
	10.20	24.46	78.12
0 to 0.630	2.40	40.42	62.62
	3.00	37.76	65.40
	3.60	35.63	67.60
	4.20	33.51	68.67
	4.80	31.38	68.75
	5.40	29.78	69.20
	6.00	28.19	69.05
	7.20	26.59	71.35
	8.40	25.00	72.46
	9.60	23.94	74.17
	10.80	22.87	75.16

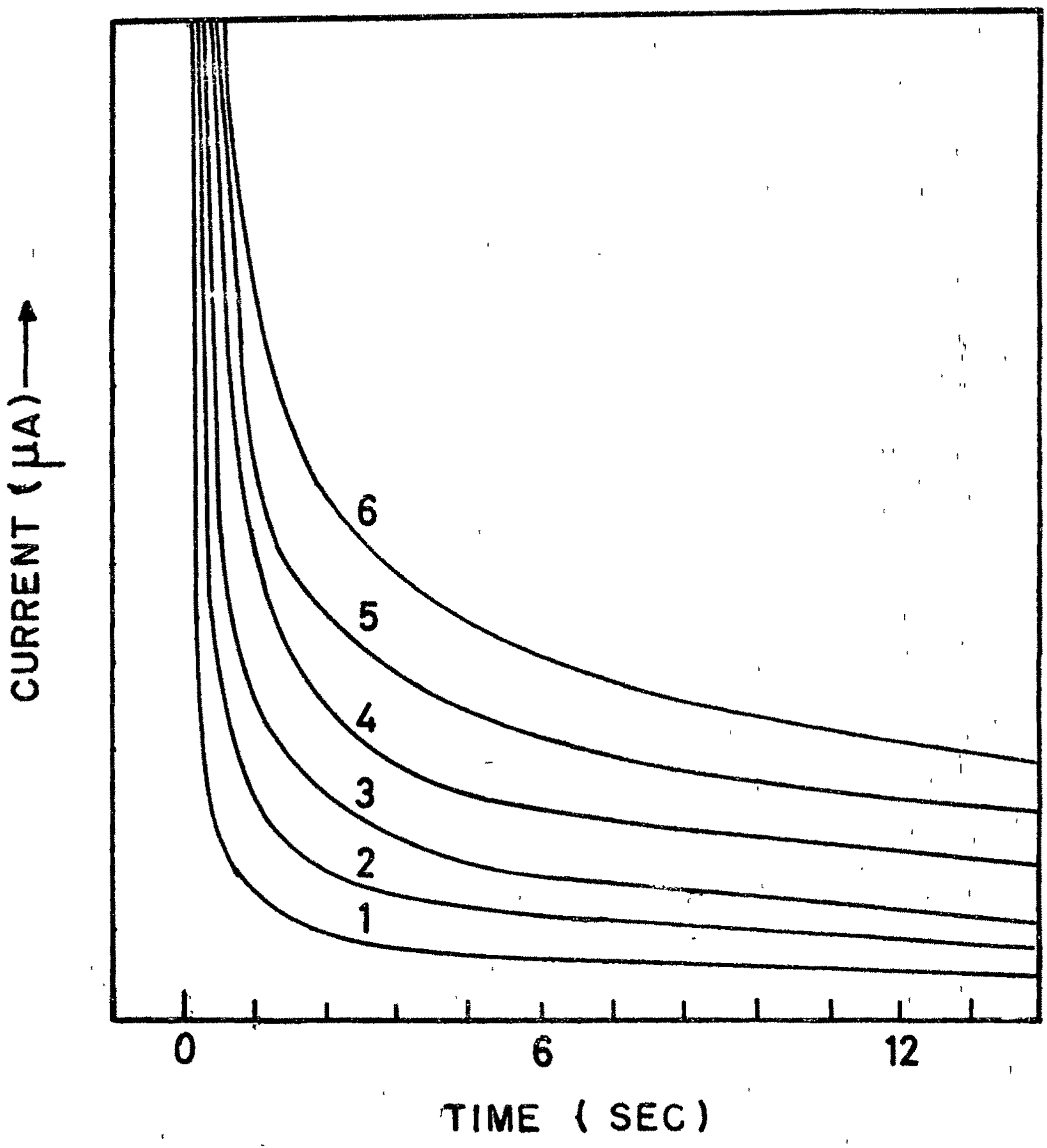

FIG. 4.4.3. CHRONOAMPEROGRAMS OF 2.05×10^{-6} mole cm^{-3} Co^{++} ION RECORDED AT POTENTIAL STEPS FROM 0.0 V TO (1) -0.143, (2) -0.193, (3) -0.444, (4) -0.490, (5) -0.531 AND (6) -0.581 V Vs Ag/Ag^{+} ELECTRODE.

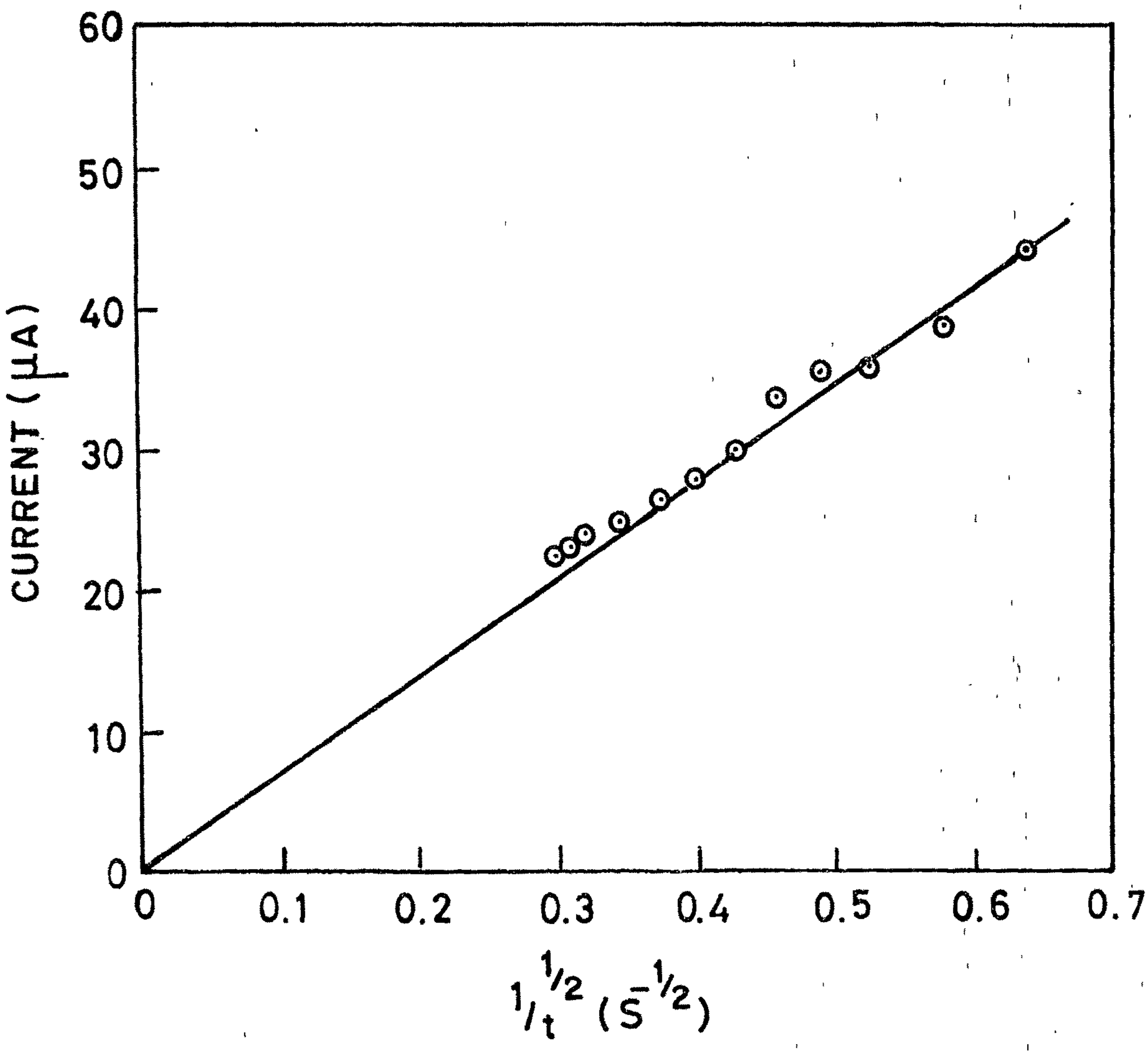

FIG.4.4.4. A TYPICAL PLOT OF RELATIONSHIP BETWEEN $1/t^{1/2}$ AND $i_{(t)}$ FOR Co^{++} ION, POTENTIAL STEP 0 TO -0.630 V Vs Ag / Ag^{+}.

The consolidated data for the potential steps, viz., 0 to -0.143 V, 0 to -0.241 V, 0 to -0.341 V, 0 to -0.444 V, 0 to -0.490 V, 0 to -0.581 V and 0 to -0.630 V are given in Table 4.4.2 together with the factor $i(t)\,t^{1/2}$. As can be seen from this Table, this factor remains constant within experimental errors for each potential step, thus providing evidence that the process is diffusion controlled. In several cases the straight line passes through zero when extrapolated, but in some cases it gave a small intercept as in the case of lead. Fig. 4.4.3 gives some of the typical curves obtained in the series of chronoamperograms taken for Co^{++} in the nitrate melt at 423 K. Fig. 4.4.4 gives the $t - i(t)$ relationship for one out of the series of chronoamperograms taken.

As in the case of lead, the diffusion coefficient of Co^{++} ion in the nitrate melt at 423 K was calculated using Cottrell's equation and the mean value was found to be 2.09×10^{-6} $cm^2\,s^{-1}$. The other relevant data has been given in the Tables and Figures.

4.4.3 Nickel

Chronoamperometry of Ni^{++} ions was done using $Ni(NO_3)_2$ as the solute, dissolved in 50 gm of solvent, i.e., the (Li, Na, K) NO_3 eutectic. Various potentials were used, right direct from 0 to -0.400 V to 0 to -0.800 V, in steps of 0.05 V, i.e., 0 to -0.400 V, 0 to -0.450, 0 to -0.500 V etc. The series

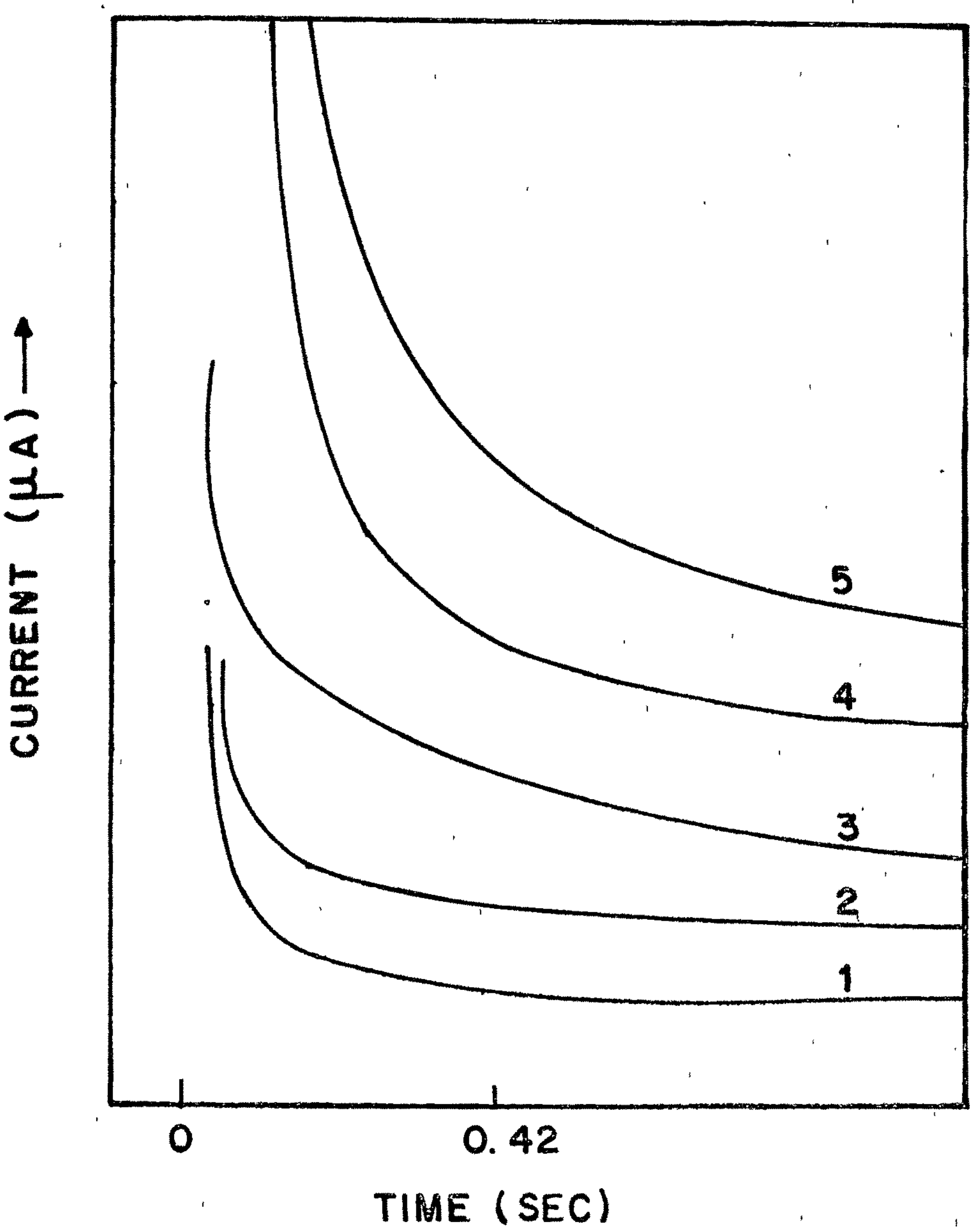

FIG. 4.4.5. CHRONOAMPEROGRAMS OF 1.37 x 10^{-6} mole cm^{-3} Ni^{++} ION RECORDED AT POTENTIAL STEPS FROM 0.0 V TO (1) -0.300, (2) -0.350, (3) -0.401, (4) -0.452, (5) -0.501 V Vs Ag/Ag^{+} ELECTRODE.

Table 4.4.3

Chronoamperometric Data on Ni^{++} Ion in
(Li, Na, K) NO_3 Eutectic at 423 ± 2 K

Concentration of Ni^{++} = 1.37×10^{-6} mole cm^{-3}

Potential step V vs Ag/Ag^+	Time s	Current $i_{(t)}$ µA	$i_{(t)}\ t^{\frac{1}{2}}$ µA $s^{\frac{1}{2}}$
0 to -0.4	0.72	6.0	5.09
	1.44	4.25	5.10
	2.16	3.40	4.99
	2.88	2.98	5.05
	3.60	2.59	4.91
	4.32	2.34	4.86
	5.04	2.17	4.87
	6.48	2.04	5.19
	7.20	1.91	5.12
0 to -0.45	0.72	6.80	5.77
	1.44	4.76	5.71
	2.16	3.91	5.74
	2.88	3.32	5.63
	3.60	2.89	5.48
	4.32	2.80	5.81
	5.04	2.55	5.72
	5.76	2.21	5.30
	6.48	2.12	5.39
	7.20	2.04	5.47
0 to 0.50	0.72	6.80	5.77
	1.44	4.76	5.71
	2.16	3.91	5.75

Contd.

Table 4.4.3 (Contd.)

Potential step V vs Ag/Ag^+	Time s	Current $i_{(t)}$ µA	$i_{(t)}\ t^{\frac{1}{2}}$ µA $s^{\frac{1}{2}}$
0 to 0.50	2.88	3.32	5.63
	3.60	2.89	5.48
	4.32	2.64	5.48
	5.04	2.47	5.55
	5.76	2.30	5.52
	6.48	2.13	5.42
	7.20	2.04	5.47
0 to 0.55	0.72	6.98	5.92
	1.44	5.10	6.12
	2.16	4.25	6.24
	2.88	3.74	6.34
	3.60	3.40	6.45
	4.32	3.06	6.36
	5.04	2.98	6.69
	5.76	2.80	6.72
	6.48	2.64	6.72
	7.20	2.55	6.84
0 to 0.60	0.72	9.70	8.23
	1.44	7.49	8.99
	2.16	6.30	9.26
	2.88	5.45	9.24
	3.60	5.10	9.67
	4.32	4.68	9.73
	5.04	4.42	9.92
	5.76	4.17	10.00
	6.48	4.00	10.18
	7.20	3.82	10.25

Contd.

Table 4.4.3 (Contd.)

Potential step V vs Ag/Ag^+	Time s	Current $i_{(t)}$ μA	$i_{(t)}\ t^{\frac{1}{2}}$ $\mu A\ s^{\frac{1}{2}}$
0 to -0.65	0.72	11.74	9.96
	1.44	9.02	10.82
	2.16	7.83	11.50
	2.88	6.89	11.69
	3.60	6.30	11.95
	4.32	5.96	11.68
	5.04	5.62	12.62
	5.76	5.28	12.67
	6.48	5.02	12.77
	7.20	4.94	13.25
0 to 0.70	0.72	17.04	14.46
	1.44	12.99	15.59
	2.16	10.22	15.02
	2.88	9.37	15.90
	3.60	8.52	16.16
	4.32	7.67	15.94
	5.04	7.24	16.25
	5.76	7.03	16.87
	6.48	6.82	17.36
	7.20	6.60	17.70
0 to -0.75	0.72	23.85	20.24
	1.44	19.59	23.50
	2.16	17.04	25.04
	2.88	14.19	24.08
	3.60	13.84	26.26

Contd.

Table 4.4.3 (Contd.)

Potential step V vs Ag/Ag^+	Time S	Current $i_{(t)}$ μA	$i_{(t)}\ t^{\frac{1}{2}}$ $\mu A\ s^{\frac{1}{2}}$
0 to -0.75	4.32	12.78	26.56
	5.04	11.93	26.78
	5.76	11.50	27.60
	6.48	11.07	28.18
	7.20	10.65	28.58
0 to -0.80	0.72	27.30	23.16
	1.44	24.30	29.16
	2.16	20.20	29.69
	2.88	18.10	30.72
	3.60	16.80	31.87
	4.32	16.00	33.26
	5.04	15.55	34.90
	5.76	14.27	34.25
	6.48	14.05	35.76
	7.20	13.84	37.13

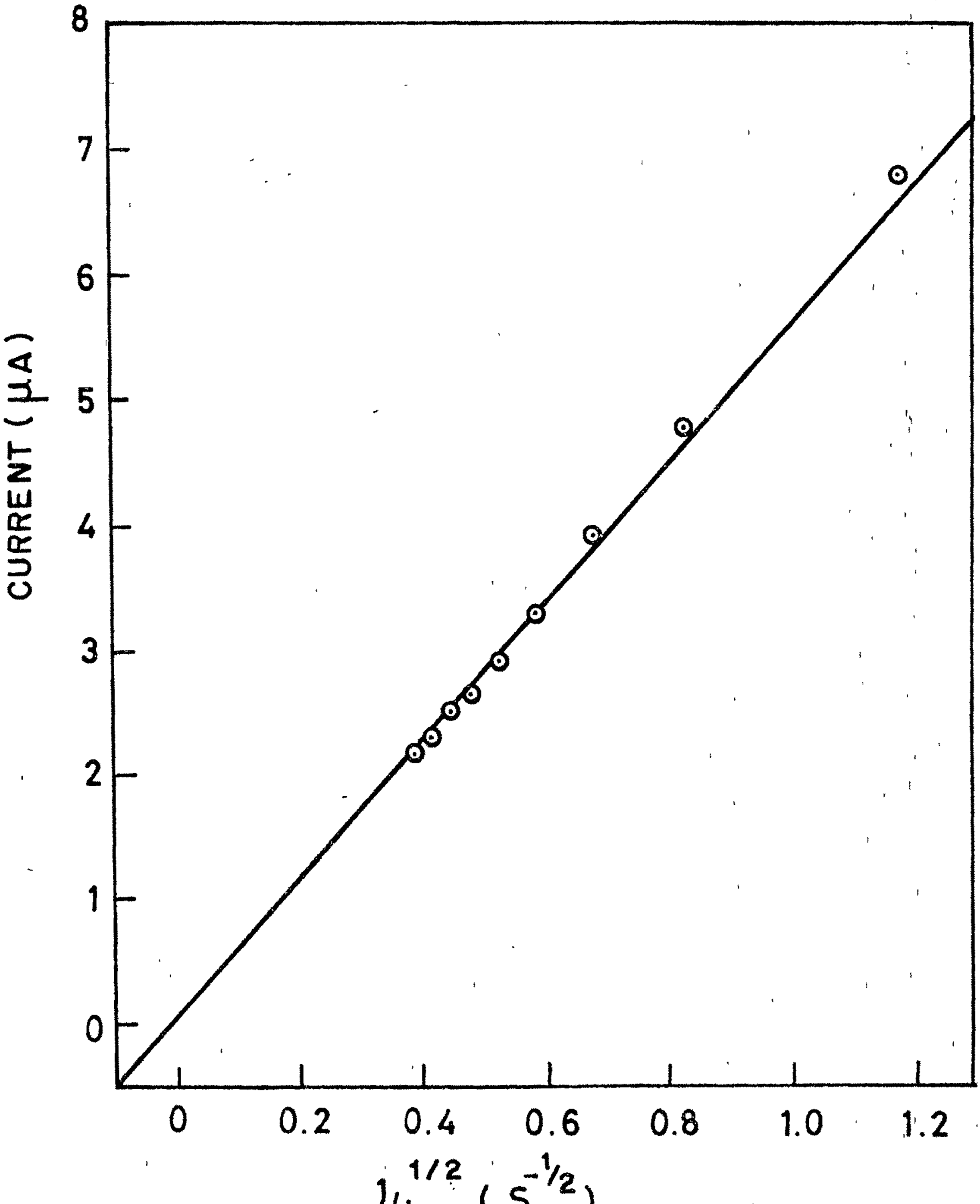

FIG. 4.4.6. A TYPICAL PLOT OF RELATIONSHIP BETWEEN $1/t^{1/2}$ AND $i_{(t)}$ FOR Ni^{++} ION, POTENTIAL STEP 0 TO -0.500 V Vs Ag/Ag^{+}.

of chronoamperograms obtained is depicted in Fig. 4.4.5 as a function of current i (t) and time. The factors i (t) $t^{\frac{1}{2}}$ and the measured quantities of i (t) and current are given in Table 4.4.3. As can be seen from this Table, the factor i (t) $t^{\frac{1}{2}}$ remains constant for each potential step indicating that the reduction process is diffusion controlled. A typical plot of t vs $t^{-\frac{1}{2}}$ for one of the potential steps is given in Fig. 4.4.6. As in the case of both lead and cobalt, in most of the cases the straight line passed through the origin, but in one or two cases there was a small intercept obtained. The implication of this intercept has already been explained in section 4.4.1. The diffusion coefficient of the Ni^{++} ion in the nitrate melt was calculated to be 3.59×10^{-7} cm^2 s^{-1} and some of the relevant data like concentration of the solute etc. are given in the Figures and Tables.

4.4.4 Iron

Chronoamperometry of iron or Fe^{+++} ions in the nitrate melt was done by taking $Fe(NO_3)_3$ as the solute. Various potential steps were taken and each of the curve so obtained was analysed for the current i (t) – t relationship. The various potential steps were from 0 to −0.095 V, 0 to −0.197, 0 to −0.291, 0 to −0.338, 0 to −0.390, 0 to −0.434, 0 to −0.467 and 0 to −0.666 V and consolidated data of i (t) and t together with the factor i (t) $t^{\frac{1}{2}}$ are given in Table 4.4.4. The series of curves obtained for the various potential steps is given in Fig. 4.4.7. The near constancy of the factor $i(t)\,t^{\frac{1}{2}}$ indicates that the process is diffusion controlled. This constancy is not as good as for the values of lead, nickel and cobalt; this may, perhaps, be due to the slightly erratic behaviour of the system due to atmospheric conditions. Another situation which was noticed was that none of the straight lines obtained by plotting $i(t)$ against $t^{-\frac{1}{2}}$ passed through the origin. At almost all the potential steps an intercept was found. A typical graph is given in Fig. 4.4.8.

The diffusion coefficient of Fe^{+++} ion was calculated using Cottrell's equation and the mean value from the various currents and potential steps was $6.33 \times 10^{-5}\ cm^2\ s^{-1}$. This was an order of ten, more than the values obtained for Pb^{++}, Co^{++} and Ni^{++}. The significance of this increase is discussed in the next chapter.

4.4.5 Copper

Chronoamperometry of copper in the nitrate melt was done by dissolving $Cu(NO_3)_2$ in the nitrate melt at 423 K. The data acquired were $i(t)$, current with respect to t, time. Various potential steps were used and the data consolidated, are given in Table 4.4.5. The series of curves obtained for various potential steps from 0 to -0.800 V vs Ag/Ag^+ is given in Fig. 4.4.9. The factor $i(t)\,t^{\frac{1}{2}}$, expressed as uA $s^{\frac{1}{2}}$, is seen to be constant for the various potential steps used.

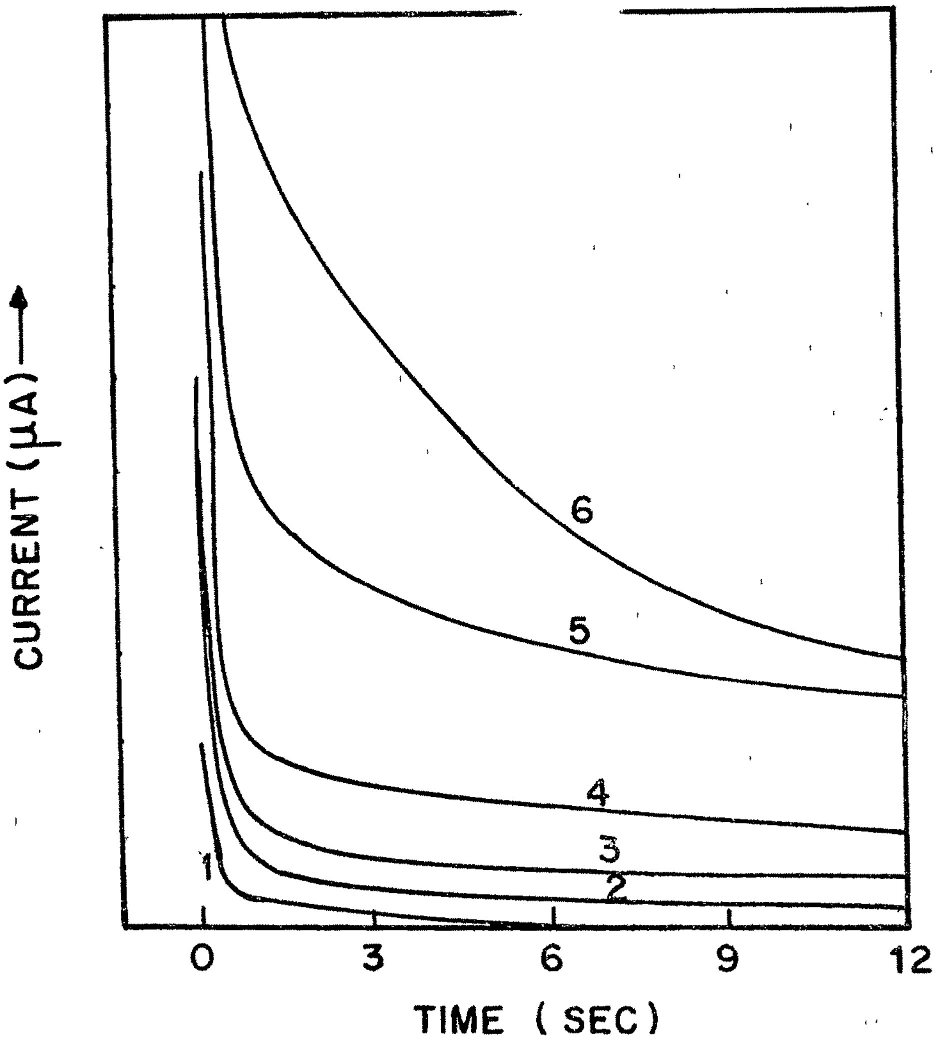

FIG. 4.4.7. CHRONOAMPEROGRAMS OF 1.39 x 10^{-6} mole cm^{-3} Fe^{+++} ION RECORDED AT POTENTIAL STEPS FROM 0.0 V TO (1) -0.095, (2) -0.197, (3) -0.244, (4) -0.338, (5) -0.390, (6) -0.434 V Vs Ag/Ag^{+} ELECTRODE.

Table 4.4.4

Chronoamperometric Data on Fe^{++} Ion in (Li, Na, K) NO_3 Eutectic at 423 ± 2 K

Concentration Fe^{++} = 1.39×10^{-6} mole cm^{-3}

Potential step V vs Ag/Ag^+	Time t s	Current $i_{(t)}$ μA	$i_{(t)}\ t^{1/2}$ μA $s^{1/2}$
0 to -0.95	0.3	9.57	5.24
	0.6	7.45	5.77
	0.9	4.26	4.04
	1.2	2.66	2.91
	1.8	1.86	2.49
	2.4	1.59	2.46
	3.6	1.06	2.02
0 to -0.197	1.2	5.05	5.53
	1.5	4.50	5.51
	2.4	3.52	5.43
	3.0	3.00	5.20
	3.6	2.65	5.03
	4.2	2.40	4.92
0 to -0.291	1.2	8.31	9.10
	1.8	7.00	9.39
	2.4	6.22	9.64
	3.6	4.79	9.09
	5.4	4.00	9.30
	7.8	3.48	9.72

Contd.

Table 4.4.4 (Contd.)

Potential step V vs Ag/Ag^+	Time t s	Current $i_{(t)}$ µA	$i_{(t)}\ t^{\frac{1}{2}}$ µA $s^{\frac{1}{2}}$
0 to 0.338	1.2	16.10	17.63
	1.8	13.20	17.71
	2.4	11.88	18.40
	3.0	10.02	17.36
	3.6	9.04	17.15
	4.2	8.41	17.23
	7.2	3.92	18.56
0 to 0.390	0.3	58.51	32.05
	0.6	42.55	32.96
	0.9	35.10	33.30
	1.2	31.91	34.96
	1.5	29.79	36.48
	2.4	26.59	41.19
	3.0	25.26	43.75
	3.6	24.20	45.91
	4.2	23.40	47.95
	6.0	21.28	52.12
0 to 0.434	2.4	42.10	65.22
	3.0	39.20	67.90
	3.6	36.30	68.87
	4.2	33.80	69.27
	5.4	30.20	70.18
	7.2	26.00	69.76
	9.0	23.35	70.05

Contd.

Table 4.4.4 (Contd.)

Potential step V vs Ag/Ag^+	Time t S	Current $i_{(t)}$ μA	$i_{(t)}\ t^{\frac{1}{2}}$ μA $s^{\frac{1}{2}}$
0 to -0.467	1.8	60.15	80.70
	2.4	49.10	76.07
	3.0	45.22	78.32
	3.6	42.50	80.64
	4.8	36.80	80.62
	7.2	30.40	81.57
	9.0	28.10	84.30
	10.0	26.00	82.22
	12.0	24.10	83.48
0 to -0.666	2.4	79.78	123.59
	3.0	69.15	119.77
	3.6	62.00	117.64
	4.2	59.04	120.99
	5.4	53.19	123.60
	6.0	51.06	125.07
	7.2	47.34	127.02
	8.4	44.68	129.49
	10.8	40.42	132.83
	12.0	38.30	132.67
	15.0	34.57	133.88
	18.0	31.91	135.88

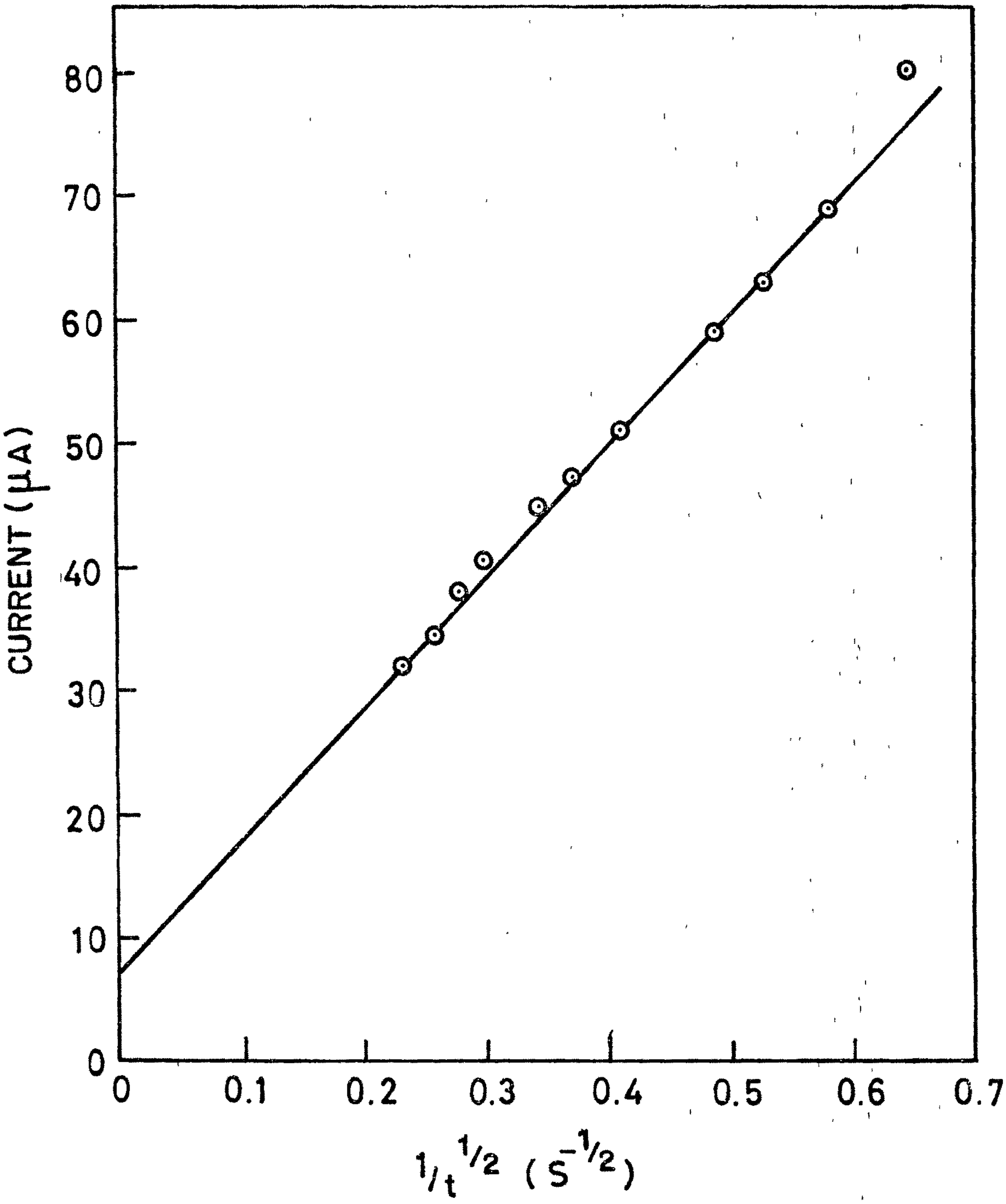

FIG.4.4.8. A TYPICAL PLOT OF RELATIONSHIP BETWEEN $1/t^{1/2}$ AND $i_{(t)}$ FOR Fe^{+++} ION, POTENTIAL STEP O TO −0.666 V Vs Ag/Ag^{+}.

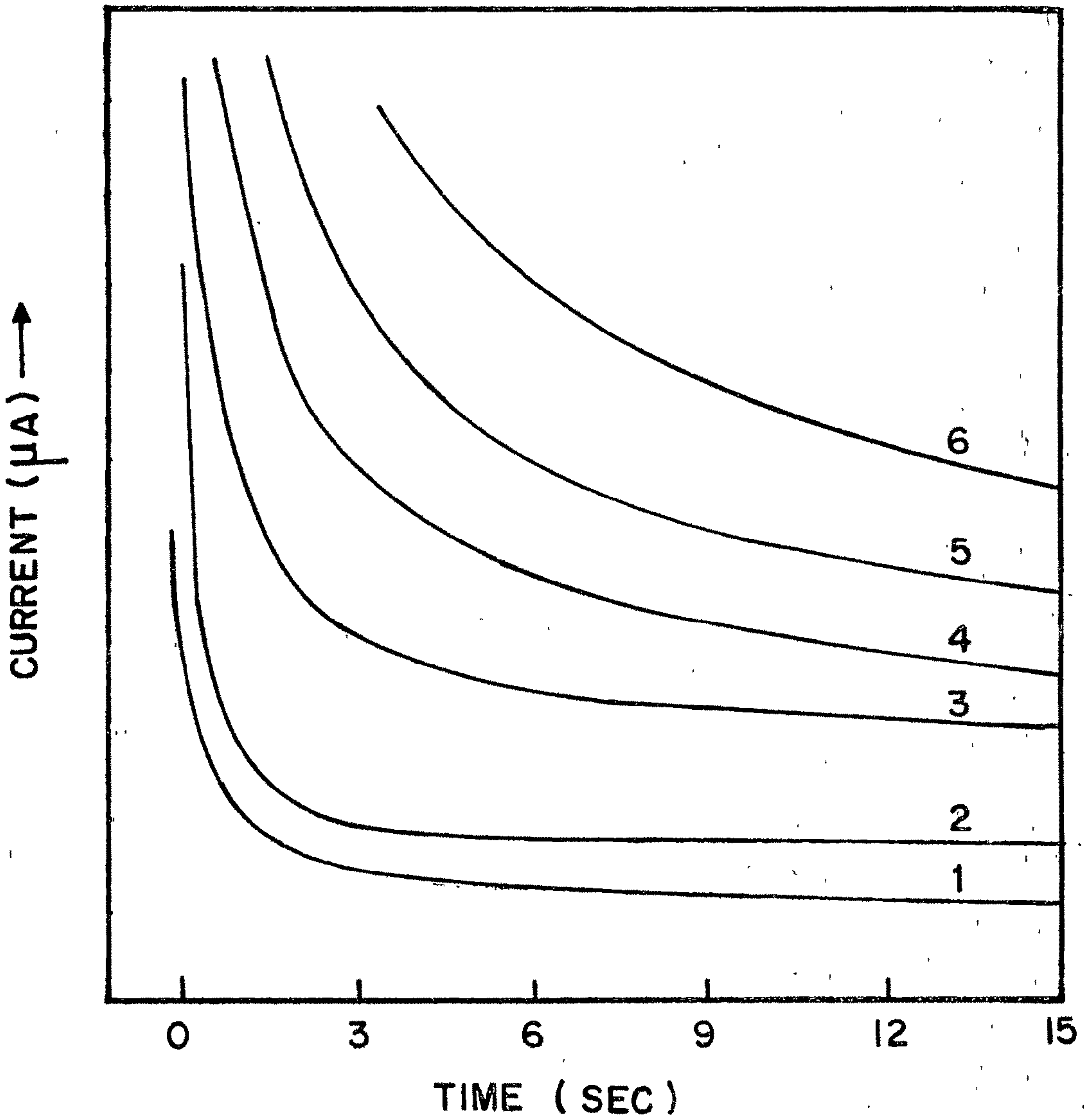

FIG. 4.4.9. CHRONOAMPEROGRAMS OF 4.36 x 10^{-6} mole cm^{-3} Cu^{++} ION RECORDED AT POTENTIAL STEPS FROM 0 V TO (1)-0.147,(2)-0.241, (3)-0.341,(4)-0.426,(5)-0.577,(6)-0.675 V Vs Ag/Ag^{+} ELETRODE.

Table 4.4.5

Chronoamperometric Data on Cu^{++} Ion in
(Li, Na, K) NO_3 Eutectic at 423 $\pm$ 2 K

Concentration of Cu^{++} = 4.36×10^{-6} mole cm^{-3}

Potential step V vs Ag/Ag^+	Time t s	Current $i_{(t)}$ µA	$i_{(t)}\ t^{\frac{1}{2}}$ µA $s^{\frac{1}{2}}$
0 to -0.147	0.6	20.21	15.65
	0.9	17.02	15.14
	1.2	14.89	16.31
	1.8	12.77	17.13
	2.4	11.70	18.12
	3.0	10.64	18.42
	4.2	9.57	19.61
	4.8	7.40	16.21
	9.0	6.45	19.35
	15.0	5.40	20.99
0 to -0.241	0.9	27.66	26.24
	1.2	23.34	24.47
	1.5	19.15	23.45
	1.8	16.49	22.12
	2.4	15.42	23.88
	3.0	14.09	24.40
	4.2	12.76	26.15
	4.8	11.17	26.54
0 to -0.341	0.6	58.51	45.32
	0.9	45.74	43.39
	1.2	40.95	44.86

Contd.

Table 4.4.5 (Contd.)

Potential step V vs Ag/Ag^+	Time t S	Current $i_{(t)}$ μA	$i_{(t)}\ t^{\frac{1}{2}}$ $\mu A\ s^{\frac{1}{2}}$
0 to -0.341	1.5	38.29	46.89
	1.8	36.17	48.53
	2.4	32.98	51.09
	3.0	30.32	52.51
	3.6	28.19	53.49
	4.2	26.57	54.49
	4.8	23.60	51.71
	7.2	18.78	50.39
0 to -0.426	1.8	58.51	78.50
	2.4	52.66	81.58
	3.0	47.87	82.29
	3.6	43.88	83.25
	4.2	40.95	83.92
	4.8	35.10	76.90
	5.4	36.70	85.28
	7.2	32.98	88.50
	9.0	30.85	92.55
0 to -0.525	3.0	59.57	103.20
	3.6	52.13	98.90
	4.2	47.87	104.88
	4.8	39.40	86.32
	5.4	38.92	90.44
	6.0	37.64	91.85
	7.8	34.04	95.07
	9.0	31.91	95.73

Contd.

Table 4.4.5 (Contd.)

Potential step V vs Ag/Ag^+	Time t S	Current $i_{(t)}$ µA	$i_{(t)}\ t^{\frac{1}{2}}$ µA $s^{\frac{1}{2}}$
0 to -0.525	10.8	29.79	97.90
	12.0	28.19	97.65
	15.0	26.06	100.90
	18.0	23.93	101.53
0 to -0.577	3.0	70.21	121.60
	3.6	61.70	117.06
	4.2	56.38	115.54
	4.8	46.80	102.53
	5.4	43.14	100.22
	7.8	42.55	118.84
	9.0	40.42	120.66
	10.2	38.30	122.33
	12.0	35.64	123.46
	15.0	32.97	127.73
0 to -0.675	3.0	95.50	165.41
	4.8	74.50	163.22
	6.6	71.27	183.09
	7.8	65.96	184.22
	9.0	61.17	183.51
	10.2	57.44	183.44
	11.4	54.25	183.17
	13.2	50.53	183.58
	14.4	48.40	183.67
	15.6	46.80	184.85
	16.8	44.68	183.13
	18.0	43.08	182.77
	21.0	39.89	182.80
	24.0	37.76	184.98

Contd.

Table 4.4.5 (Contd.)

Potential step V vs Ag/Ag^+	Time t S	Current $i_{(t)}$ μA	$i_{(t)}\ t^{\frac{1}{2}}$ μA $s^{\frac{1}{2}}$
0 to -0.805	3.0	112.50	195.00
	4.8	85.10	186.44
	7.2	77.65	208.35
	8.4	72.33	209.63
	9.6	68.08	210.94
	10.8	64.89	213.25
	12.0	61.70	213.74
	13.2	59.04	214.50
	14.4	56.65	214.97
	15.6	54.78	216.36
	16.8	52.65	215.80
	18.0	51.33	217.77
	21.0	47.87	219.36
	24.0	45.21	221.48
	30.0	30.95	224.29

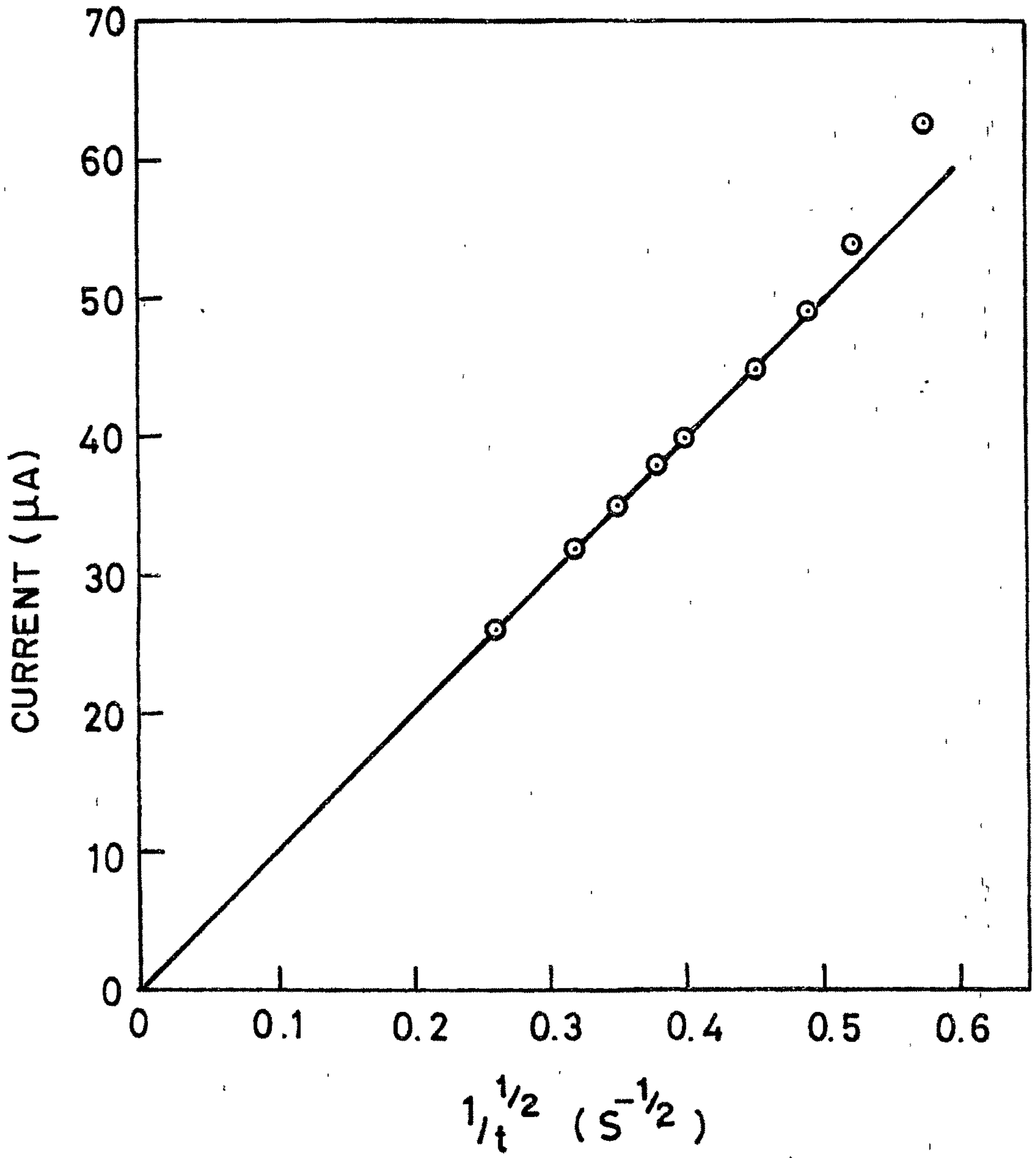

FIG. 4.4.10. A TYPICAL PLOT OF RELATIONSHIP BETWEEN $1/t^{1/2}$ AND $i_{(t)}$ FOR Cu^{++} ION, POTENTIAL STEP 0 TO −0.480 V Vs Ag/Ag^{+}.

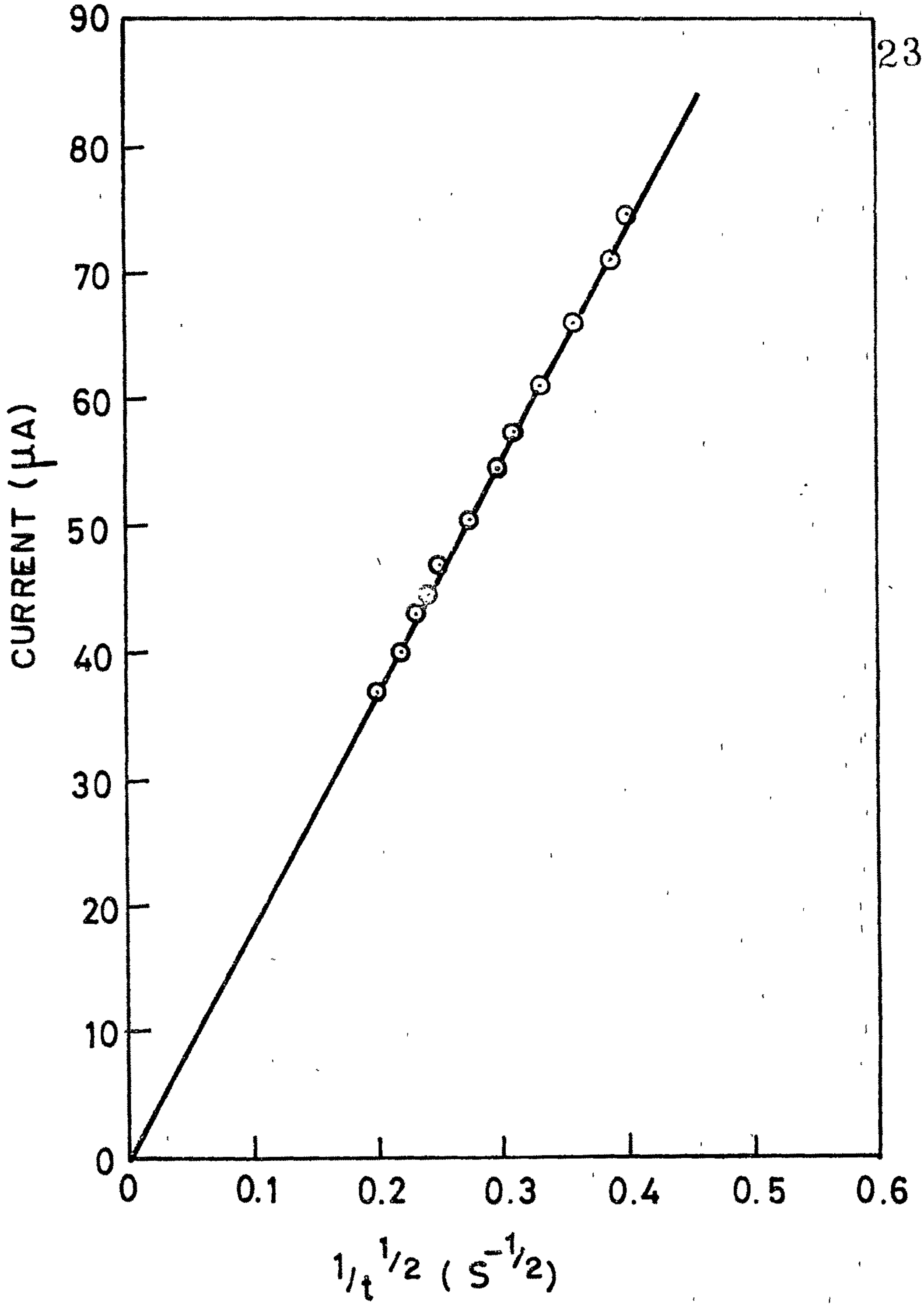

FIG. 4.4.11. A TYPICAL PLOT OF RELATIONSHIP BETWEEN $1/t^{1/2}$ AND $i_{(t)}$ FOR Cu^{++} ION, POTENTIAL STEP 0 TO −0.675 V Vs Ag/Ag^{+}

Fig. 4.4.10 and Fig. 4.4.11 depict the relationship between i (t) and $t^{\frac{1}{2}}$ and it can be seen from the figures that for both the relations i (t) = t = 0 holds good. In some of the plots a small intercept was found. The constancy of the factor i (t) $t^{\frac{1}{2}}$ shows that the reaction was controlled by diffusion and that Cottrell's equation can be applied. The mean value of the diffusion coefficient was found to be 5.23×10^{-6} $cm^2 s^{-1}$ for the Cu^{++} ion, of the same order as those for Pb^{++}, Co^{++} and Ni^{++}. The reason, behind the two figures, viz., Figs. 4.4.10 and 4.4.11 being mentioned, will be given in the next chapter. The diffusion coefficients were calculated at different potential steps, the lowest and highest, and they were not found to vary in their order.

4.5 SAMPLED CURRENT VOLTAMMETRY

In sampled current voltammetry one utilises the data obtained on the chronoamperometric experiments of a system. The only quantitative data which can be obtained from chronoamperometry is the diffusion coefficient and this, too, only if it is confirmed that the reaction is diffusion controlled. The standard electron transfer rate constant values can be obtained under certain circumstances, but it was not attempted in the present case, as the other conditions, discussed in section 4.4.1 have not been fulfilled. As discussed in chapter 2, the current obtained at different potential steps were sampled at different times, designated as τ and such values of currents are plotted as a function of potentials to obtain a sampled current voltammogram. In the next few pages are given the results of this technique.

4.5.1 Lead

As discussed earlier, in sampled current voltammetry potential step (under diffusion control) data, i.e., the relationship between i (t) and t, are used for further calculations. No further experiments are to be performed.

Fig. 4.4.1 gives the relationship between i (t) and t for the various potential steps and the data is given in Table 4.4.1. All the potential steps performed are not given in this Table because of the paucity of space. On the basis of the fair indication that the reaction is not reversible, a certain value of τ is to be fixed at which the value of the current i (t) has to be measured. Table 4.5.1 gives the list of the 16 potential steps performed. Several values of τ were chosen, viz., 4, 5, 6, 7 s etc. The currents at $t = \tau = 6$ s are listed in this Table. This current can now be termed as i (τ). This i (τ) is then plotted against the potential of the 16 steps in Fig. 4.5.1. An S - shaped curve is obtained. The shape of S - curve becomes more drawn out as the reversible nature of the process is reduced. The more irreversible the process is, the more drawn out the curve will be. In this respect the curve is similar to a

Table 4.5.1

Data on Sampled Current Voltammetry of Pb^{++} Ion in (Li, Na, K) NO_3 Eutectic at 423 $\pm$ 2 K

Concentration of Pb^{++} = 2.02×10^{-6} mole cm^{-3}

τ = 6.0 s

Potential E V vs Ag/Ag^+	$i_{(\tau)}$ μA
-0.136	0.96
-0.191	1.60
-0.240	2.30
-0.289	3.40
-0.306	4.47
-0.424	8.50
-0.472	15.20
-0.520	15.40
-0.570	20.20
-0.613	24.50
-0.669	28.70
-0.718	29.80
-0.766	38.80
-0.824	55.90
-0.890	92.60

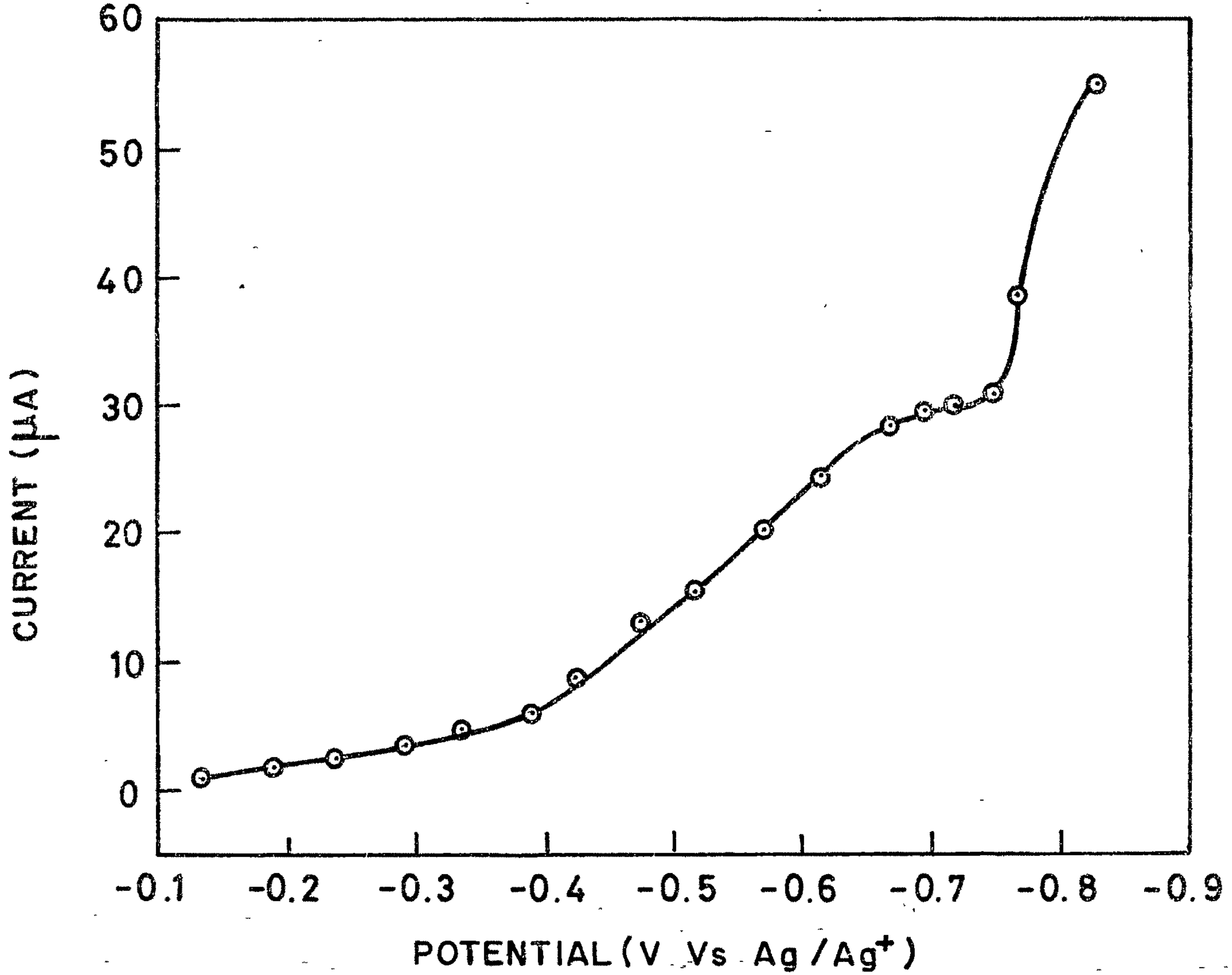

FIG. 4:5.1. A TYPICAL SAMPLED CURRENT VOLTAMMOGRAM OF Pb^{++} ION.

polarographic wave. The current becomes limiting current after a certain voltage and thus remains constant. This current is measured and is termed i_d and can be considered as the diffusion current of the polarographic wave. In the present case this was measured as 20.00 μA. The value of the potential at $i_{d(\tau)}/2$ or at half the diffusion current is equal to $E_{\frac{1}{2}}$ or the half-wave potential. This value was found to be -0.535 V vs Ag/Ag^+. The analysis of the S-shaped curve was then done by measuring the current at potentials on the ascending portion of the graph. These values of the potentials and currents are listed in Table 4.5.2. This quantity is termed as $i_{d(\tau)}$. The factor $i_{d(\tau)} / i_{d(\tau)} - i_{(\tau)}$ was then calculated and the square root of this factor is also given in Table 4.5.2. The quantity $k_{f,h}$ is then calculated from the formula

$$k_{f,h} = \left[\left(\frac{D_o}{2\tau}\right)\right]^{\frac{1}{2}} \left[\frac{i_{d(\tau)}}{i_{d(\tau)} - i_{(\tau)}}\right]^{\frac{1}{2}} \qquad 2.77$$

Here the value of D_o has been taken as 2.01×10^{-6} cm^2 s^{-1}, the value determined from chronoamperometry.

The values of $k_{f,h}$ then calculated are given in Table 4.5.2. The equation

$$\log k_{f,h} = \log k_{s,h} \; \frac{-\alpha_c n_\alpha F}{2.303\,RT} (E - E^o) \qquad 2.79$$

is then utilised to obtain the transfer coefficient $\alpha_c n_\alpha$ and

Table 4.5.2

Relationship between Potential E and log $k_{f,h}$ at $\tau = 6.0$ s

Diffusion current $i_{d(\tau)} = 20.00\ \mu A$

Potential E V vs Ag/Ag^+	$i_{(\tau)}$ μA	$\left[\frac{i_{d(\tau)}}{i_{d(\tau)} - i_{(\tau)}}\right]^{\frac{1}{2}}$	$k_{f,h}$ x 10^4 cm s^{-1}	log $k_{f,h}$
-0.425	2.5	1.069	4.01	-3.397
-0.450	4.0	1.118	4.20	-3.377
-0.475	5.5	1.174	4.41	-3.356
-0.500	7.5	1.265	4.75	-3.324
-0.525	9.0	1.348	5.06	-3.296
-0.550	11.0	1.491	5.60	-3.252
-0.575	13.0	1.690	6.34	-3.198
-0.600	14.5	1.907	7.16	-3.145
-0.625	16.5	2.390	9.00	-3.047
-0.650	18.0	3.160	11.86	-2.926
-0.675	19.0	4.472	16.78	-2.775

also $k_{s,h}$. A plot of log $k_{f,h}$ vs E (Fig. 4.5.2) gives a straight line with the slope equal to $\frac{\alpha_c n_\alpha F}{2.303 RT}$ and the intercept equal to log $k_{s,h}$. The value of the slope was found to be 1.356 from which the transfer coefficient $\alpha_c n_\alpha$ worked out to be 0.114. The value of $k_{s,h}$ is the value of $k_{f,h}$ when $E = 0$, i.e., when $E = E^o$, where E^o is the formal potential of the system. This value was taken as -0.535 V, i.e. $E_{\frac{1}{2}}$ obtained from Fig. 4.5.1. The value of $k_{s,h}$ was calculated to be 5.32×10^{-4} cm s^{-1} and log $k_{s,h}$ is equal to -3.27. As per equation 2.79, log $k_{f,h}$ has to be plotted against $E - E^o$, but in all the cases the plots are made as a function of E and the intercept taken when $E = E^o$.

4.5.2 Cobalt

The chronoamperometric data obtained in section 4.4.2 have been used in the present case for the calculations on the sampled current voltammetry of Co^{++} ions. The measured parameters in this case were i (t) in μA and t in seconds.

First of all a choice was made to select a particular value of τ for the calculation of $i(\tau)$. τ selected were 2, 2.5, 2.88, 3 and 3.5 seconds. Out of these the data at $\tau = 3.6$ s have been selected and listed in Table 4.5.3 which gives the potentials E against the corresponding value of $i_{(\tau)}$. This data was plotted in Fig. 4.5.3 and gave a S-shaped curve with a diffusion current $i_{d(\tau)}$ of 28.00 μA.

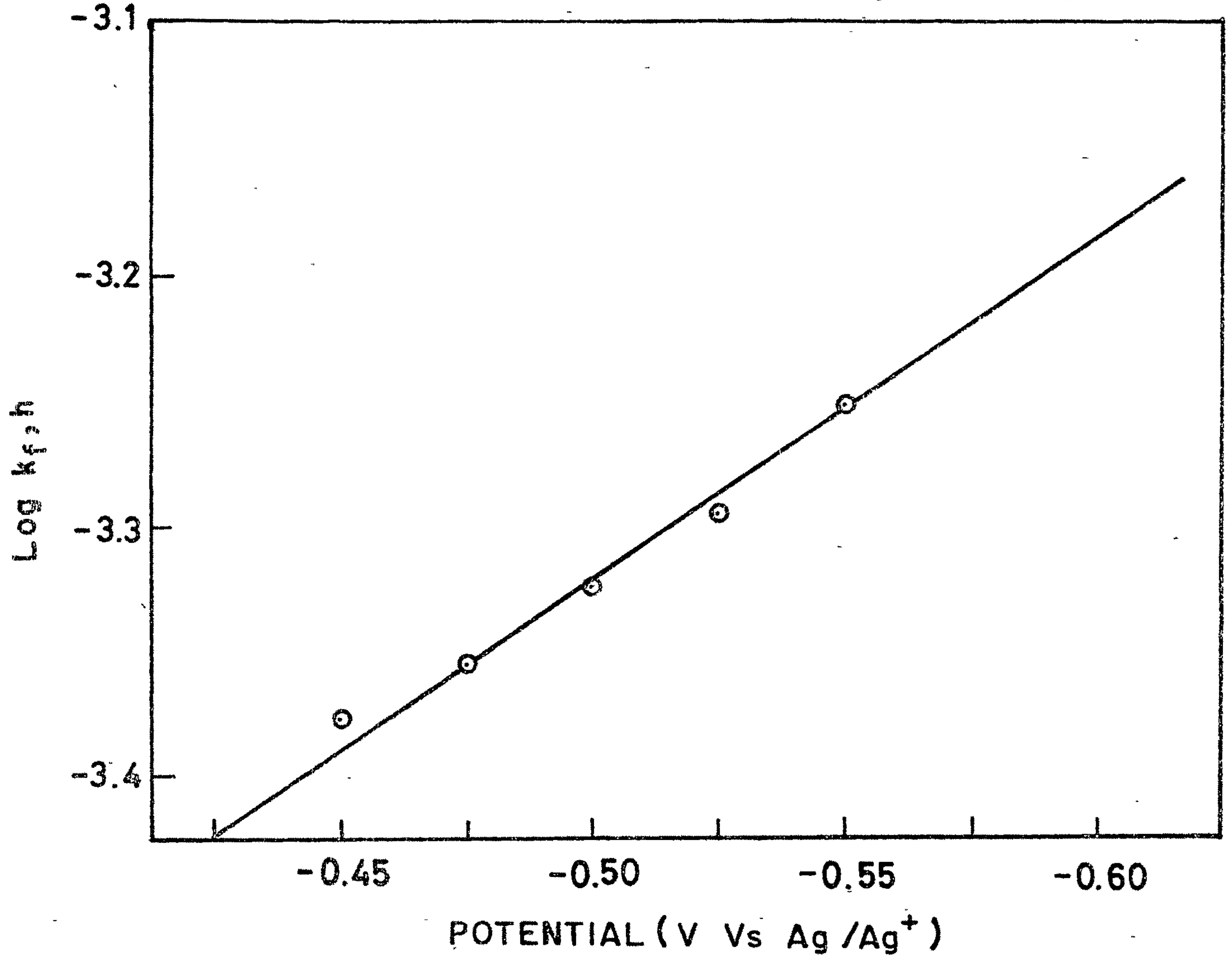

FIG.4.5.2. A PLOT OF E Vs LOG k_f,h FOR FINDING OUT $\alpha_c n_\alpha$ AND k_s,h FOR Pb^{++} ION.

Table 4.5.3

Data on Sampled Current Voltammetry of Co^{++} Ion in (Li, Na, K) NO_3 Eutectic at 423 ± 2 K

Concentration of Co^{++} = 2.054×10^{-6} mole cm^{-3}

τ = 3.6.0 s

Potential E V vs Ag/Ag^+	$i_{(\tau)}$ μA
-0.097	0.70
-0.143	1.30
-0.197	2.20
-0.241	3.20
-0.290	4.80
-0.314	5.30
-0.396	11.70
-0.444	16.50
-0.490	24.50
-0.513	30.90
-0.581	38.30
-0.678	44.70
-0.725	63.80

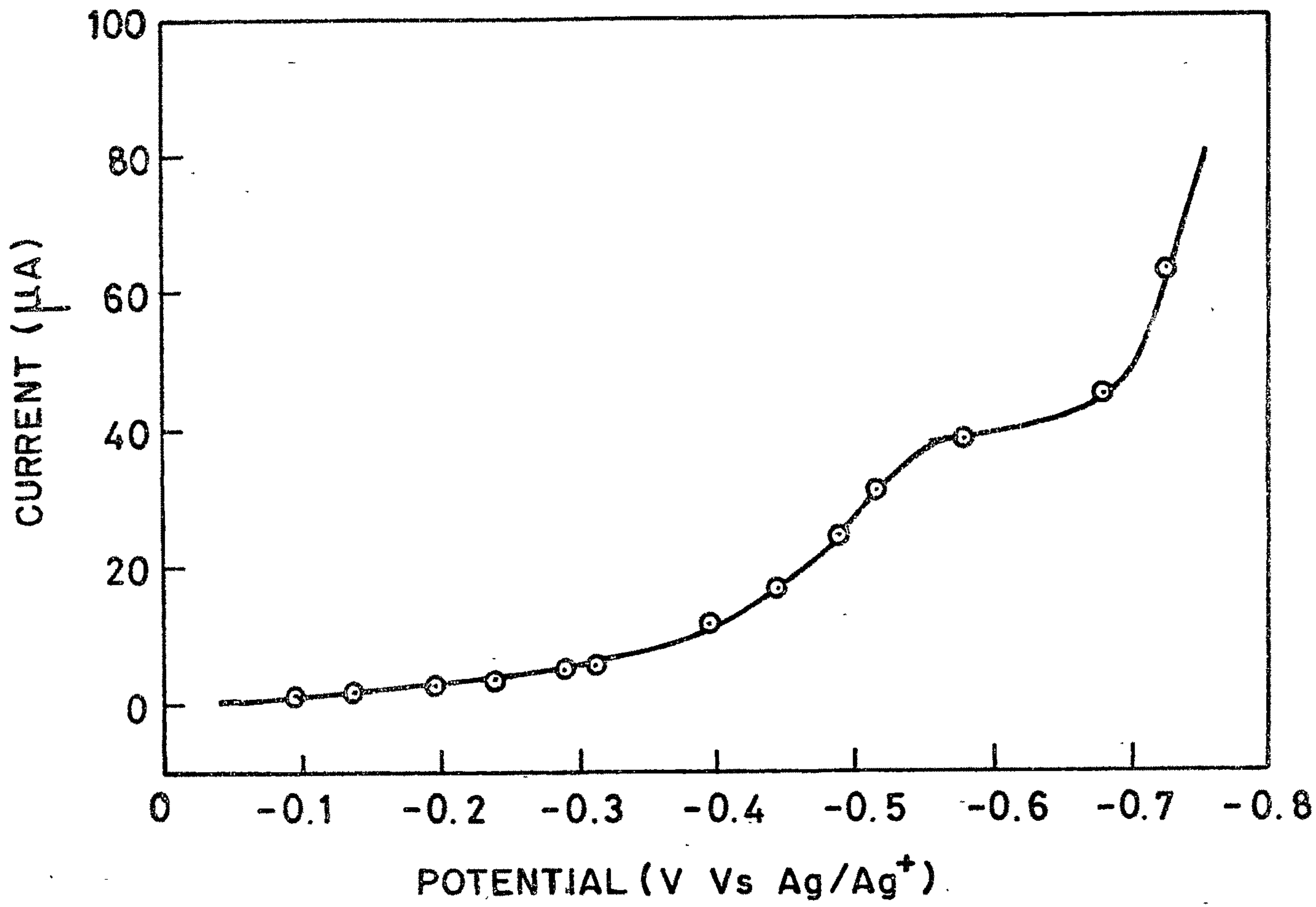

FIG. 4.5.3. A TYPICAL SAMPLED CURRENT VOLTAMMOGRAM OF Co^{++} ION.

The curve was drawn out as can be seen from Fig. 4.5.3 showing the irreversible nature of the process. The $E_{\frac{1}{2}}$ value, i.e., the value of the potential at which current was 14.00 μA, was found to be -0.475 V vs Ag/Ag^+. A discussion of this value will be given in the next chapter. Table 4.5.4 then gives the values on the analysis of this wave. As in the case of lead, several potentials were chosen along the lower and upper limiting potentials and along the ascending part of the curve and the corresponding $i_{(\tau)}$ were measured and calculated. This data together with the values of $\left[i_{d(\tau)} / i_{d(\tau)} - i_{(\tau)} \right]^{\frac{1}{2}}$ are given in Table 4.5.4. The $k_{f,h}$ values were calculated, then, using the equation

$$\log k_{f,h} = \frac{(D_o)^{\frac{1}{2}}}{\sqrt{2} \quad \tau^{\frac{1}{2}}} \quad \left[\frac{i_{d(\tau)}}{i_{d(\tau)} - i_{(\tau)}} \right]^{\frac{1}{2}} \qquad 2.77$$

The values of $k_{f,h}$ and $\log k_{f,h}$ are also given in Table 4.5.4. The plot of $\log k_{f,h}$ vs E is given in Fig. 4.5.4. The value for D_o for the computation of $k_{f,h}$ values was taken from section 4.4.1 and was 2.09×10^{-6} cm^2 s^{-1} and τ was 3.6 s. The relationship was linear and gave the value of $\alpha_c n_\alpha$ as 0.201 and $\log k_{s,h}$ as -2.66. The value of $k_{s,h}$ works out to be 2.19×10^{-3} cm s^{-1}. The discussion of the significance of these values is given in chapter 5.

4.5.3 Nickel

As in the case of lead and coblt, the chronoamperometric data given in Table 4.4.3 were utilised to calculate the sampled

Table 4.5.4

Relationship between Potential E and log $k_{f,h}$ at τ = 6.0 s

Diffusion current $i_{d(\tau)}$ = 28.00 μA

Potential E V vs Ag/Ag^+	$i_{(\tau)}$ μA	$\left[\dfrac{i_{d(\tau)}}{i_{d(\tau)} - i_{(\tau)}}\right]^{1/2}$	$k_{f,h}$ x 10^4 cm s^{-1}	log $k_{f,h}$
-0.400	5.00	1.10	8.89	-3.05
-0.425	7.00	1.15	9.29	-3.03
-0.450	9.50	1.22	9.86	-3.01
-0.475	13.00	1.38	11.15	-2.95
-0.500	18.00	1.62	13.09	-2.88
-0.525	23.00	2.20	17.77	-2.75
-0.550	26.50	3.40	27.47	-2.56

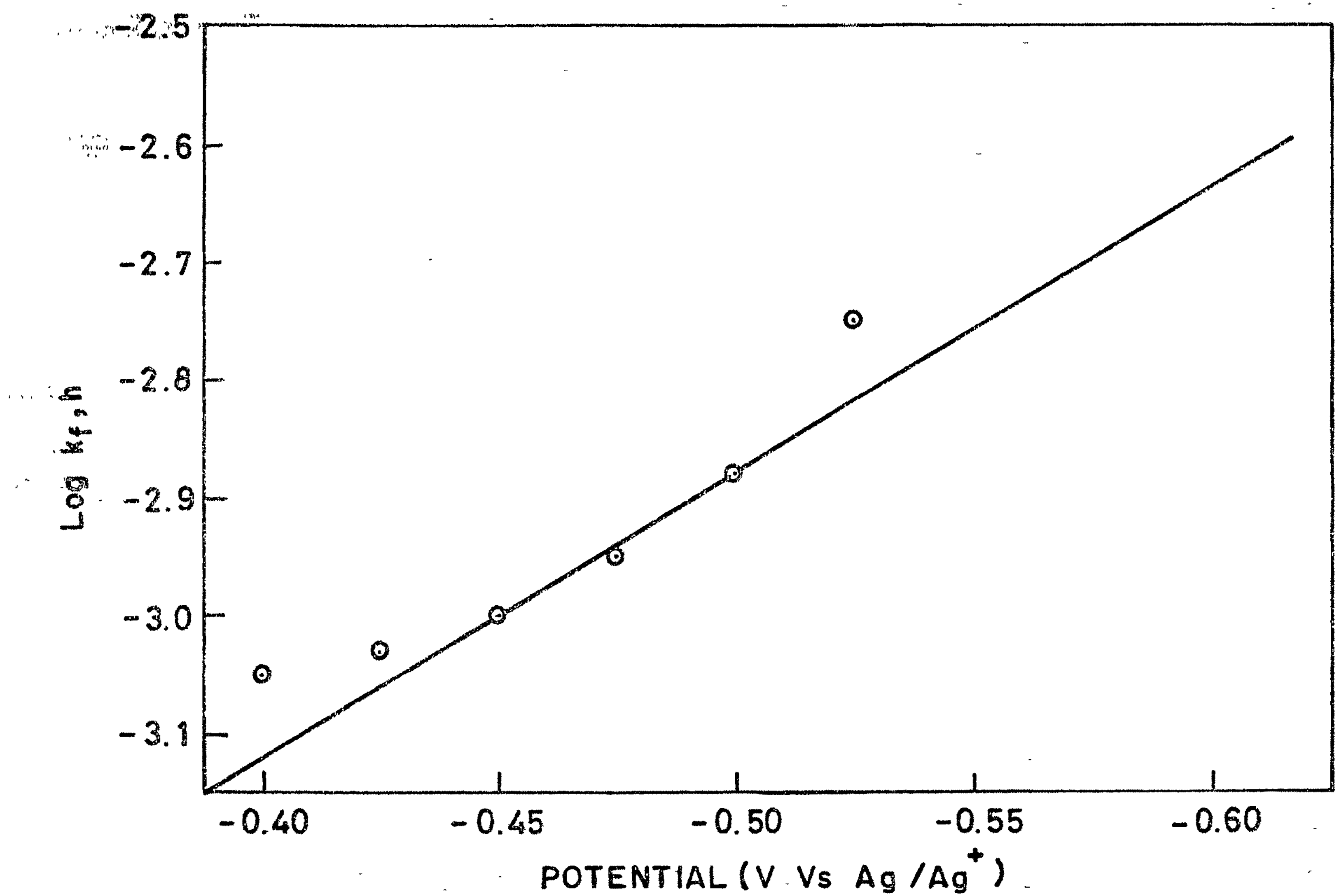

FIG. 4.5.4. A POLT OF E Vs LOG $k_{f,h}$ FOR FINDING OUT $\alpha_c n_\alpha$ AND $k_{s,h}$.

current voltammogram of nickelous ion. The measured quantities in this Table were $i_{(t)}$ and t. As in the earlier cases suitable time intervals τ_i were chosen. One typical case where $\tau = 6.48$ s has been cited here and data for this value of τ is given in Table 4.5.5. This data has been plotted in Fig. 4.5.5 and gave an S-shaped curve with an $i_{d(\tau)}$ value of 2.60 μA. The $E_{\frac{1}{2}}$ value was found to be −0.585 V. The long drawn-out nature of the graph points out to the irreversible nature of the process. The curve was then analysed and $i_{(\tau)}$ values were found out for the potential values connected with the curve. These values are given in Table 4.5.6 together with the factor $\left[i_{d(\tau)} / i_{d(\tau)} - i_{(\tau)} \right]^{\frac{1}{2}}$.

These values were utilised to calculate $k_{f,h}$ values using equation 2.77. The log $k_{f,h}$ values so obtained were plotted against the respective potentials (Fig. 4.5.6) and from the slope the value of the transfer coefficient $\alpha_c n_\alpha$ was calculated to be 0.315. The intercept value at $E = E_{\frac{1}{2}}$ was equal to log $k_{s,h}$ equal to −3.62. The value of $k_{s,h}$ was found to be 2.4×10^{-4} cm s^{-1}.

4.5.4 Iron

The chronoamperometric data given in section 4.4.4 have been used in this section to obtain sampled current voltammogram of Fe^{+++} ion in nitrate melt at 423 K. The relevant data are given in Table 4.4.4.

As usual in sampled current voltammetry values of τ were chosen for the construction of voltammograms. Out of these values

Table 4.5.5

Data on Sampled Current Voltammetry of Ni^{++} Ion in (Li, Na, K) NO_3 Eutectic at 423 $\pm$ 2 K

Concentration of Ni^{++} = 1.37×10^{-6} mole cm^{-3}

τ = 6.48 s

Potential E V vs Ag/Ag^+	$i_{(\tau)}$ μA
-0.400	1.83
-0.450	2.12
-0.500	2.13
-0.550	2.64
-0.600	4.00
-0.650	5.02
-0.700	6.82
-0.750	11.07
-0.800	14.05

Table 4.5.6

Relationship between Potential E and log $k_{f,h}$ at $\tau = 6.48$ s

Diffusion current $i_{d(\tau)} = 2.6$ μA

Potential E V vs Ag/Ag^+	$i_{(\tau)}$ μA	$\left[\frac{i_{d(\tau)}}{i_{d(\tau)} - i_{(\tau)}}\right]^{1/2}$	$k_{f,h}$ $\times 10^4$ cm s^{-1}	log $k_{f,h}$
-0.550	0.50	1.11	1.85	-3.73
-0.563	0.70	1.17	1.94	-3.71
-0.575	1.00	1.28	2.12	-3.67
-0.588	1.30	1.41	2.35	-3.63
-0.600	1.60	1.61	2.68	-3.57
-0.613	2.10	2.28	3.79	-3.42
-0.625	2.30	2.95	4.89	-3.31

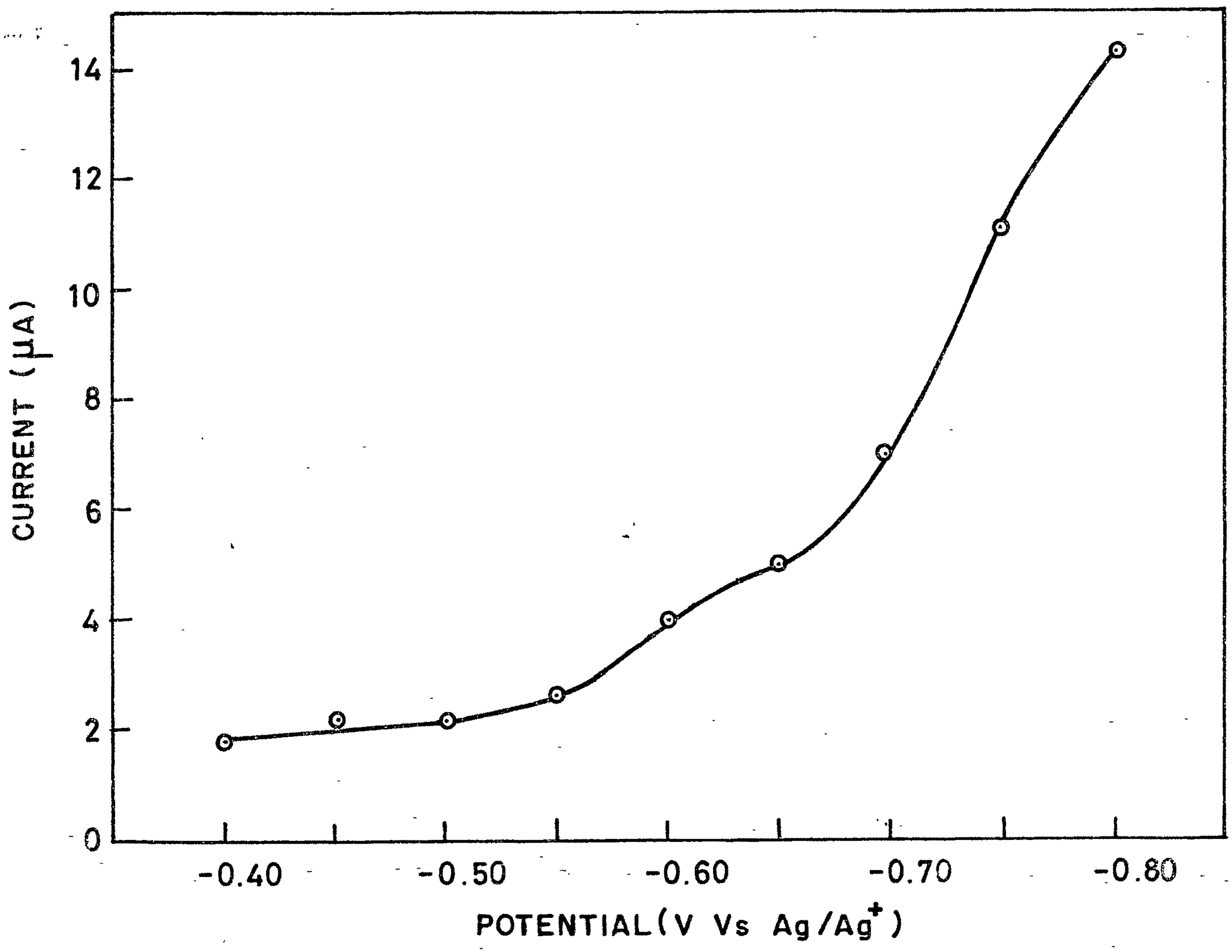

FIG. 4:5.5. A TYPICAL SAMPLED CURRENT VALTAMMOGRAM OF Ni^{++} ION.

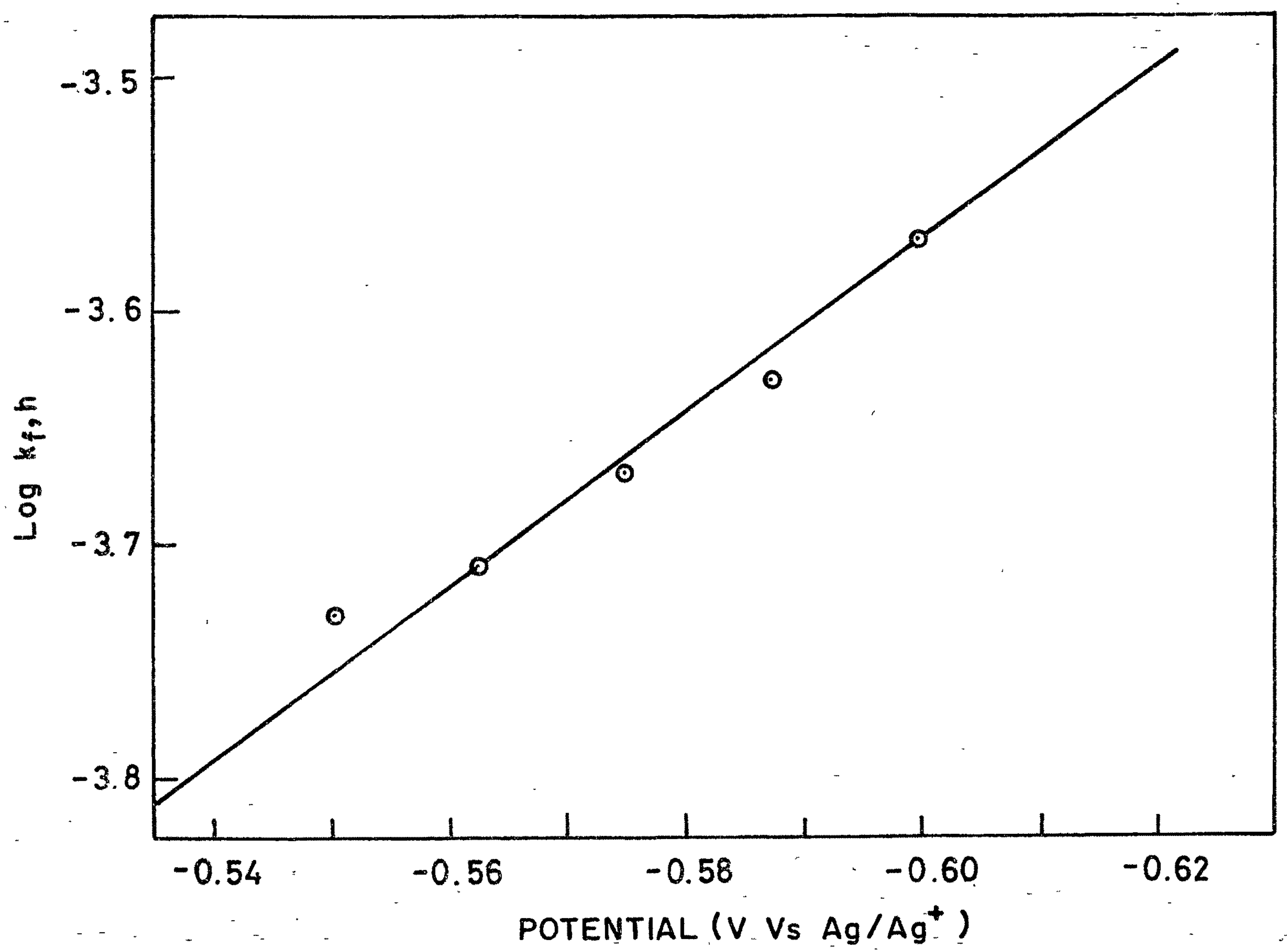

FIG. 4.5.6. A PLOT OF E Vs LOG k_f, h FOR FINDING OUT $\alpha_c n_\alpha$ AND k_s, h.

the data at $\tau = 4.8$ s are given here. This data is listed in Table 4.5.7 and consists of the potential values E and the currents $i_{(\tau)}$. This data was used for plotting the sampled current voltammogram and the relationship is depicted graphically in Fig. 4.5.7. As can be seen from this figure the curve is not very much drawn out, but at the same time the rise in the current is not very sharp. The $i_{d(\tau)}$ was measured to be 50.00 µA and the $E_{\frac{1}{2}}$ was found to be -0.415 V. The curve was then analysed for $i_{(\tau)}$ - E relationship. The values of $i_{(\tau)}$ for the various values of potential are given in Table 4.5.8 together with the factor $\left[i_{d(\tau)} / i_{d(\tau)} - i_{(\tau)} \right]^{\frac{1}{2}}$. Fig. 4.5.8 gives the relationship between $k_{f,h}$ and the potential E. Here $k_{f,h}$ was calculated using equation 2.77. The linear relationship gave a slope of 3.2 from which the transfer coefficient was calculated to be 0.269. The intercept gave the value of log $k_{s,h}$ as -2.83 and $k_{s,h}$ was calculated to be 1.50×10^{-3}.

4.5.5 Copper

The chronoamperometric data given in section 4.4.5 have been used to construct sampled current voltammograms for Cu^{++} ion in nitrate melt at 423 K. The relevant data are given in Table 4.4.5 and Fig. 4.4.9. As usual values of were chosen for the sampling the current and ranged from $\tau = 4.8$ to $\tau = 8.0$ s. The data at $\tau = 4.8$ s only is being cited in the present text due to paucity of space and for

Table 4.5.7

Data on Sampled Current Voltammetry of Fe^{+++} Ion in (Li, Na, K) NO_3 Eutectic at 423 ± 2 K.

Concentration of Fe^{+++} = 1.39×10^{-6} mole cm^3

τ = 3.60 s

Potential E V vs Ag/Ag^+	$i(\tau)$ µA
-0.095	1.06
-0.143	2.12
-0.197	2.65
-0.244	3.18
-0.291	4.79
-0.338	9.04
-0.390	24.20
-0.434	36.30
-0.467	42.55
-0.579	57.00
-0.666	62.00

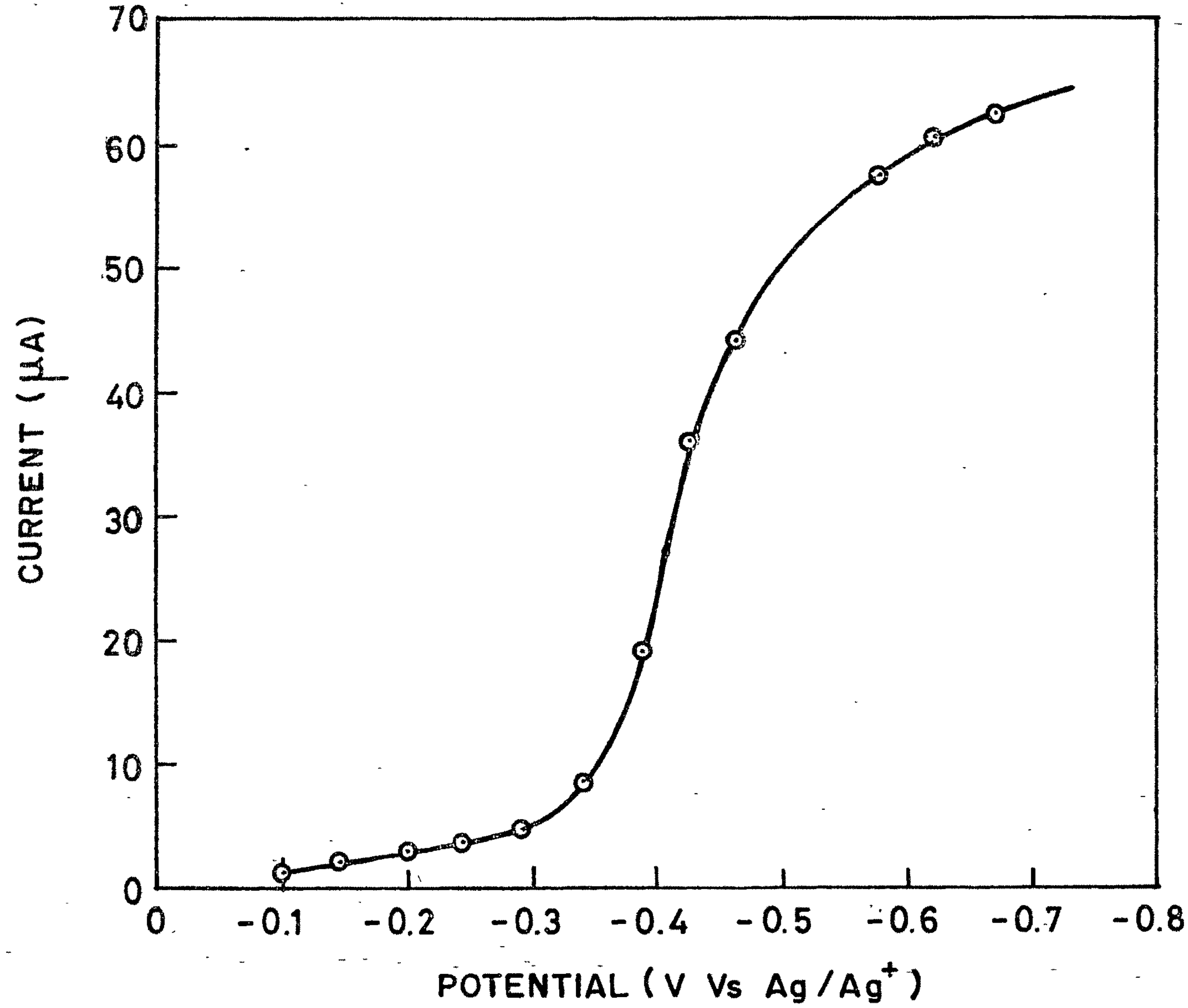

FIG. 4:5.7. A TYPICAL SAMPLED CURRENT VOLTAMMOGRAM OF Fe^{+++} ION.

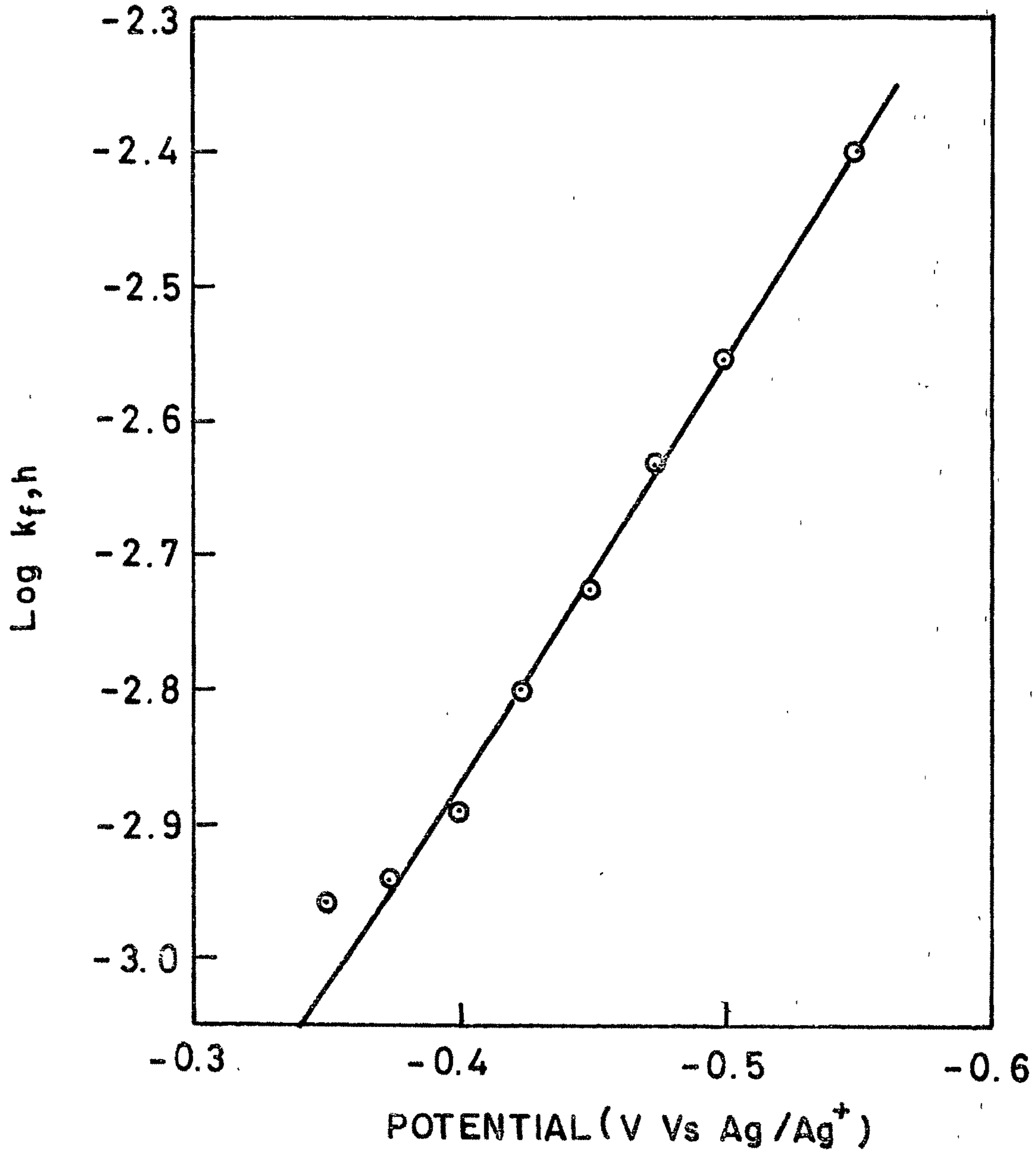

FIG.4:5.8. A PLOT OF E Vs LOG k_f,h FOR FINDING OUT $\alpha_c n_\alpha$ AND k_s,h.

Table 4.5.8

Relationship between Potential E and log $k_{f,h}$ at $\tau = 3.60$ s

Diffusion current $i_{d(\tau)} = 50.00$ μA

Potential E V vs Ag/Ag^+	$i_{(\tau)}$ uA	$\left[\dfrac{i_{d(\tau)}}{i_{d(\tau)} - i_{(\tau)}}\right]^{\frac{1}{2}}$	$k_{f,h}$ x 10^3 cm s^{-1}	log $k_{f,h}$
-0.350	4.0	1.04	1.09	-2.96
-0.375	8.5	1.10	1.15	-2.94
-0.400	17.0	1.23	1.29	-2.89
-0.425	28.5	1.53	1.60	-2.80
-0.450	34.5	1.80	1.88	-2.73
-0.475	40.0	2.24	2.34	-2.63
-0.500	43.0	2.67	2.80	-2.55
-0.550	46.5	3.78	4.00	-2.40

fear of the text becoming too bulky. The data on E, the potential and $i_{(\tau)}$, the current at $\tau = 4.8$ s are given in Table 4.5.9 and were used to plot the sampled current voltammogram given in Fig. 4.5.9. As can be seen from this figure, two well defined S-shaped curves were obtained indicating that the Cu^{++} ion is being reduced in two steps, most probably in stages of one electron each, i.e., from Cu^{++} to Cu^{+} and Cu^{+} to Cu^{o}. The $E_{\frac{1}{2}}$ values for the two waves were found to be -0.350 V and -0.650 V vs Ag/Ag^{+} respectively and the $i_{d(\tau)_1}$ and $i_{d(\tau)_2}$ were obtained as 22.00 uA and 40.50 μA respectively. These curves were then analysed for their $i_{(\tau)}$ - E relationships and the respective values of the potentials and $i(\tau)_1$ and $i(\tau)_2$ are given in Tables 4.5.10 and 4.5.11 respectively together with the values of $\left[\dfrac{i_{d(\tau)_1}}{i_{d(\tau)_1} - i_{(\tau)_1}}\right]^{\frac{1}{2}}$ and $\left[\dfrac{i_{d(\tau)_2}}{i_{d(\tau)} - i_{(\tau)_2}}\right]^{\frac{1}{2}}$.

The values of $(k_{f,h})_1$ and $(k_{f,h})_2$ were then calculated using the equation

$$k_{f,h} = \frac{(D_o)^{\frac{1}{2}}}{\sqrt{2}\ \tau^{\frac{1}{2}}} \left[\frac{i_{d(\tau)_i}}{i_{d(\tau)_i} - i_{(\tau)_i}}\right]^{\frac{1}{2}} \qquad 2.77$$

The D_o value was taken as the same for both the waves and equal to 5.23×10^{-6} cm^2 s^{-1}. The respective $(k_{f,h})_i$ values are given in Table 4.5.10 and Table 4.5.11 respectively. The plots of $(k_{f,h})_i$ against the potential E are given in

Table 4.5.9

Data on Sampled Current Voltammetry of Cu^{++} Ion in (Li, Na, K) NO_3 Eutectic at 423 $\pm$ 2 K.

Concentration of Cu^{++} = 4.36×10^{-6} mole cm^{-3}

τ = 4.80 s

Potential E V vs Ag/Ag^+	$i_{(\tau)}$ μA
-0.147	7.4
-0.190	9.6
-0.241	11.2
-0.291	14.0
-0.341	23.6
-0.384	31.4
-0.426	35.1
-0.525	39.4
-0.577	46.8
-0.621	56.4
-0.675	74.5
-0.720	85.1
-0.805	85.1

Table 4.5.10

Relationship between Potential E and log $(k_{f,h})_1$ at $\tau = 4.8$ s

Diffusion current $i_{d(\tau)_1}$ = 22.00 µA

<u>First Wave</u>

Potential E V vs Ag/Ag^+	$i_{(\tau)_1}$ µA	$\left[\frac{i_{d(\tau)_1}}{i_{d(\tau)_1} - i_{(\tau)_1}}\right]^{1/2}$	$(k_{f,h})_1$ x 10^4 cm s^{-1}	log $(k_{f,h})_1$
-0.300	3.0	1.05	7.53	-3.12
-0.325	6.0	1.17	8.42	-3.07
-0.350	10.5	1.38	9.93	-3.00
-0.375	16.0	1.92	13.75	-2.86
-0.400	19.0	2.70	19.45	-2.71

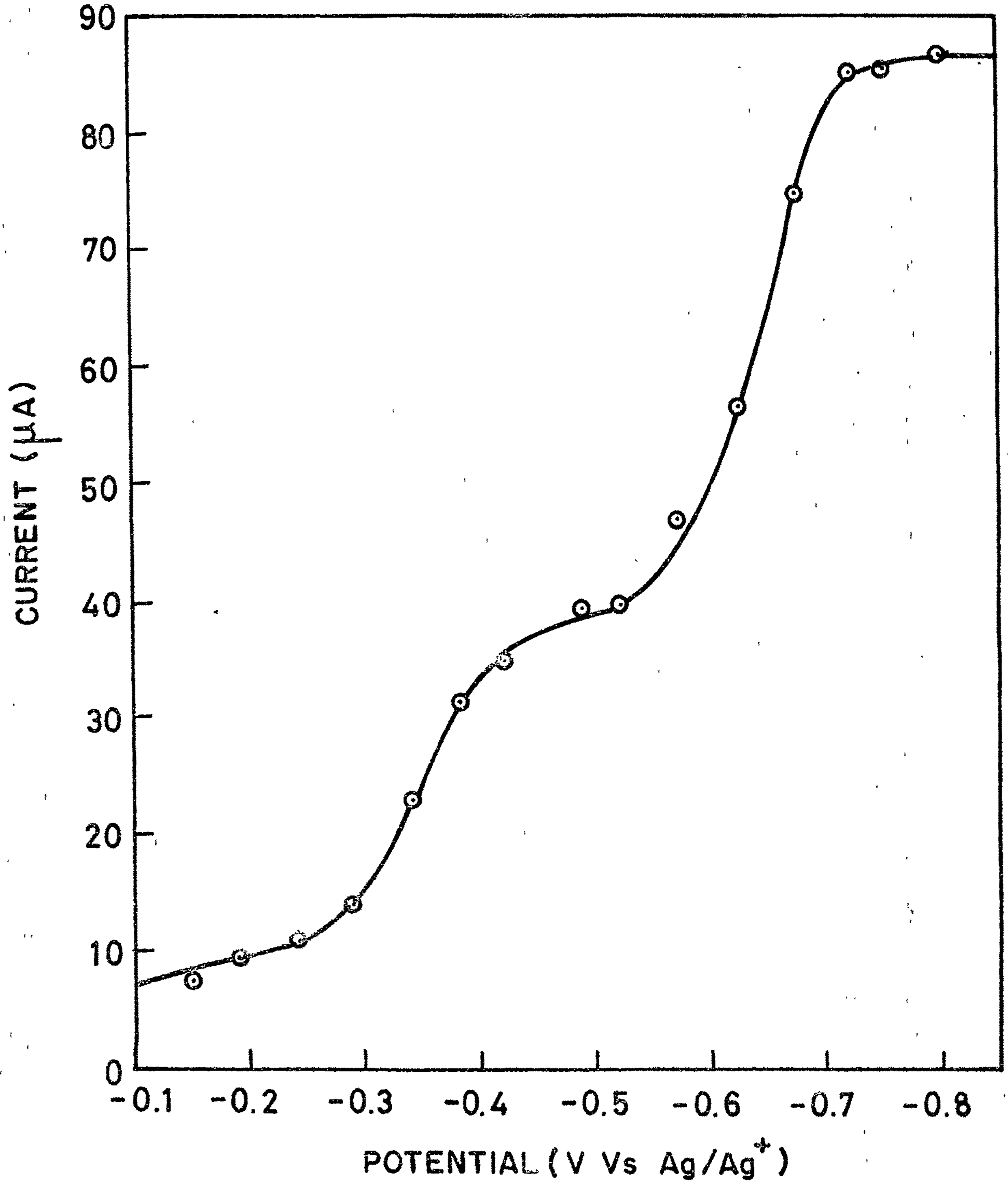

FIG. 4.5.9. A TYPICAL SAMPLED CURRENT VALTAMMOGRAM OF Cu^{++} ION.

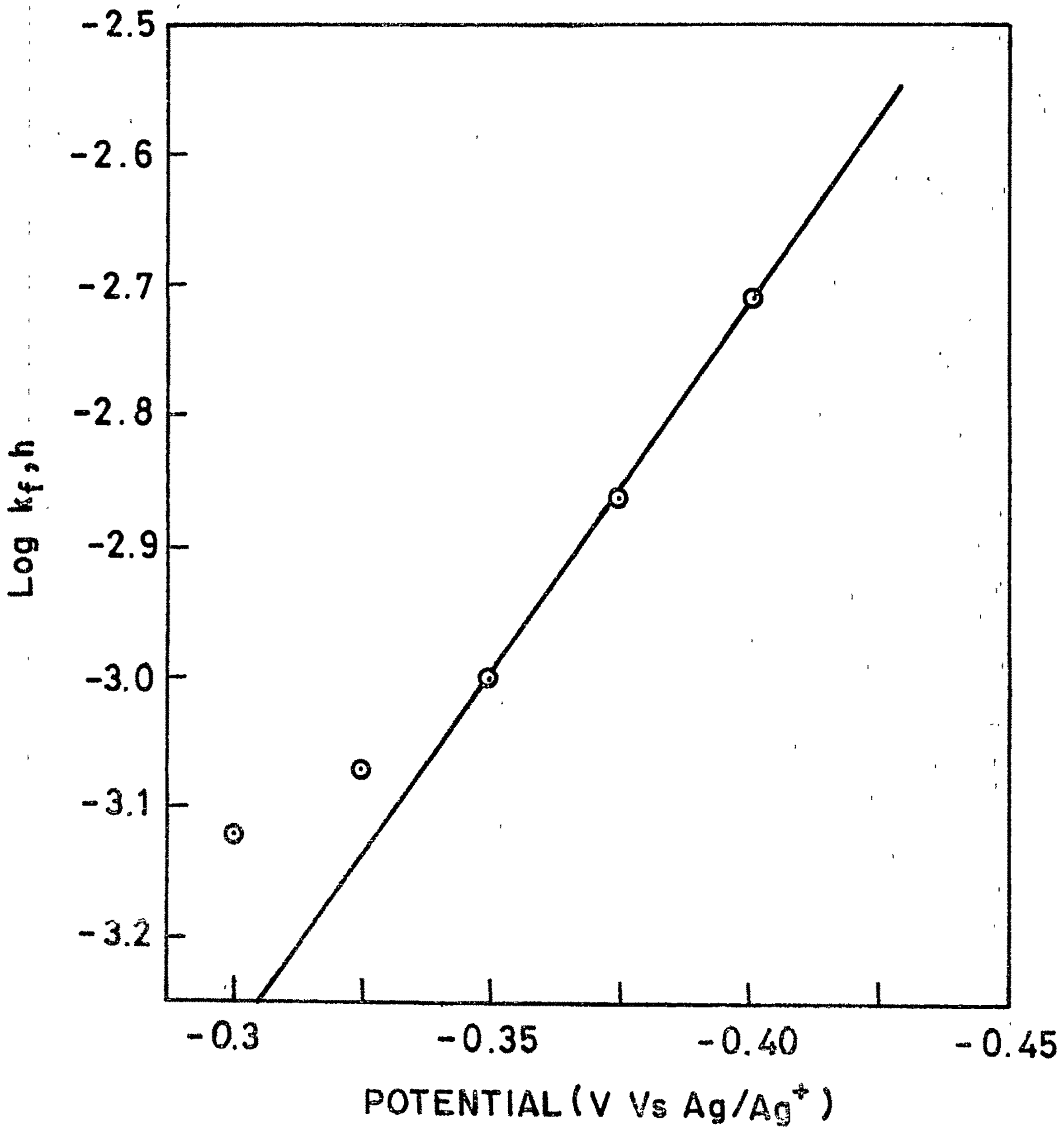

FIG.4.5.10. A PLOT OF E Vs LOG k_f,h (FIRST WAVE) FOR FINDING OUT $(\alpha_C n_\alpha)_1$ AND $(k_s,h)_1$.

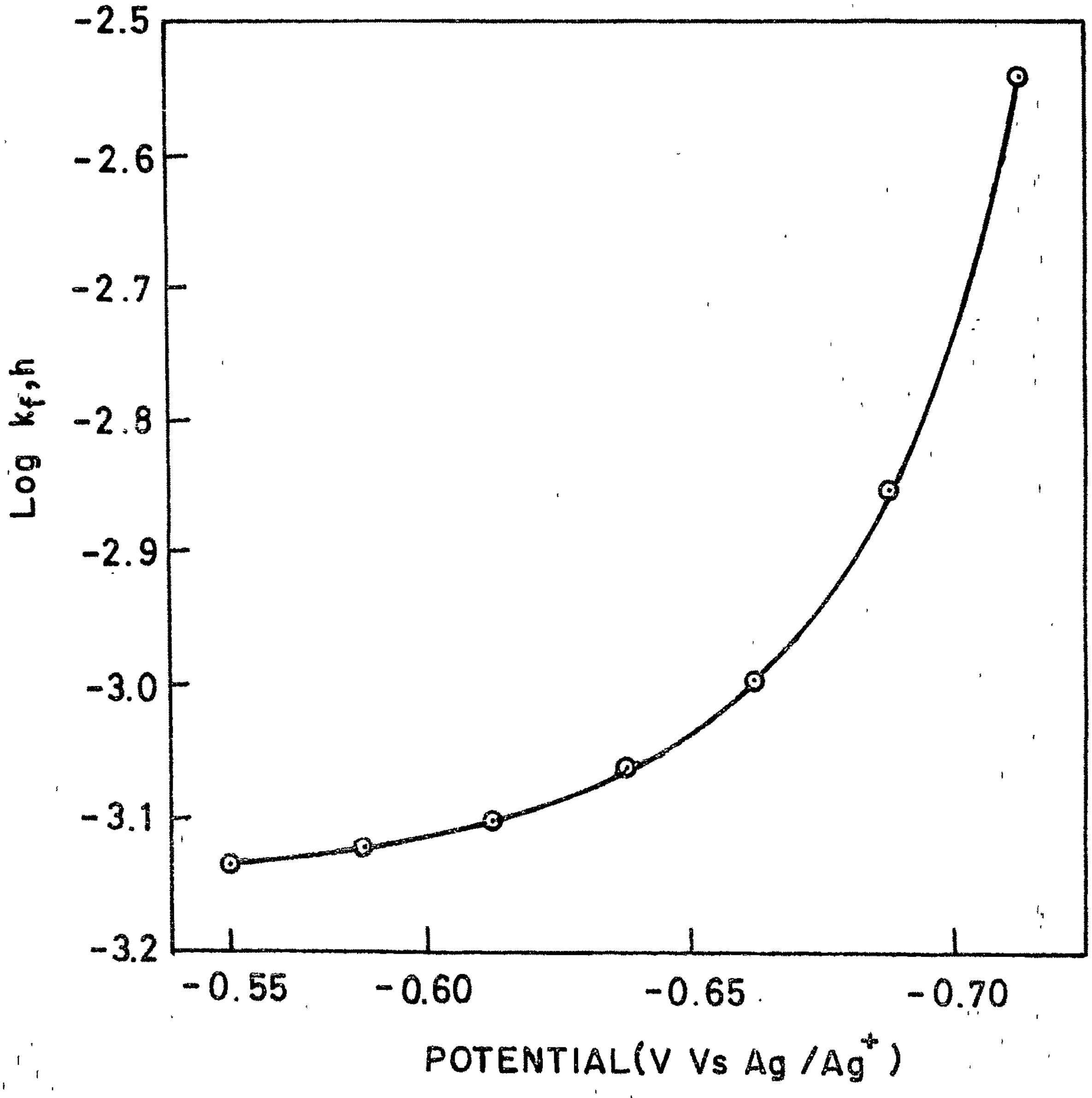

FIG.4.5.11. A PLOT OF E Vs LOG $k_{f,h}$ (SECOND WAVE) FOR FINDING OUT $(\alpha_c n_\alpha)_2$ AND $(k_{s,h})_2$.

Figs. 4.5.10 and 4.5.11. The equation connecting $(k_{f,h})_i$ with potentials can be written as

$$\log (k_{f,h})_i = (k_{s,h})_i - \frac{(\alpha_c n_\alpha)_i F}{2.303 RT} \left[E - (E^o)_i \right] \qquad \ldots\ldots\ldots \quad 2.79$$

According to this equation $\log (k_{f,h})_i$ if plotted against $E - (E^o)_i$ should give a straight line with a slope equal to $(\alpha_c n_\alpha)_i F / 2.303 RT$ and the intercept should be equal to $(k_{s,h})_i$ at $E = (E^o)_i$. As can be seen from Fig. 4.5.10, a linear relationship is found between $(k_{f,h})_1$ and E, with a slope of 5.66, from which the value of $(\alpha_c n_\alpha)_1$ works out to be 0.475. A perusal of Fig. 4.5.11 shows that $\log (k_{f,h})_2$ values do not vary in a linear manner with E. The curve obtained, however, can be resolved into two straight lines which intersect at exactly -0.650 V, i.e., at the $E_{1/2}$ value of the second wave. The implication of this is not immediately explainable as this is, perhaps, the first time that a clear cut second wave has been reported in sampled current voltammetry. The theoretical basis behind the calculation and the treatment of the two waves, as if they were separate entities, is not entirely sound. As in chronopotentiometry the second wave should be treated as a cumulative effect of the first and the second. This attempt has not been made here and the data as the second wave should be treated only to that extent.

The intercept on the x-axis, i.e., the value of $k_{f,h}$ when E = -0.350 V was found to be 1×10^{-3} cm s^{-1} which would give a value of log $k_{f,h}$ equal to -3.00. The slopes of the two straight lines into which the curve of the second wave can be resolved work out to be 1.0 and 9.1, which would yield values of $(\alpha_c n_\alpha)$, will be 0.086 and 0.786. The intercept on the y-axis which gives the value of log $(k_{s,h})_2$ will be again -3.00 which gives a value of $(k_{s,h})_2$ as 1×10^{-3}. Not withstanding the theoretical explanation it is clear that the lower part of the curve represents a one electron reduction while the upper portion of curve in Fig. 4.5.11 represents an irreversible reduction involving two faradays mol^{-1}. The discussion of the mechanism of the reduction of Cu^{++} ion, whether it is the simple coordinated copper ion or the nitrato complex that is being reduced, will be followed up in the next chapter.

Table 4.5.11

Relationship between Potential E and log $(k_{f,h})_2$ at $\tau = 4.8$ s

Diffusion current $i_{d(\tau)_2} = 40.5$ μA

Second Wave

Potential E V vs Ag/Ag$^+$	$i_{(\tau)_2}$ μA	$\left[\dfrac{i_{d(\tau)_2}}{i_{d(\tau)_2} - i_{(\tau)_2}}\right]^{\frac{1}{2}}$	$(k_{f,h})_2$ x 10^4 cm s^{-1}	log $(k_{f,h})_2$
-0.550	1.5	1.02	7.32	-3.14
-0.575	4.0	1.05	7.56	-3.12
-0.600	7.0	1.10	7.90	-3.10
-0.625	13.0	1.21	8.72	-3.06
-0.650	20.0	1.41	10.10	-3.00
-0.675	30.0	1.96	14.10	-2.85
-0.700	38.0	4.03	28.90	-2.54